

Deciphering the mode of regulation and understanding protein-protein interactions of human HtrA serine proteases

By

K. RAGHUPATHI

LIFE09201304015

**Tata Memorial Centre (TMC),
Advanced Centre for Treatment, Research and Education in Cancer (ACTREC),
Kharghar, Navi Mumbai – 410210.**

*A thesis submitted to the
Board of Studies in Life Sciences
(as applicable)
In partial fulfillment of requirements
for the Degree of*

DOCTOR OF PHILOSOPHY

of

HOMI BHABHA NATIONAL INSTITUTE



April, 2020

Homi Bhabha National Institute

Recommendations of the Viva Voce Committee

As members of the Viva Voce Committee, we certify that we have read the dissertation prepared by Mr. K.Raghupathi entitled "**Deciphering the mode of regulation and understanding protein-protein interactions of human HtrA serine proteases**" and recommend that it may be accepted as fulfilling the thesis requirement for the award of Degree of Doctor of Philosophy.



Chairperson—Dr. Sorab Dalal

Date:28-04-2020



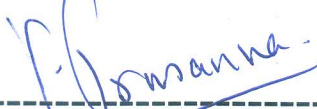
Guide/Convener —Dr. Kakoli Bose

Date: 28-04-2020



External Examiner—Dr.R.Sankaranarayanan

Date: 28-04-2020



Member —Dr. P. Venkatraman

Date: 28-04-2020




Member —Dr. Dibyendu Bhattacharyya

Date: 28-04-2020



Member -Dr. Manoj Bhat

Date: 28-04-2020



Invitee - Prof. S.V. Chiplunkar

Date: 28-04-2020



Invitee -Dr. Kaushik Sengupta

Date: 28-04-2020

Final approval and acceptance of this thesis is contingent upon the candidate's submission of the final copies of the thesis to HBNI.

I hereby certify that I have read this thesis prepared under my direction and recommend that it may be accepted as fulfilling the thesis requirement.

Date: 28-04-2020

Place: Navi Mumbai



Dr. Kakoli Bose
Guide

STATEMENT BY AUTHOR

This dissertation has been submitted in partial fulfillment of requirements for an advanced degree at Homi Bhabha National Institute (HBNI) and is deposited in the Library to be made available to borrowers under rules of the HBNI.

Brief quotations from this dissertation are allowable without special permission, provided that accurate acknowledgement of source is made. Requests for permission for extended quotation from or reproduction of this manuscript in whole or in part may be granted by the Competent Authority of HBNI when in his or her judgment the proposed use of the material is in the interests of scholarship. In all other instances, however, permission must be obtained from the author.



K. Raghupathi

DECLARATION

I, hereby declare that the investigation presented in the thesis has been carried out by me. The work is original and has not been submitted earlier as a whole or in part for a degree / diploma at this or any other Institution / University.



K. Raghupathi

List of Publications arising from the thesis

Journal

1. “Discerning the mechanism of action of HtrA4: a serine protease implicated in the cell death pathway”, Raghupathi Kummari, Shubhankar Dutta, Lalith K. Chaganti & Kakoli Bose, *Biochemical Journal*, May 21, 2019, 476(10)1445-1463; DOI: 10.1042/BCJ20190224

Chapters in books and lectures notes: NA

Conferences

1. **Horizons in Molecular Biology Symposium 2019**, Max Planck Institute for Biophysical Chemistry in Göttingen, Germany, 10th September -13th September 2018
Nature of Participation: Poster presentation (Title: Deciphering the Mode of Regulation and Functional Redundancy of HtrA4 – a Serine Protease Implicated in the Cell Death Pathway)
2. **42nd Annual Indian Biophysical Society (IBS) titled “Emerging Trends in Biophysics” 2018**, IISER Pune, Pune, India, 9th March to 11th March 2018
Nature of Participation: Poster presentation (Title: Biochemical and functional characterization of serine protease HtrA4)
3. **42nd Annual Indian Biophysical Society Meeting & Workshop on Archiving and Enriching Structural Data in Biology**, IISER Pune, Pune, India, 12th March to 13th March 2018
Nature of Participation: Attended the workshop (Title: Workshop on archiving and enriching structural data in biology)
4. **Science Communication Workshop**, Bhabha Atomic Research Centre, Mumbai, India, February 2018
Nature of Participation: Attended the workshop (Title: Science Communication Workshop- Sci comm 101)

5. **Fundamentals of Scientific Manuscript Writing and Submission**, Tata Memorial Centre, Mumbai, India, January 2018: Nature of Participation: Attended the workshop
6. **11th Biophysics Paschim Meeting**, IISER Pune, Pune, India, November 2017
Nature of Participation: Oral presentation (Title: Biochemical and functional characterization of serine protease HtrA4)
7. **10th Biophysics Paschim Meeting**, TIFR Mumbai, Mumbai, India, March 2017
Nature of Participation: Attended the lectures
8. **Advances in Enzymology: Implications in Health, Diseases and Therapeutics (INDO-US)**, ACTREC, India, January 2017
Nature of Participation: Poster presentation (Title: Biochemical and functional characterization of serine protease HtrA4)
9. **Tata Memorial Centre Platinum Jubilee Conference “HEALTHCARE: A Commodity or Basic Human Need?” 2017**, TIFR, Mumbai, India, January 2017
Nature of Participation: Attended the lectures
10. **National Research Scholar Meet 2016**, ACTREC, India, December 2016
Nature of Participation: Attended the lectures
11. **A conference of new ideas in cancer – Challenging dogmas**, Tata Theatre, NCPA, Mumbai, India, February 2016
Nature of Participation: Poster presentation (Title: Designing allosteric activators of proapoptotic HtrA2 and their implications in cancer therapeutics)
12. **National Research Scholar Meet 2015**, ACTREC, Mumbai, India, December 2015
Nature of Participation: Attended the lectures
13. **6th Biophysics Paschim Meeting**, IISER Pune, Pune, India, March 2014
Nature of Participation: Attended the lectures



K. Raghupathi

Dedicated to
my
beloved parents and teachers

Acknowledgment

Pursuing a Ph.D. is a challenge in every aspect; it demands passion, optimism, dedication and perseverance. Now, as I stand on the edge of its completion, I look back in retrospection and indispensable assistance and guidance of those who were vital in letting me achieve my goals. I want to thank all people without whom this project would have been a distant reality. Most importantly the very priority should be given to my mentor; Dr. Kakoli Bose, for giving an opportunity to work under her thoughtful and valuable guidance. Her intriguing suggestions and constructive criticism supplemented with the freedom of thought that she granted, has not only helped to discover my potential but also contributed a new dimension to my scientific career. I am also thankful to her as she has given me lot of opportunities to improve in many aspects and helped in acquiring excellent professional and communication skills. I am indebted to her more than she knows. Ma'am, I can never thank you enough for all that I have learned from you.

I am thankful to Dr. Sudeep Gupta (Director, ACTREC), Dr. Shubhada Chiplunkar (Ex-Director, ACTREC) and Dr. Prasanna Venktraman (Deputy Director, ACTREC) for their help and support directly or indirectly. I'm also thankful to the Department of Science and Technology (DST), ACTREC and Homi Bhabha National Institute (HBNI) for funding. I was privileged to have critical, supportive and inspiring Doctoral Committee members. I am indebted and highly obliged to Dr. Sorab Dalal (Chairperson) for all his support and guidance in my research. I want to thank him for teaching how to critically analyze and evaluate the data, improving my scientific understanding, his guidance and motivation that he provided during this tenure. I want to thank Dr. Prasanna Venktraman for her invaluable suggestions and guidance that had an impact on shaping up my scientific aptitude. I would like to express my deepest gratitude to Dr. Manoj Bhat (Our Santa Claus) not only for his valuable suggestions as my DC member but also for his support in providing the reagents and chemicals very promptly whenever I needed. I also extend my gratitude to thank Dr. Dibyendu Bhattacharyya for his motivation and support.

I am extremely thankful to the common instrument facility for their help and support specially Mr. Dandekar who is a very dedicated and resourceful person and always keen and kin to help everyone. I am thankful to Mrs. Maya and Mrs. Sharwari from Program office, Mr. Shashi Dolas and all members of Mass Spectrometry facility, Mrs. Sharada and Mr. Naresh from sequencing

facility for all their help. I am also thankful to the electrical department, Security department for the safety and watchfulness.

I want to express my warmest thanks to all Bose lab members (Padale sir, Snehal Ma'am, Saujanya, Ajay, Shubhankar, Rashmi, Aasna, Rucha, Sucheta, and Shubham) for creating such a joyful work environment and always being there for support. I am extremely thankful to all my trainees (Revathi, Rashi, Ankita Bhavasar, Nidhi, Vipshayana, Fatima and Zafar) and all others who have helped me with their presence, honest support and affection during their tenure in my Ph.D. I am glad and thankful to all my seniors, Dr. Nitu for her help and guidance during my initial Ph.D. days, and Dr. Raja for his constant support and affection. I am very thankful to late Dr. Lalith for helping me in many ways and I always miss him a lot. I am extremely thankful to Shubhankar Dutta for his help and support for in silico data. Special thanks to Rashmi Puja for proofreading and helping me in thesis writing. I owe my peace, happiness, success and progress to all such people in my life.

I am thankful to my batchmates of 2013 for their support and all the good times we had together. It would be another small chapter if I express all my feelings and gratitude towards them. Therefore to make it short I would say, it feels awesome being with them. Everyone has a vibrant and unique personality; they positively shaped my character and taught many life lessons. I had huge bunch of memorable, funny moments with everyone to cherish for a long time and I love immensely each one of them. I hope and wish our batch mates always stay happy and playful together forever. Additionally, my batch mate Raghav deserves special thanks for being such a wonderful roommate.

I am thankful to all the students of ACTREC for providing timely support whenever needed. I would specifically like to acknowledge Prasanna Lab and Dibyendu lab. I am especially grateful to all my teachers, who made me realize that the world is a beautiful place to live in. I am incredibly thankful to my parents for their sacrifice, trust, support, and confidence in me and for always standing by me whenever needed. I thank my sister and brothers for the strength, courage, unconditional love and affection they provided. I take immense pleasure in thanking my family. Words cannot express how grateful I am to my parents and others in the family for their love and support. I want to thank everyone who interacted with me and taught me lessons of life that shaped my integral personality.

Thank you all.

CONTENTS

SYNOPSIS	- 2 -
LIST OF FIGURES	- 18 -
LIST OF TABLES	- 21 -
CHAPTER 1: INTRODUCTION	- 23 -
Aims and objectives	- 28 -
CHAPTER 2: REVIEW OF LITERATURE	- 30 -
2.1 HtrA family Proteins	- 30 -
2.2 Bacterial HtrA proteins and other lower eukaryotic proteins	- 31 -
2.3 Human HtrAs	- 33 -
2.3.1 HtrA1	- 35 -
2.3.2 HtrA2	- 36 -
2.3.3 HtrA3	- 37 -
2.3.4 HtrA4	- 37 -
2.4 Structural assembly, oligomerization and role of domains in human HtrAs	- 38 -
2.5 Allostery, activation and cleavage mechanism of HtrAs	- 41 -
2.6 HtrA4 overview	- 45 -
2.7 HtrA2 overview	- 48 -
Caspase-dependent pathway	- 50 -

Caspase-independent pathway	51 -
2.8 GRIM-19 Overview	56 -
Functions of GRIM-19 and alterations in cancer	57 -
Physiological relevance of HtrA2 and GRIM-19 Interaction.....	59 -
CHAPTER 3: MATERIALS AND METHODS	61 -
3.1 MATERIALS	61 -
3.1.1 Bacterial Strains.....	61 -
3.1.2 Plasmids used for cloning.....	63 -
3.1.3 Resins used for protein purification.....	63 -
3.1.4 Kits used	64 -
3.1.5 Specialized instruments	64 -
3.1.6 Buffers and Reagents.....	65 -
3.1.6.1 Antibiotics.....	65 -
3.1.6.2 Bacterial culture media	66 -
3.1.6.3 For cloning and site directed mutagenesis	66 -
3.1.6.4 Buffers for protein expression and purification	68 -
Ni -IDA Column Purification buffers	69 -
Amylose column purification buffers	70 -
Urea denaturation buffers	71 -
3.1.6.5 5X SDS sample loading buffer (10 ml)	73 -

3.1.6.6	30% acrylamide	- 73 -
3.1.6.7	SDS-PAGE Running Buffer (for 1 L)	- 73 -
3.1.6.8	Staining / Destaining solution (for 1L)	- 74 -
3.1.6.9	Tris-Tricine SDS-PAGE buffers.....	- 74 -
3.2	Methods.....	- 75 -
3.2.1	Primer reconstitution	- 75 -
3.2.2	Determination of DNA concentration	- 78 -
3.2.3	Polymerase chain reaction (PCR).....	- 78 -
3.2.4	Agarose gel electrophoresis of DNA.....	- 80 -
3.2.5	Restriction digestion reaction	- 80 -
3.2.6	Cloning/Ligation.....	- 81 -
3.2.7	Plasmid construction.....	- 82 -
3.2.7.1	HtrA4 constructs	- 82 -
3.2.7.2	GRIM19 constructs	- 83 -
3.2.8	Transformation	- 83 -
3.2.9	Recombinant protein expression and purification	- 84 -
3.2.10	General protocol for protein purification.....	- 86 -
3.2.10.1	Ni-NTA agarose affinity chromatography	- 86 -
3.2.10.2	Amylose affinity chromatography	- 87 -
3.2.11	Purification of HtrA2 variants	- 88 -

3.3.13 Urea denaturation protocols.....	- 89 -
3.3.14 Urea denaturation modified protocols	- 89 -
3.3.15 Concentration of the protein using millipore centricon.....	- 89 -
3.3.16 Gel filtration chromatography	- 90 -
3.3.17 Determination of Protein concentration	- 90 -
3.3.17.1 Bradford protein assay	- 91 -
3.3.17.2 Absorbance at 280 nm	- 91 -
3.3.18 SDS polyacrylamide gel electrophoresis (SDS-PAGE)	- 92 -
3.3.19 12% TRIS TRICINE- SDS PAGE	- 92 -
3.3.20 Biophysical studies	- 93 -
3.3.20.1 Circular Dichroism (CD) spectroscopy	- 93 -
3.3.20.2 Fluorescence spectroscopy.....	- 95 -
3.3.21 Biochemical studies	- 95 -
3.3.21.1 Affinity pull down studies	- 95 -
3.3.21.2 Western Blotting	- 96 -
3.3.21.3 Serine protease enzymatic assays	- 99 -
Protease assays with β -casein as substrate:.....	- 99 -
Protease assays with GRIM-19 as substrate:	- 100 -
3.3.21.4 N-terminal sequencing	- 100 -
3.3.22 Crystallization.....	- 101 -

Methods of crystallization:	103 -
3.3.23 Molecular modeling, docking, and simulation	105 -
3.3.23.1 HtrA4	105 -
3.3.23.2 GRIM-19	108 -
3.3.23.3 Types of interactions	111 -
3.3.24 Animal cell culture	113 -
3.3.24.1 Materials	113 -
3.3.24.2 Protocols	114 -
a) Revival of cells	114 -
b) Trypsinization and Subculture	115 -
c) Freezing and cryopreservation	115 -
d) Preparation of whole cell lysate	116 -
e) Protein estimation using Bradford method	116 -
 CHAPTER 4: DISCERNING THE MECHANISM OF ACTION OF HTRA4 AND	
FUNCTIONAL REDUNDANCY	118 -
4.1 Introduction	118 -
4.2 Results	121 -
4.2.1 Sequence alignment of HtrA4 with other family members	121 -
4.2.2 Endogenous level of HtrA4 in different cell lines	123 -
4.2.3 Cloning of different domains, expression, and purifications	125 -

4.2.4 Secondary and tertiary structural characterization of HtrA4.....	128 -
4.2.5 Native oligomerization status of HtrA4 and its domains	130 -
4.2.6 Oligomerization status of HtrA4 in the presence of substrate.....	134 -
4.2.7 Protease assays to understand the role of different domains and the effect of temperature on catalytic activity.....	135 -
4.2.8 Substrate specificity of HtrA4	140 -
4.2.9 Mechanism of cleavage and the role of PDZ in substrate cleavage:	145 -
4.2.10 Crystallization of the PDZ domain of HtrA4 protein	148 -
4.2.11 Functional analysis: Binding and cleavage analysis with X-Linked Inhibitor of Apoptosis:.....	150 -
4.2.12 Selective binding pocket identification in HtrA4 and structural changes associated with peptide binding	155 -
4.2.12.1 Structural analysis and identification of binding pocket of HtrA4	155 -
4.2.12.2 Docking analysis reveals the important interacting residues in SBP_HtrA4	163 -
4.2.12.3 MDS analysis showing the structural reorientation of HtrA4 model upon binding with β -casein peptide	165 -
4.2.12.4 Comparative analysis of HtrA2 and HtrA4 catalytic triads to understand their role in enzymatic activity.....	167 -
4.3 Discussion and Conclusion.....	169 -

CHAPTER 5: TO UNDERSTAND THE INTERACTION BETWEEN HTRA2 AND ITS

BINDING PARTNER–GRIM-19.....	- 177 -
5.1 Introduction	- 177 -
5.2 Results	- 179 -
5.2.1 Cloning, expression, and purification of GRIM-19.....	- 179 -
5.2.1.1 Cloning and expression standardization of human GRIM-19 protein	- 179 -
5.2.1.2 GRIM-19 protein solubility analysis	- 180 -
5.2.1.3 GST tagged GRIM-19 purification.....	- 181 -
5.2.1.4 Co-expression and purification with chaperones	- 183 -
5.2.1.5 MBP tagged GRIM-19 purification	- 186 -
5.2.1.7 GRIM-19 protein Purification with urea denaturation method.....	- 188 -
5.2.2 Biophysical and structural characterization of GRIM-19 protein	- 190 -
5.2.2.1 Tertiary structure analysis of GRIM-19.....	- 190 -
5.2.2.2 <i>In-silico</i> modelling of GRIM-19	- 191 -
5.2.3 Mapping the minimal binding region important for interaction.....	- 193 -
5.2.3.1 Docking of full-length GRIM-19 with HtrA2	- 193 -
5.2.3.2 Binding assays of HtrA2 and GRIM-19	- 195 -
5.2.4 Substrate specificity of HtrA2 determined using natural substrate GRIM-19	- 199 -
5.2.5 Activation assays of HtrA2 with GRIM-19.....	- 204 -
5.2.6 Structural changes in HtrA2 associated with GRIM-19 peptide binding	- 207 -

5.2.6.1 Docking analysis of the GRIM-19 peptides with HtrA2 trimer	207 -
5.2.6.2 Structure-based comparative analysis of the GRIM-19 peptide bound and unbound HtrA2 using MD simulation	211 -
5.3 Discussion and conclusion:	214 -
CHAPTER 6: CONCLUSIONS AND FUTURE PERSPECTIVES.....	219 -
CHAPTER 7: REFERENCES	226 -
PUBLICATION	256 -

SYNOPSIS



Homi Bhabha National Institute

SYNOPSIS OF Ph. D. THESIS

1. **Name of the Student:** K.Raghupathi
2. **Name of the Constituent Institution:** Tata Memorial Centre, ACTREC
3. **Enrolment No. :** LIFE09201304015
4. **Title of the Thesis:** Deciphering the mode of regulation and understanding protein-protein interactions of human HtrA serine proteases
5. **Board of Studies:** Life Science

SYNOPSIS

Introduction:

High-temperature requirement protease A (HtrA) is a family of oligomeric serine proteases that are conserved from prokaryotes to humans. In humans, four HtrA homologs (HtrA1-4) have been identified¹⁻³. These proteins share a common domain architecture that comprise an N-terminal region, serine protease domain (SPD) for enzymatic activity and PDZ domain (postsynaptic density of 95 kDa, disk large, and zonula-occludens 1 domain) for protein-protein interactions. Apart from these common domains, all except HtrA2, harbor a Kazal like domain that acts as an inhibitor for serine protease activity, insulin-like growth factor binding protein domain (IGFBP) and a signal peptide. While, HtrA1, HtrA3, and HtrA4 share very similar domain organizations, the uniqueness of HtrA2 is manifested through the absence of Kazal and IGFBP domains and existence of a distinct N-terminal region, which includes a prominent IAP (inhibitor of apoptosis) binding motif (IBM) and a transmembrane domain⁴.

In humans, these proteases are involved in numerous cellular processes ranging from maintenance of mitochondrial homeostasis to cell death. Therefore, deregulation of their normal functions leads to various diseases that include neurodegeneration, neuromuscular disorders, arthritis, age-related macular degeneration, pregnancy-specific pre-eclampsia, and cancer. Among human HtrA homologs, HtrA1 and HtrA2 are well characterized with available high-resolution crystal structures. However, HtrA4 is the least characterized human HtrA protease concerning both structure as well as its functions. It has been found to be up-regulated in pre-eclampsia (PE) and hence has been suggested to be used as a biomarker of PE⁵. Meta-analyses of available microarray data suggested that HtrA4 is up-regulated in glioblastoma multiforme and breast carcinoma, whereas, down-regulated in metastatic prostate cancer; making it an emerging therapeutic target^{6,7}. Therefore, an intricate dissection of HtrA4 structure with an understanding of its functional reciprocity becomes imperative to harness its properties with desired characteristics.

Specific objectives:

Objective 1:

1) Characterization of human HtrA4 and its subdomains using biophysical, biochemical, enzymology and structural biology probes.

Results:

1.1. Purification and secondary structural characterization of HtrA4 and its variants:

Different variants of HtrA4 were generated using polymerase chain reaction (PCR) and site-directed mutagenesis (SDM) to understand the role of different domains and their combinations in regulating HtrA4 stability and functions. Pairwise sequence alignment of HtrA4 with mature HtrA2 showed 54% sequence similarity and also displayed a conserved N-terminal ¹⁴⁴AVPV motif similar to that of ¹³³AVPS motif (IAP binding motif) in HtrA2. Based on this observation, we cloned HtrA4 starting from ¹⁴⁴AVPV residues. Several literature reports highlighted the importance of the N-terminal region in regulating enzymatic activity of HtrA family proteins. Therefore, to understand the role of the N-terminal region in oligomerization, stability, and functions of HtrA4, we generated N-terminal deleted construct (SPD-PDZ). Similarly, only SPD variant was also generated to understand its function as a single domain. Similarly, different

domain combinations of HtrA4 with active-site (S326A) mutation were purified using Ni-IDA affinity chromatography and characterized.

To check for structural perturbation, if any, in the inactive (S326A) HtrA4 variant, far UV CD of the protein was performed and compared with its active counterpart. The similarity in secondary structure suggests that the mutation is not structurally perturbing. Melting curves of HtrA4 and the catalytically inactive (S326A) HtrA4 implicate that the proteins have similar thermal stability with a $T_m \sim 58^\circ\text{C}$.

1.2. Oligomerization status of various HtrA4 domains and mutants:

Prokaryotic HtrA family members are capable of forming higher-order oligomeric complexes consisting up to 24 molecules. While DegS is a stable trimer, active DegQ and DegP form higher order oligomers comprising 12 and 24 monomeric subunits respectively. Human HtrA homologs (HtrA1, HtrA2, and HtrA3) however have been reported to be in trimeric form, while no report on HtrA4's oligomeric property has been obtained so far. Therefore, to understand the oligomerization status of HtrA4, gel filtration chromatography was performed using a superdex 200 gel filtration column. Elution profiles of HtrA4 variants (N-SPD, SPD-PDZ, and SPD) were monitored, and their respective molecular weights were calculated from the calibration curve generated from protein standards. The estimated molecular weights of these proteins demonstrate that HtrA4 and N-SPD are trimers. Interestingly, unlike HtrA2⁸, some amount of monomeric population is also observed in HtrA4 suggesting lesser stability of trimeric HtrA4. However, upon incubation of inactive HtrA4 with its generic substrate β -casein, only trimeric peak was observed with complete disappearance of the monomeric population. N-SPD showed solely a trimeric ensemble implicating that the PDZ along with the linker region might provide more conformational flexibility to the protease. As expected, SPD-PDZ and SPD were found to be monomers reiterating the importance of N terminal region in trimerization.

1.3. Protease assays:

To compare enzymatic properties of HtrA4 primarily with HtrA2 as well as to understand the role of different domains and their oligomerization status in regulating its protease activity, gel-based protease assays of HtrA4 and its variants were performed using β -casein. In these studies, the active-site mutant (S326A) was used as a negative control. Different HtrA4 variants were incubated with β -casein at 37°C for 10 hrs. Uncleaved β -casein band was semi-quantified using Image J software and subsequently cleaved β -casein percentage was calculated and plotted. It

was observed that both the trimeric protein HtrA4, and N-SPD cleaved β -casein, although the activity of N-SPD was less than HtrA4, particularly at higher temperatures. However, the monomeric variants, i.e., SPD-PDZ and SPD, did not show any protease activity, highlighting the importance of trimerization for HtrA4 activity.

Moreover, to understand the rate of substrate binding and catalysis, kinetic parameters of HtrA4 were determined fluorometrically using FITC labeled β -casein as a substrate. Further to gain insights into the HtrA4 active-site orientation and conformational dynamics, these kinetic parameters were compared with HtrA2⁸. From this study, the observed V_{\max} (1.9×10^{-12} M/s), k_{cat} (0.06×10^{-6} s⁻¹) and K_{cat}/K_m (0.0123 M⁻¹ s⁻¹) were relatively low when compared to HtrA2 (V_{\max} (4.08×10^{-9} M/s), k_{cat} (0.02 ± 0.004 s⁻¹) and K_{cat}/K_m (4.5×10^3 M⁻¹ s⁻¹)), which indicates HtrA4 is catalytically less competent than HtrA2 with lower enzymatic reaction rate and turnover number under identical experimental conditions *in vitro*. However, the K_m value of HtrA4 has been found to be almost similar to that of HtrA2 (HtrA4- K_m 4.84 ± 0.8 μ M and HtrA2 K_m 4.60 ± 0.5 μ M) suggesting similar substrate binding affinity of the two proteases. The Hill coefficient of 1.3 for HtrA4 is indicative of allosteric activation like other members of the HtrA family^{8,9}.

Literature suggests that HtrA2 and its homologs show significant increase in activity with temperature. This heat activation is associated with considerable plasticity at the PDZ-protease interface similar to activation via substrate binding at PDZ^{8,10}. Since HtrA4 is a close homolog of HtrA2, we speculated that it might also exhibit similar dynamic behavior and conformational changes in the presence of temperature. Therefore, protease assays of HtrA4 were performed as a function of temperature. HtrA4 variants were incubated with β -casein in the temperature range of 30°C to 45°C for 10 hrs and analyzed using Tris-tricine gels. The uncleaved β -casein band after 10 hrs was semi-quantified using Image J software and subsequently cleaved β -casein percentage was calculated and plotted. Activity of HtrA4 was found to be high at higher temperatures (>30°C). However for N-SPD, a subsequent decrease in activity was observed beyond 35°C, which might be due to lack of necessary conformational changes in absence of the regulatory PDZ domain and protease destabilization.

1.4. Substrate specificity of HtrA4:

Cleavage specificities of HtrA1, HtrA2, and HtrA3 have been well documented in the literature; therefore, to understand whether HtrA4 shares similar substrate specificity as its human counterparts, we determined the substrate specificity of HtrA4 using β -casein. Proteolytically

cleaved fragments (~23kDa, 19kDa, 13kDa, 7kDa and less than 5kDa) of β -casein were subjected to N-terminal sequencing by Edman degradation. The specificity profile of N-terminal sequence analysis of these fragments identified three preferred cleavage sites on β -casein. The first cleavage site is between 15A-16R, second between 108M-109G and third cleavage site is between 170V-171M amino acids respectively. Cleavage at single or multiple sites resulted in a combination of different peptide fragments.

Our observations suggest that HtrA4 has a strong preference for aliphatic residues at P1 (A, V, and M) position similar to the other three human HtrA homologs. The P2 position is occupied by aliphatic (L and V) and polar (T) residues, HtrA1 and HtrA2 also preferred similar aliphatic residues (L) at this position. At P3 and P4 positions, HtrA4 preferred aliphatic (A and L) and polar residues (P and E), which also matches with HtrA1 and HtrA3 specificity. At P1' position HtrA4 preferred aliphatic (G and M) and polar amino acids (R) that is similar to other family members. At P2' position like other family members, HtrA4 also preferred aromatic (F) and aliphatic (V) residues. At P3' position, HtrA4 preferred polar (S and P) and aliphatic (L) residues. At the same position, HtrA2 and HtrA3 showed preference for similar polar residues (S and P) only. At P4' position, other family members showed a preference for mostly aromatic (F, Y, and W) and polar (S), while HtrA4 preferred polar (P, E and K) residues¹¹⁻¹⁶. Overall, these results suggest that HtrA family members have similar but not identical substrate specificities.

1.5. Binding and cleavage of XIAP:

Identification of substrates and binding partners of HtrA4 is important for providing insight into its specific role in physiological processes. It has been reported that HtrA1, HtrA2, and HtrA3 cleave XIAP to induce apoptosis, which has been very well characterized in HtrA2. XIAP is an antiapoptotic protein that interacts with downstream caspase-3 and prevents activation of the caspase cascade. HtrA4 shares a very high sequence similarity with other human HtrAs, that implies functional overlap within the family. Our sequence alignment demonstrated that HtrA4 shares an N-terminal IAP binding tetrapeptide ¹⁴⁴AVPV similar to ¹³³AVPS motif of HtrA2. Based on this observation, we performed *in vitro* binding and proteolytic assays of HtrA4 using XIAP.

For *in vitro* binding studies, pull-down assays were performed with GST-fused XIAP as bait and inactive HtrA4 (S326A) as prey. Pull-down demonstrated that HtrA4 interacts with GST-XIAP but not with GST-tag alone. To determine the role of the N-terminal ¹⁴⁴AVPV in binding to

XIAP if any, we performed pull-down studies with Δ AVPV construct of HtrA4. Absence of AVPV abrogated the interaction thus highlighting its importance in HtrA4-XIAP complex formation. This interaction was further confirmed by western blot analysis using anti-His antibody. The observed result indicates that XIAP is an N-terminal binding partner of HtrA4.

Further to understand whether XIAP is a substrate for HtrA4, protease assays were performed. Since XIAP was less stable, GST tagged XIAP was used as a substrate for our study. Interestingly, HtrA4 cleaved GST-XIAP but not GST alone in a time dependent manner suggesting XIAP might be a novel substrate of HtrA4. Further to investigate the rate of protease activity semi-quantitatively, time-based degradation of GST-XIAP was monitored. The rate of hydrolysis was quantitated by measuring the intensity of the proteolytically degraded GST-XIAP band at 24 hr relative to uncleaved GST-XIAP using *Image J* software. HtrA4 cleaved GST-XIAP in a time-dependent fashion with 80% of the substrate being hydrolyzed in 24 hrs.

Further to corroborate our binding studies, we performed protease assays with Δ AVPV construct. No cleavage of GST-XIAP was observed with this deletion construct of HtrA4 as expected. These observations suggest binding to ¹⁴⁴AVPV might be a pre-requisite for subsequent cleavage of XIAP by HtrA4. In all the protease assays, inactive HtrA4 (S326A) was used as a negative control. We could not do further analysis of the cleaved products as the cleaved fragments of XIAP were very small and remained undetected even in Tris-tricine gel.

1.6. Structural analysis and identification of binding pocket of HtrA4:

HtrA4 model (**PM0081859**), generated from I-TASSER server was analyzed to understand the orientation of the secondary structures using PSIPRED tool. PSIPRED showed a total of five alpha helices, twenty β -strands and eight major loops traversing throughout the SPD and PDZ domain of HtrA4 model. Helices and β -strands were numbered sequentially starting from the N-terminus towards the C-terminal end of the model. SPD contains twelve β -strands (β 1- β 12) connected by evolutionarily conserved loops which were named according to the chymotrypsin nomenclature. Among these loops, LB (β 3- β 4), LC (β 6- β 7), and L1 (β 9- β 10) accommodate the catalytic triad residues His218, Asp248, and Ser326 respectively. These loops synergistically interact with LA (β 1- β 2), LD (β 7- β 8), and L3 (β 8- β 9) loops, which are found to be essential for proteolytic activity and its regulation for various serine proteases. Prior to docking analysis of HtrA4 with β -Casein, the binding pocket was identified using SiteMap.

1.7. Docking analysis reveals the important interacting residues in SBP_HtrA4

To find leads toward critical interacting residues, the affinity of the interaction and the allosteric changes associated upon peptide binding, we prepared a peptide library of β -casein (library preparation and docking discussed in the Methods section) and docked them with HtrA4. Among 23 β -casein peptides present in the library, $^{199}\text{DMPIQAF}^{205}$ (β -casein peptide- $^{199}\text{DMPIQAFLLYQEPVLGPVRGPFPIIV}^{224}$) showed the highest binding affinity with a docking score of -10.126 kcal/mole.

1.8. MDS analysis representing structural reorientations of modeled HtrA4 upon binding β -casein peptide:

RMSD plot generated from MDS analysis of HtrA4_ β -casein complex (PMDB ID: **PM0081893**) showed fluctuation in the N-terminus, linker region and PDZ domain when compared to the unbound protease. Among these three regions, N-terminus showed the maximum deviation of 0.2 nm (2 Å) as compared to the unbound HtrA4. Linker region started fluctuating after 5 ns that got stabilized beyond 10 ns of simulation. Highest deviation for linker region was 0.3 nm (3 Å) in a bound form that is 0.1 nm (1 Å) less than the same in the apo-form and subtle change in the overall RMSD values for PDZ domain were also observed upon binding the β -casein peptide.

Movement in the H3 helix was observed upon H-bond interaction between S394 in H3 with the β -casein peptide. In addition, L383 of $^{382}\text{YLGL}^{385}$ motif in PDZ domain displayed interaction with the peptide resulting in deviation of both the linker region and $^{382}\text{YLGL}^{385}$ motif. The $^{382}\text{YLGL}^{385}$ motif moved away to accommodate the heptameric β -casein peptide. Moreover, loop movement in the SPD domain contributed to the reorientation of the catalytic triad, where LC and L1 loops came closer to each other bringing H218 and S326 residues in close proximity. Moreover, the LC loop moved away from L4 causing an increment in the distance between H218 and D248. These arrangements when compared with other serine proteases have been found to be conducive for substrate binding and catalysis. For example, similar movements are observed in L1, L2 and LD loops of HtrA2 when an activator peptide binds to it, resulting in reorientation of the catalytic triad residues¹⁷.

1.9. Endogenous level of HtrA4 in different cell lines:

The expression of the endogenous level of HtrA4 was analyzed in various cancer cell lines. Using trypan blue staining and hemocytometer, an equal number of cells of MCF7, HeLa, A549, SiHA, and HEK 293 (normal) were calculated and seeded. The cells were grown in complete

media, were lysed, and protein concentration was estimated by Bradford's method. Purified HtrA4 protein expressed in Rosetta™(DE3)pLysS cells was used as a positive control for HtrA4. The bacterial cell lysate was used as a negative control for antibody specificity in the study. From our results, it is clear that all of the above-mentioned cell lines showed almost similar protein levels of HtrA4; we could also observe a 36kDa band indicating that HtrA4 also has a maturation process similar to that of HtrA2.

Summary:

Overall, we did an extensive biophysical and enzymatic characterization of serine protease HtrA4 and propose a working model of its mode of action (Fig. 1). We propose that HtrA4 exists in both trimeric and monomeric forms; trimeric one is the dominant and most favorable native oligomeric state. Addition of substrate also enhances the conversion of the residual population of monomers to trimers. The model also suggests that initial binding of the β -casein peptide at SBP_HtrA4 leads to conformational rearrangement of the N-terminal region and loops at and around the catalytic triad. The significant role of N-terminal region in fostering HtrA4's activity and maintaining its trimeric form is evident from the fact that both SPD-PDZ and SPD monomers, which are devoid of N-terminal regions are inactive. Hence, it further emphasizes the importance of trimerization to acquire a catalytically competent structure and indicates that the serine protease domain alone is not sufficient for substrate catalysis. Moreover, our study also show antiapoptotic XIAP as a binding partner cum substrate of HtrA4 *in vitro*. Thus, with the help of the comprehensive model proposed by our study, further identification of natural substrates of HtrA4 would provide a clue for devising strategies for therapeutic intervention against diseases it is associated with^{18,19}.

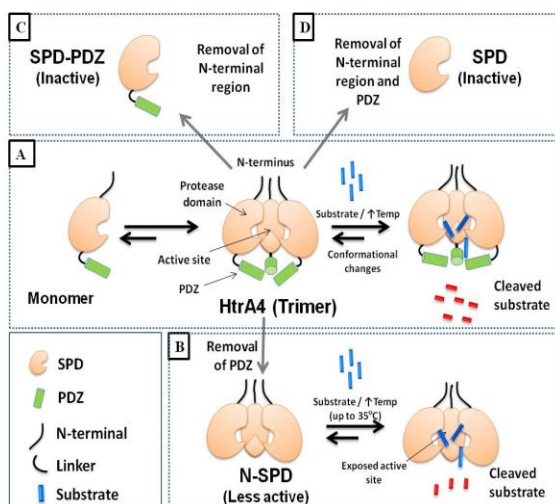


Fig. 1: A proposed simplistic model for HtrA4 mechanism of action: The model illustrates existence of HtrA4 primarily as a trimer with a small amount of monomeric population. The trimeric population is stabilized upon substrate binding. **A)** In trimeric HtrA4, initial substrate binding or increase in temperature leads to conformational changes in regulatory loops and makes protease active and cleaves substrates into shorter fragments. **B)** In trimeric N-SPD with partially exposed active site and no regulatory PDZ domain, activity is less. **C)** Removal of N-terminal makes protease monomer, and hence no catalytic activity is observed. **D)** Removal of both N-terminus and PDZ also generates monomeric protease, which lacks proteolytic activity

Objective 2: Understand the basis of interaction of GRIM-19 and HtrA2 using different biophysical and biochemical tools.

Introduction:

HtrA2 mitochondrial resident protein, upon apoptotic induction, the first 133 residues that include the mitochondrial localization signal get cleaved, leading to the formation of active mature form of HtrA2 with the exposure of the tetrapeptide motif at the N-terminus. This mature form of HtrA2 interacts and cleaves IAPs, relieving the inhibition on effector caspases and promotes apoptosis. To modulate HtrA2 functions with desired characteristics, we require a detailed understanding of its mode of activation and the other protein-protein interactions that control it. To date, HtrA2 is reported to interact with IAPs, cytoskeletal proteins, antiapoptotic proteins and also with the cell death regulatory protein called GRIM-19 (Gene associated with retinoic and interferon-induced mortality 19 protein)⁶.

Kalvakolanu et al. have identified GRIM-19 as potential activator of HtrA2. In presence of GRIM-19, the proapoptotic activity of HtrA2 is amplified resulting in elevated rate of apoptosis²⁰. This offers an excellent opportunity towards designing activators for HtrA2, which modulate its functions with desired characteristics against diseases associated with it. However, their mechanisms of activation, binding affinity as well as the region of interaction, are not known so far. Delineation of this important information will therefore be a step towards this goal.

Results:

2.1. GRIM-19 cloning, expression and protein purification:

The *GRIM-19* gene was cloned into a pET28a expression vector. *E. coli* expressed GRIM-19 was found to be in the insoluble fraction after sonication. Therefore, GRIM-19 protein from the insoluble fractions was purified using 8M urea. Urea-denatured GRIM-19 protein was refolded and dialyzed to remove the additives (which helps in refolding). Fluorescence emission maxima scans were collected to check whether the protein refolded properly or not. Refolded protein showed a blue shift (~7nm) in emission maxima when compared to unfolded, suggesting that the protein has folded properly.

2.2. Mapping the minimal binding region important for interaction:

Docking of full-length GRIM-19 with HtrA2: The best GRIM-19 model was subjected to blind docking with HtrA2. Protein-protein docking between these proteins generated complexes that were ranked based on the docking score. Most of the residues in the interaction belong to the cell death-inducing domain of GRIM-19 and the serine protease domain of HtrA2.

Binding assays of HtrA2 and GRIM-19: Although it has been previously demonstrated that GRIM-19 interacts with HtrA2 to promote the rate of apoptosis, the corresponding minimal binding region and critical residues involved in HtrA2 and GRIM-19 interaction are not known. Therefore, pull-down studies were performed with MBP fused recombinant GRIM-19 as bait and HtrA2 variants as prey. From our results, it is clear that both full-length GRIM-19 and cell death-inducing domain of GRIM-19 interacts with full length and the serine protease domain of HtrA2. No pull-down was detectable using MBP control alone.

2.3. Substrate specificity of HtrA2 determined by using natural substrate GRIM-19:

Substrate specificity of HtrA2 is limited to only two published reports with artificial substrates; to understand the substrate specificity of HtrA2, we used one of the natural substrate GRIM-19. Both HtrA2 and HtrA2 Δ PDZ (N-SPD) variants cleaved GRIM-19 suggesting that GRIM-19 is a novel substrate of HtrA2. Further to gain insights into HtrA2 cleavage site specificity, proteolytically cleaved fragments (~15, 13, 12, 9.5, 6 and 5 kDa) of GRIM-19 were subjected to N-terminal sequencing by Edman degradation. The specificity profile of the N-terminal sequence analysis of these fragments identified six preferred cleavage sites on GRIM-19. This preference corroborates well with the previously published data, and this is the first report of HtrA2 substrate specificity determined using a natural substrate.

2.4. Structural characterization:

In silico modeling of GRIM-19: Five models were given by I-TASSER Ab-Initio server whose C-score ranged from -3.08 to -2.00. ModLoop refined model was further validated using Ramachandran plot which revealed that refined structure contains no outlier residues and the number of residues in core region increased from 104 (73.2%) to 137 (96.5%).

2.5. Activation assays of HtrA2 with GRIM-19:

It was reported in the literature that GRIM-19 enhances the proapoptotic activity of HtrA2 in *ex vivo*. The minimal binding region of GRIM-19 which activates HtrA2 and the allosteric changes in HtrA2 associated with GRIM-19 binding is not known. The activation assay was performed in the presence of GRIM-19. From our docking and pull-down studies, the cell death-inducing

domain of GRIM-19 is known to interact with HtrA2, and we employed this domain of GRIM-19 for activation assays as well. Interestingly, upon pre-incubation of HtrA2 with GRIM-19, the catalytic efficiency (k_{cat}/K_m) increased by two-fold, and with cell death-inducing domain it increased to 2.8 fold.

2.6. Structural changes associated with GRIM-19 peptide binding:

Docking analysis of the GRIM-19 peptides with HtrA2 trimer: To understand more about interacting surface, in depth analysis of HtrA2 and GRIM-19 interacting residues were analyzed using docking studies with the peptides of GRIM-19. Since the cell death-inducing domain has high potential to activate HtrA2, the peptide library prepared from only cell death-inducing domain of GRIM-19 (amino acid sequence 102 to 144). Heptameric GRIM-19 peptides from the designed peptide library were docked with HtrA2 trimer at the best binding site generated from the SiteMap output.

2.7. Structure-based comparative analysis of the GRIM-19 peptide bound and unbound HtrA2 using MD simulations:

To understand more about conformational changes associated with peptide binding, we performed molecular dynamic simulations with GRIM-19 peptide bound and unbound HtrA2. Among all the peptides, HGFMWYT yielded the highest docking score of -9.191 kCal/ mole and was chosen for comparative MD simulation analysis with unbound HtrA2. Conformational changes in HtrA2-HGFMWYT complex during MD simulation indicated large fluctuation in the N-terminal region (1-32) when compared to unbound HtrA2. The RMSD difference between bound and unbound HtrA2 in the N-terminus was found to be 1.2 Å. In comparison to the unbound HtrA2, overall SPD domain movements (33-209) in the bound HtrA2 seemed to get relaxed by 0.9 Å.

Summary:

1. Successfully purified GRIM 19 for biophysical studies.
2. Pull-down assay showing the interaction between HtrA2 and GRIM 19.
3. Using *in vitro* enzymology studies, we identified that GRIM-19 is a novel substrate for HtrA2.
4. For the first time, the substrate specificity of HtrA2 determined using a natural substrate GRIM-19.
5. Identified the critical residues involved in the interaction using docking studies.

6. Activation assays of HtrA2 with GRIM-19 shows that GRIM-19 is an allosteric activator of HtrA2.
7. Structure-based comparative analysis of the GRIM-19 peptide bound and unbound HtrA2 using MD simulation have been done to know structural changes associated with GRIM-19 peptide binding.

References:

1. Clausen, T., Southan, C. & Ehrmann, M. The HtrA family of proteases: implications for protein composition and cell fate. *Mol. Cell* 10, 443–55 (2002).
2. Gray, C. W. et al. Characterization of human HtrA2, a novel serine protease involved in the mammalian cellular stress response. *Eur. J. Biochem.* 267, 5699–710 (2000).
3. Nie, G.-Y., Hampton, A., Li, Y., Findlay, J. K. & Salmons, L. A. Identification and cloning of two isoforms of human high-temperature requirement factor A3 (HtrA3), characterization of its genomic structure and comparison of its tissue distribution with HtrA1 and HtrA2. *Biochem. J.* 371, 39–48 (2003).
4. Bose, K. Proteases in apoptosis: Pathways, protocols and translational advances. *Proteases in Apoptosis: Pathways, Protocols and Translational Advances* (2015). doi:10.1007/978-3-319-19497-4
5. Inagaki, A. et al. Upregulation of HtrA4 in the placentas of patients with severe pre-eclampsia. *Placenta* 33, 919–926 (2012).
6. Zurawa-Janicka, D., Skorko-Glonek, J. & Lipinska, B. HtrA proteins as targets in therapy of cancer and other diseases. *Expert Opin. Ther. Targets* 14, 665–679 (2010).
7. Chien, J., Campioni, M., Shridhar, V. & Baldi, A. HtrA serine proteases as potential therapeutic targets in cancer. *Curr. Cancer Drug Targets* 9, 451–68 (2009).
8. Chaganti, L. K., Kuppli, R. R. & Bose, K. Intricate structural coordination and domain plasticity regulate activity of serine protease HtrA2. *FASEB J.* 27, 3054–66 (2013).
9. Singh, N., D'Souza, A., Cholleti, A., Sastry, G. M. & Bose, K. Dual regulatory switch confers tighter control on HtrA2 proteolytic activity. *FEBS J.* 281, 2456–2470 (2014).
10. Zurawa-Janicka, D. et al. Temperature-induced changes of HtrA2(Omi) protease activity and structure. *Cell Stress Chaperones* 18, 35–51 (2013).
11. Glaza, P. et al. Structural and functional analysis of human HtrA3 protease and its subdomains. *PLoS One* 10, e0131142 (2015).
12. Vande Walle, L. et al. Proteome-wide Identification of HtrA2/Omi Substrates. *J. Proteome Res.* 6, 1006–1015 (2007).
13. Martins, L. M. et al. Binding specificity and regulation of the serine protease and PDZ domains of HtrA2/Omi. *J. Biol. Chem.* 278, 49417–27 (2003).
14. Chaganti, L. K., Singh, N. & Bose, K. Cathepsins and HtrAs – Multitasking Proteases in Programmed Cell Death. in *Proteases in Apoptosis: Pathways, Protocols and Translational Advances* 95–141 (Springer International Publishing, 2015). doi:10.1007/978-3-319-19497-4_4
15. Eigenbrot, C. et al. Structural and Functional Analysis of HtrA1 and Its Subdomains. *Structure* 20, 1040–1050 (2012).
16. Truebestein, L. et al. Substrate-induced remodeling of the active site regulates human HTRA1 activity. *Nat. Struct. Mol. Biol.* 18, 386–388 (2011).

17. Bejugam, P. R. et al. Allosteric Regulation of Serine Protease HtrA2 through Novel Non-Canonical Substrate Binding Pocket. PLoS One 8, e55416 (2013).
18. Cilenti, L. et al. Omi/HtrA2 protease mediates cisplatin-induced cell death in renal cells. Am. J. Physiol. Physiol. 288, F371–F379 (2005).
19. Salvesen, G. S. & Duckett, C. S. Apoptosis: IAP proteins: blocking the road to death's door. Nat. Rev. Mol. Cell Biol. 3, 401–410 (2002).
20. Ma, X. et al. GRIM-19 associates with the serine protease HtrA2 for promoting cell death. Oncogene 26, 4842–4849 (2007).

Publications in Refereed Journal:

- a. Published: Kummari Raghupathi, Shubhankar Dutta, Lalith K Chaganti, and Kakoli Bose. 2019. “Discerning the Mechanism of Action of HtrA4: A Serine Protease Implicated in the Cell Death Pathway.” The Biochemical Journal 476 (10): 1445–63. <https://doi.org/10.1042/BCJ20190224>.
- b. Accepted: NA
- c. Communicated: NA

Other Publications:

- a. Book/Book Chapter: NA
- b. Conference/Symposium:
 - Horizons in Molecular Biology Symposium 2019, Max Planck Institute for Biophysical Chemistry in Göttingen, Germany, 10th September -13th September 2018
Nature of Participation: **Poster presentation** (Title: **Deciphering the Mode of Regulation and Functional Redundancy of HtrA4 – a Serine Protease Implicated in the Cell Death Pathway**)
 - 42nd Annual Indian Biophysical Society (IBS) titled “Emerging Trends in Biophysics” 2018, IISER Pune, Pune, India, 9th March to 11th March 2018
Nature of Participation: **Poster presentation** (Title: **Biochemical and functional characterization of serine protease HtrA4**)
 - 11th Biophysics Paschim Meeting, IISER Pune, Pune, India, November 2017
Nature of Participation: **Oral presentation** (Title: **Biochemical and functional characterization of serine protease HtrA4**)
 - Advances in Enzymology: Implications in Health, Diseases and Therapeutics (INDO-US), ACTREC, India, January 2017
Nature of Participation: **Poster presentation** (Title: **Biochemical and functional characterization of serine protease HtrA4**)



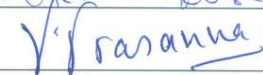


- A conference of new ideas in cancer – Challenging dogmas, Tata Theatre, NCPA, Mumbai, India, February 2016
Nature of Participation: **Poster presentation (Title: Designing allosteric activators of proapoptotic HtrA2 and their implications in cancer therapeutics)**



Signature of Student:

Date: 14-06-19

Doctoral Committee:

S. No.	Name	Designation	Signature	Date
1.	Dr. Sorab Dalal	Chairman		13/6/19
2.	Dr. Kakoli Bose	Guide/ Convener		14/6/19
3.	Dr. P. Venkatraman	Member		13/6/19
4.	Dr. Dibyendu Bhattacharyya	Member		29/05/2019
5.	Dr. Manoj Bhat	Member		28/05/2019

Forwarded Through:



Prof. S.V. Chiplunkar,
Chairperson, Academic &
Training Programme, ACTREC

Prof. Dr. S. V. Chiplunkar)
Chairperson, Academic &
Training Programme, ACTREC



Prof. S. D. Banavali,
Dean (Academics)
T.M.C.

PROF. S. D. BANAVALI, MD
DEAN (ACADEMICS)
TATA MEMORIAL CENTRE
MUMBAI - 400 012.

LIST OF FIGURES

Serial No	Figure No	Figure title	Page No.
1	2.1	Schematic representation of domain organization of HtrA family of proteases	32
2	2.2	Functions of HtrA family	34
3	2.3	Models of allosteric activation of HtrA2 protease	44
4	2.4	Apoptotic pathways	49
5	2.6	HtrA2 mediated apoptotic pathway	54
6	2.7	The anti-tumor mechanisms of GRIM-19	58
7	3.1	The phase diagram of crystallization	103
8	4.1	Multiple sequence alignment (MSA) analysis of HtrA proteins	122
9	4.2	The endogenous level of HtrA4 in various cancer and normal cell lines	124
10	4.3	Schematic representation HtrA4 and various other different subdomains generated for the study	126
11	4.4	Sequence alignment of mature HtrA2 and HtrA4	127
12	4.5	Purification of HtrA4 protein expressed in Rosetta (DE3) pLysS expression system	128
13	4.6	Comparison of secondary and tertiary structural properties of HtrA4 and its variant	129
14	4.7	Fluorescence emission spectra of HtrA4 protein	130
15	4.8	Gel filtration results of HtrA4 and its domains	132
16	4.9	Gel filtration results of HtrA4 in presence and absence of substrate	135
17	4.10	Proteolytic activity of HtrA4 and its variants with β -casein as a substrate	138
18	4.11	Proteolytic assays of HtrA2 and HtrA4 with substrates	140

19	4.12	Generic substrate β -casein cleavage by HtrA4	142
20	4.13	Mechanism of cleavage and the role of PDZ in substrate cleavage.	146
21	4.14	Crystallization of PDZ domain	149
22	4.15	Binding and protease assays of HtrA4 using GST-XIAP as a putative binding partner and substrate	153
23	4.16	<i>In silico</i> modeling of HtrA4 protein	157
24	4.17	Selective binding pocket identification (SBP) and Multiple sequence alignment (MSA) analysis of HtrA proteins	160
25	4.18	Electrostatic potential map of peptide-bound HtrA4 model	164
26	4.19	MDS analysis of HtrA4- β -Casein complex	166
27	4.20	Structural comparison of catalytic triad and oxyanion hole residues.	168
28	4.21	A proposed simplistic model for HtrA4 mechanism of action	175
29	5.1	Cloning and expression standardization of human GRIM-19 protein	180
30	5.2	GRIM-19 protein solubility analysis	181
31	5.3	GST tagged GRIM-19 purification	183
32	5.4	Co-expression and purification with chaperones	185
33	5.5	MBP tagged GRIM-19 purification	187
34	5.6	GRIM-19 protein purification with urea denaturation method	189
35	5.7	Fluorescence Emission scans of unfolded and refolded GRIM-19	190
36	5.8	Quality analysis of the I-TASSER generated GRIM-19 models	192
37	5.9	Ramachandran plot analysis of the GRIM-19 model	193
38	5.10	Interaction analysis of HtrA2 and GRIM-19 docked complex	194
39	5.11	Purification of HtrA2 and GRIM-19 variants	196
40	5.12	Pull-down assay with different HtrA2 variants with various GRIM-19 constructs	198

41	5.13	Proteolytic activity of HtrA2 and its variants with GRIM-19 as a substrate	201
42	5.14	Activity of wild-type HtrA2 in presence and absence of activator	206
43	5.15	Interaction analysis of the top-ranked docked complex	209
44	5.16	Ligplot of the docked complexes	210
45	5.17	Domain specific conformational changes in HtrA2 resulted from the GRIM-19 (HGFMWYT) peptide binding.	212
46	5.18	Interatomic distance analysis resulting structural reorientation of the catalytic triad and oxyanion hole residues	213

LIST OF TABLES

Serial No	Table No	Table Name	Page No
1	2.1	List of HtrA2 interacting partners	55
2	3.1	List of HtrA4 and GRIM-19 primers	76
3	3.2	12% Tris tricine SDS gel preparation	93
4	4.1	Comparison of HtrA4 with other family members	123
5	4.2	Oligomeric properties of different HtrA4 constructs	133
6	4.3	Kinetics of HtrA family proteins	139
7	4.4	Substrate specificity of HtrA family members	144
8	4.5	SiteMap analysis of putative binding sites in HtrA4	162
9	5.1	Table showing list of chaperone plasmids used for the co-expression studies	184
10	5.2	Substrate specificity of HtrA2 using GRIM-19 as a substrate	203
11	5.3	Substrate specificity of HtrA2	204
12	5.4	Enzymatic parameters for HtrA2 in the presence of GRIM-19 full length and CID domain (cell death-inducing domain)	207
13	5.5	SiteMap analysis of the putative binding sites of HtrA2	208
14	5.6	Docking analysis showing the H-bond interactions and docking score	211

CHAPTER 1

INTRODUCTION

CHAPTER 1: INTRODUCTION

In maintaining homeostasis, multicellular organisms tightly couple the rate of cell proliferation and cell death. Disruption of this fine balance due to altered regulation of apoptosis (programmed cell death) leads to several life-threatening diseases such as neurodegenerative disorders and cancer. Cancer, which is characterized by a breakdown in the cellular apoptotic machinery, might occur due to alteration of structural and functional properties of critical proteins in the apoptotic pathway and hence interaction between pro- and anti-apoptotic proteins is closely related to the genesis and progression of this deadly disease. Tremendous progress in apoptotic research has occurred toward understanding the classical caspase-dependent apoptotic pathways with an aim at targeting them for disease intervention. However, the complexity of cancer biology draws interest in identifying alternative mechanisms that can promote cell death. Therefore, characterizing the structural and functional properties of these pro-apoptotic proteins as well as identifying their binding partners will not only delineate their biological functions but will also help understand the apoptotic pathway better and the role of these proteins in cell death and cancer.

Part I: Discerning the mechanism of action of HtrA4 and functional redundancy

High-temperature requirement protease A (HtrA) is a family of oligomeric serine proteases that are conserved from prokaryotes to humans. In humans, four HtrA homologs (HtrA1-4) have been identified [1–3]. These proteins share a common domain architecture that comprise an N-terminal region, serine protease domain (SPD) for enzymatic activity and PDZ domain (postsynaptic density of 95 kDa, disk large, and zonula-occludens 1 domain) for protein-protein interactions. Apart from these common domains, all except HtrA2, harbor a Kazal like domain that acts as an inhibitor for serine protease activity, insulin-like growth factor binding protein domain (IGFBP) and a signal peptide. While, HtrA1, HtrA3, and HtrA4 share very similar domain organizations, the uniqueness of HtrA2 is manifested through the absence of Kazal and IGFBP domains and existence of a distinct N-terminal region, which includes a prominent IAP (inhibitor of apoptosis) binding motif (IBM) and a transmembrane domain [4].

In humans, these proteases are involved in numerous cellular processes ranging from maintenance of mitochondrial homeostasis to cell death. Therefore, deregulation of their normal functions leads to various diseases that include neurodegeneration, neuromuscular disorders, arthritis, age-related macular degeneration, pregnancy-specific pre-eclampsia, and cancer. Among human HtrA homologs, HtrA1 and HtrA2 are well characterized with available high-resolution crystal structures. However, HtrA4 is the least characterized human HtrA protease concerning both structure as well as its functions. It has been found to be up-regulated in pre-eclampsia (PE) and hence has been suggested to be used as a biomarker of PE [5]. Meta-analyses of available microarray data suggested that HtrA4 is up-regulated in glioblastoma multiforme

and breast carcinoma, whereas, down-regulated in metastatic prostate cancer; making it an emerging therapeutic target [6, 7]. Therefore, an intricate dissection of HtrA4 structure with an understanding of its functional reciprocity becomes imperative to harness its properties with desired characteristics.

Part II: To understand the interaction between HtrA2 and its binding partner– GRIM-19

HtrA2 is involved in several critical biological functions such as protein quality control, unfolded protein response (UPR), cell growth, apoptosis, arthritis, cancer and neurodegenerative disorder [8–10] Under normal physiological conditions, it acts as regulator of mitochondrial homeostasis where its protective function switches into proapoptotic behavior in response to stress-inducing agents. HtrA2 mediates apoptosis through classical pathways via caspase activation by displacing XIAP from caspases [11, 12]. There is also evidence that interaction with IAPs is not the only mechanism involved in HtrA2 induced cell death, as the proteolytic activity of HtrA2 is sufficient to promote caspase independent cell death. HtrA2, via its protease activity degrades several cellular substrates such as Pea15 [13], FLIP [14], Hax1 [15]. It also cleaves cytoskeletal proteins such as actin, vimentin, α - and β -tubulin [16]. Moreover, eukaryotic translation Initiation Factor-4 gamma 1 (eIF-4 γ 1) and Elongation Factor-1 alpha (EF-1 α) are also substrates of HtrA2[16]. Despite substantial evidence of involvement of HtrA2 in triggering apoptosis, little is known about its mode of regulation, substrate recognition and specificity. A clear understanding of the molecular mechanism of HtrA2 interaction with its binding partners or substrates will define ways of regulating its functions. Therefore, we performed the comprehensive binding and enzymology studies with tumor suppressor protein GRIM-19. Our interaction studies with GRIM-19 provide first mechanistic insight into the substrate recognition

and specificity of HtrA2. Enzymology studies with GRIM-19 suggest allosteric activation of HtrA2 might be required for activating the resting or inactive protease in the cell to cleave other physiological substrates. These studies will help to delineate a unified model of HtrA2 activation and lead toward designing activators for HtrA2 that could modulate its functions with desired characteristics against diseases associated with it.

AIMS AND OBJECTIVES

AIMS AND OBJECTIVES

In the present study, our goal is to characterize structural and functional properties and dissect the mechanism of these unique serine proteases.

Aim I

Among the four human HtrAs, HtrA4 is the least characterized protein with respect to both structure as well as its functions. Our aim is to decipher the mechanism of action of HtrA4 and its functional redundancy.

Objectives:

1. Structural characterization of HtrA4 and its domains
2. Oligomerization status of HtrA4 and its domains (Oligomerization status in presence of substrate)
3. Enzyme kinetics of HtrA4, role of different domains and effect of temperature on catalytic activity
4. Substrate specificity of HtrA4 and mechanism of substrate cleavage
5. Identification of HtrA4 functional similarity with its family members
6. Identification of its binding pocket and allosteric changes associated with peptide binding

Aim II

To understand the interaction of proapoptotic serine protease HtrA2 with tumor suppressor protein GRIM-19

Objectives:

- 1) Biophysical and structural characterization of GRIM-19
- 2) Identifying whether GRIM-19 is a substrate for HtrA2, and if yes, determining the pattern of cleavage and substrate specificity of HtrA2
- 3) Mapping the minimal binding region of GRIM-19 and HtrA2 that is important for the interaction
- 4) Identifying the minimal region of GRIM-19 important for activating HtrA2 and structural changes associated with binding

CHAPTER – 2

REVIEW OF LITERATURE

CHAPTER 2: REVIEW OF LITERATURE

2.1 HtrA family Proteins

High temperature requirement protein A (HtrA) family proteases are highly conserved oligomeric serine proteases present in prokaryotes as well as eukaryotes and perform diversified functions. In *E. coli* these were initially identified as heat shock-induced envelope-associated serine proteases [17]. Alterations or mutations in these proteases may lead to various diseases in humans like neurodegenerative, neuromuscular disorders, arthritis, age-related macular degeneration, cancer and the pregnancy-specific disease pre-eclampsia [18–22]. Although maintenance of protein quality is major function they also perform various other functions like unfolded protein response, cell growth, homeostasis, apoptosis, molecular chaperones and proteases [23–26]. HtrA proteins belong to family of oligomeric serine proteases which generally characterized by presence of a trypsin-like fold domain, and found to be highly conserved from humans to prokaryotes. There are four human homologues of HtrA have been identified: HtrA1 (PRSS11 or L56), HtrA2/Omi, HtrA3 and HtrA4. In case of mammalian HtrA proteins, in spite of having complexity and variations in their structure and functions, all of them share a basic domain organization which consists of an N-terminal sequence, serine protease domain (SPD) and PDZ domain (Postsynaptic density of 95 kDa, Disk large, and Zonula-occludens 1 domain). The PDZ domain is responsible for protein-protein interactions which bind specifically to the natural interacting partners and substrate in the cell to

regulate various functions. N-terminal region helps in the formation of functional oligomers which are mostly trimeric in nature. In case of prokaryotes e.g. in *Escherichia coli* HtrA (DegP), this trimeric unit may further oligomerize to form higher order oligomers upon substrate binding [27]. In *E. coli*, DegQ, DegP, and Deg S comprise the HtrA family of proteins and they exhibit a high degree of sequence homology in their protease domains [27]. These proteins have dual role: at normal physiological temperatures they act as chaperones and at elevated temperatures (above 30°C) they act as proteases [17, 28].

2.2 Bacterial HtrA proteins and other lower eukaryotic proteins

After the identification of HtrA as an important protein for survival of the cell, different homologues of HtrA were isolated from a variety of species. Many organisms express more than one family member in different cellular compartments. Including microorganisms (bacteria), fungi, plants, and mammals, there are hundreds of different HtrA proteases have been detected in many cell genome databases. For example, there are three HtrAs found in *E.coli* ; two to five in cyanobacteria; sixteen in *Arabidopsis thaliana*; and four in humans [23, 24]. In *E.coli*, DegP, DegQ and DegS proteins show a high degree of sequence homology in SPD protease domains. However, DegP and DegQ have two PDZ domains; DegS contain only one PDZ domain. HtrA proteases share a common architecture (trimeric pyramidal) where each monomer comprises two or three major domains and have similar activation mechanism [29, 30].

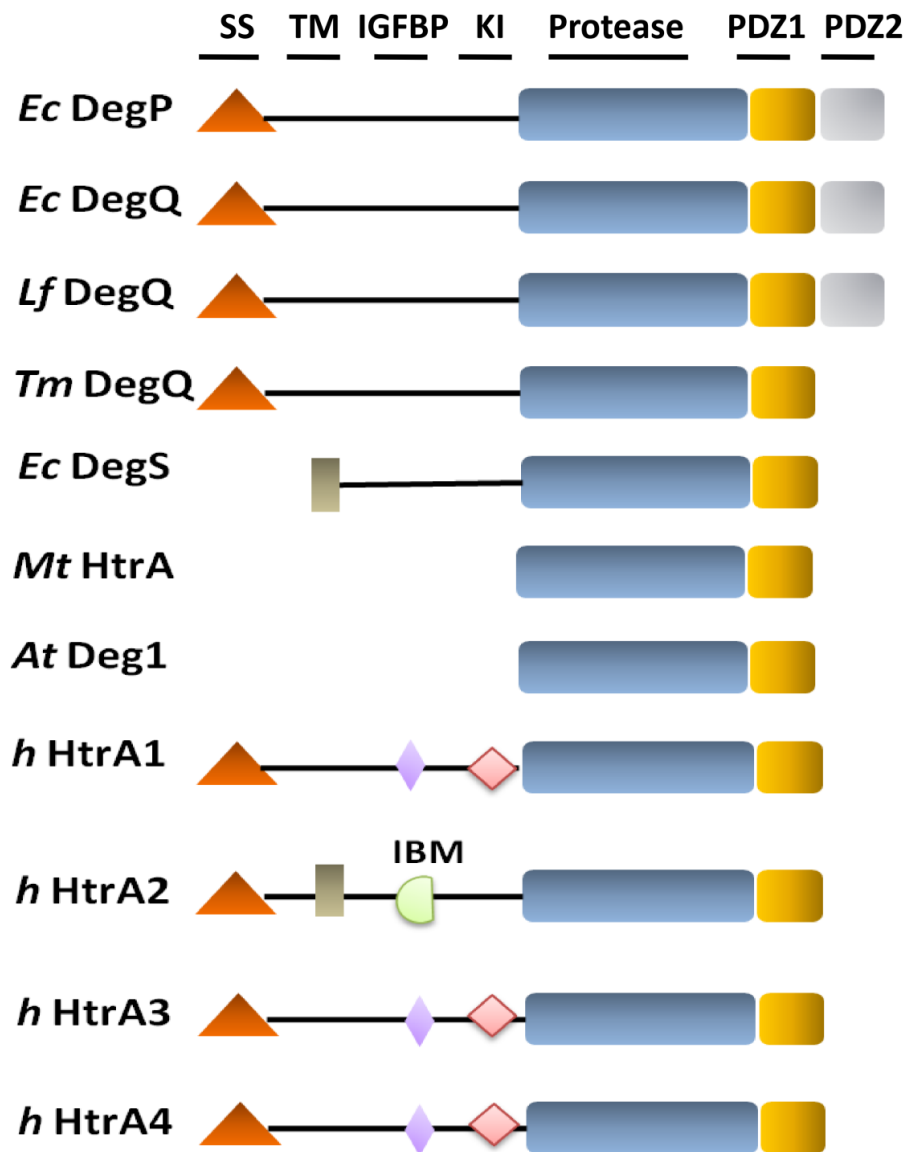


Figure 2.1: Schematic representation of domain organization of HtrA family of proteases. The protease domain is in blue rectangles, PDZ1 and PDZ2 domains are in yellow and gray rectangles respectively, SS (signal sequence) in orange triangles, TM (transmembrane domain) in dark green rectangles, IGFBP (Insulin-like growth factor binding) in purple diamonds, and KI (Kazal protease inhibitor domain) in light red.

2.3 Human HtrAs

In humans, four HtrA homologs (HtrA1, HtrA2, HtrA3 and HtrA4 [23, 31–33]) have been identified. Among these members HtrA1 and HtrA2 have been well studied [34]. Except for HtrA4, structures of other HtrA homologs have been solved. These proteins share a common N-terminal, SPD and PDZ domain which are very well conserved across the family. They also have some additional domains consist of signal peptides and regions identified as insulin-like growth factor binding proteins (IGFBP) and Kazal like domain. HtrA1, HtrA3 and HtrA4 share identical domain organization, while HtrA2 has a marginally different N-terminal domain which includes IBM (IAP binding motif) and transmembrane domain [4]. HtrA3 and HtrA4 proteins are found to be associated with Pre-eclampsia (PE), which is a pregnancy-specific syndrome and it accounts for 15-20% of the pregnancy-associated mortalities [35]. All four homologs of human HtrAs have their respective regulating mechanism to maintain these functions defined by their localization in the body [4].

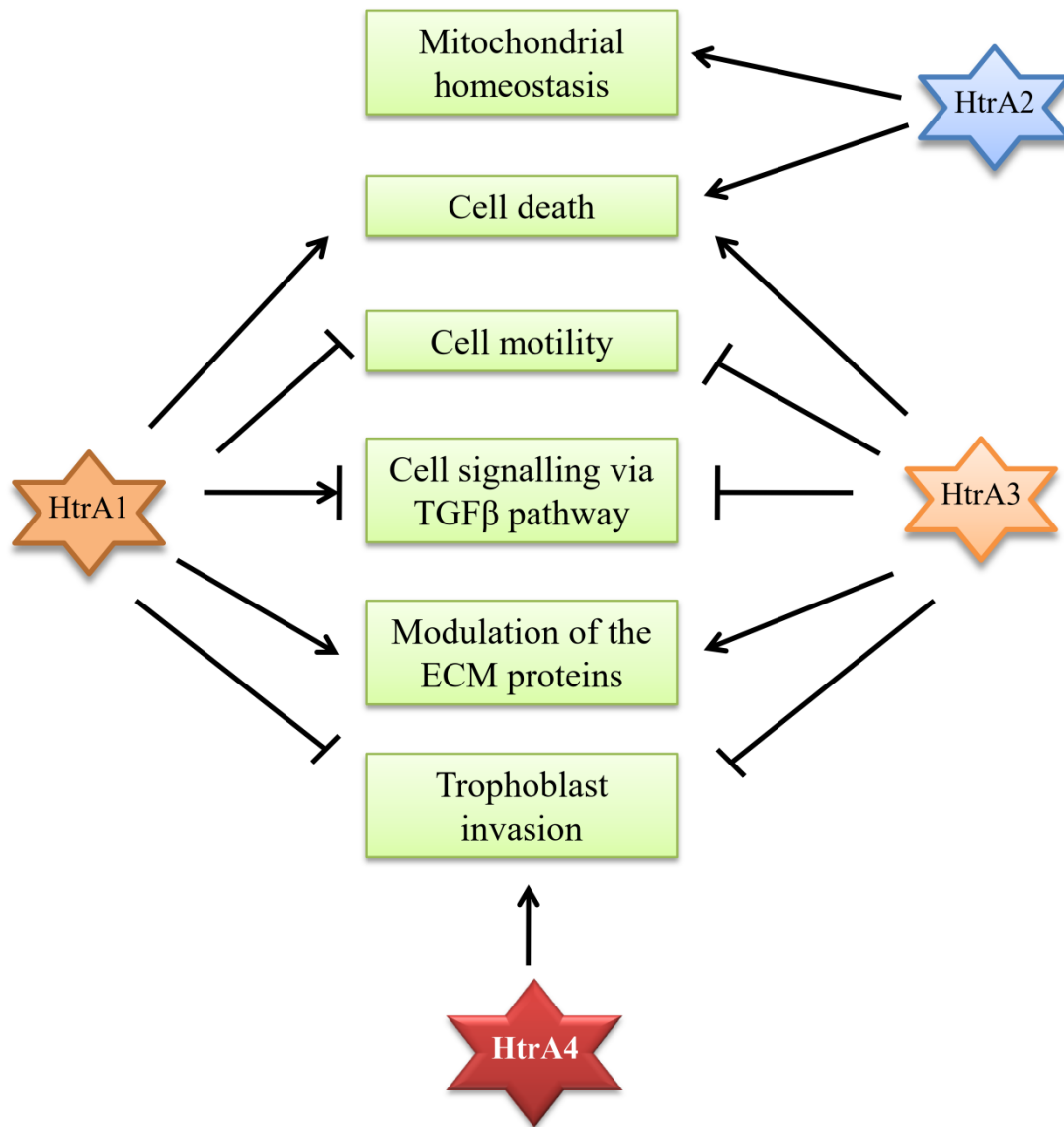


Figure 2.2: Functions of HtrA family proteins: The main functions of HtrAs are regulation and modulation of cell death, TGF- β pathway, mitochondrial homeostasis, ECM proteins, cell motility, trophoblast invasion and bone formation. These processes are interconnected and affect each other. In some cases like regulation of cell death and motility, TGF- β signaling, and in ECM proteins modulation HtrAs may act synergistically. Modified from[36] ,

2.3.1 HtrA1

HtrA1 (PRSS11) is the first human homolog of DegP identified and it has chromosomal locations of 10q26.2 containing 9 exons. It is normally expressed in human adult tissues with an up-regulation during pregnancy showing its function in placental formation and embryogenesis. It regulates biological processes by modulating growth factor systems such as TGF- β family. This ubiquitously expressed protein, plays important roles in cellular physiology and is associated with diseases such as arthritis, cancer, Alzheimer's disease and age-related macular degeneration. Secreted HtrA1 is observed to be involved in the degradation of extra-cellular matrix proteins and its down regulation is seen in melanomas and ovarian cancer [37].

Among HtrA homologues, HtrA1 and HtrA2 are well characterized with available high resolution crystal structures. The human secreted serine protease HtrA1 exhibits endo-proteolytic activity, including autocatalytic cleavage [38]. It has also been reported that neither N-terminal region nor the C-terminal PDZ domain of HtrA1 has involvement in its protease activity. HtrA1 binds, cleaves and activates a variety of targets which are involved in important physiological processes such as maintenance of cell death and cell signaling. The HtrA1 is involved in osteoarthritis, transformed fibroblasts, ovarian cancer, melanoma and various diseases [39, 40]. The expression of HtrA1 can be regulated by the chemotherapeutic drugs [41]. Related with ovarian cancer, the Chien et al. group showed that expression of HtrA1 in primary tumors correlates with a better response to cisplatin based chemotherapy [41]. It was observed that HtrA1 was activated during drug treatment *in vitro* and active HtrA1 increases caspases 3/7 and participated in cytotoxicity [41]. In addition, over expression of HtrA1 inhibits proliferation and tumor growth *in vivo* as well as *in vitro*. These data suggest that HtrA1 might function as tumor

suppression and play a role in guiding apoptosis [41]. These studies highlight the important role of HtrA1 and provide a rationale to target HtrA1 cancer therapy and therapeutics due to its pro-apoptotic, anti growth properties and its regulation by therapeutic drugs [41].

2.3.2 HtrA2

Human HtrA2, also known as Omi, is a well studied member of HtrA family. It has chromosomal location of 2p13.1, and contains 8 exons. It is a mitochondrial serine protease showing extensive homology with bacterial HtrAs (High temperature requirement A) [19]. As in case of bacterial HtrA, HtrA2 also show an increase in proteolytic activity during heat shock or stress. HtrA2 has been found to be involved in both caspase dependent and independent apoptosis. Apart from its pro-apoptotic function, HtrA2 has been involved in neurodegenerative disorders such as Parkinson's and Alzheimer's [6].

HtrA2 being distinctive member of this serine protease family localizes in the mitochondrion where it serves as a protein quality control factor at physiological conditions and is released into the cytosol upon apoptotic stimuli [11]. It regulates apoptosis in both caspase-dependent and caspase-independent manner. The precursor form of HtrA2/Omi protein contains an N-terminal signal peptide that directs localization to the mitochondria. Due to its auto-proteolytic activity, cleavage of the N-terminal 133 residues (containing the TM transmembrane region) exposes an IAP binding motif [11, 42, 43]

2.3.3 HtrA3

In humans, the *HTRA3* gene is located on the chromosome 14p16.1 and the overall intron/exon structure of *HTRA3* is very well conserved in evolution. HtrA 3 is localized in the cytoplasm and it is ubiquitously expressed in both adult and fetal heart, ovary, uterus, placenta and bladder. Alternative splicing produces two isoforms of HtrA3, a long form (50kDa) and a short form (40kDa). Both these forms have serine protease activity, however the short form lacks the PDZ domain. Excessive expression of HtrA3 has been observed during early pregnancy, indicating its importance in the development of embryo and in placenta formation [44]. Because of having high structural similarity with HtrA1, it has also been reported that HtrA3 displays similar functions to HtrA1 [32]. HtrA3 was first identified in developing placenta and found to be associated with pregnancy both in mouse and human. Like other family members, it also has four domains including an IGFB, Kazal, trypsin-like serine protease domain and PDZ domain. The N-terminal domain is not required for protease activity; its deletion resulted in increased proteolytic activity (~3fold) and at higher temperature HtrA3 undergoes auto proteolysis.

2.3.4 HtrA4

HtrA4 is a novel protein from the HtrA family which is the least characterized. The relevant gene has chromosomal location of 8p11.22. It is a nuclear encoded secreted protein almost restricted to the placenta, although a small amount of protein is observed in thyroid or uterus. It has been only studied at the transcript level [33]. The pathophysiological role and cellular functions of HtrA4 has recently started emerging. Meta-Analysis and gene expression profiling of PE

patients' placenta has resulted in association of over-expressed HtrA4 with PE [33, 45]. HtrA4 protein was also detected in the sera of normal pregnant women, where the circulating levels are significantly elevated and high levels of HtrA4 cause endothelial dysfunction [46]. Studies revealed that HtrA4 suppresses cell-cell fusion by interacting with syncytin-1 [47]. HtrA1 and HtrA3 suppress HtrA4-mediated trophoblast invasion by degradation of HtrA4 [47, 48]. High levels of HtrA4 can alter the expression of a range of genes related to inflammation, vasoactivity, angiogenesis, cell adhesion, platelet activation and coagulation [49]. Mice homozygous for the recombinant allele (HtrA4^{-/-}) appeared to be normal. These mice being viable and fertile can be used as a tool to investigate the role of HtrA4 in pathogenesis and development of preeclampsia and coronary heart disease [50].

2.4 Structural assembly, oligomerization and role of domains in human HtrAs

In human HtrAs, structural organization, domains functions and allosteric modulation have important roles in their activity regulation or activation mechanism. Available literature suggest that these HtrA proteins form oligomers which is essential for their functional activity. The N-terminal region helps in the formation of functional oligomers which are mostly trimeric in nature. In case of prokaryotes e.g. in *Escherichia coli* HtrA (DegP), this trimeric unit may further oligomerize to form higher order oligomers upon substrate binding. HtrAs form functional oligomers ranging from trimeric to 24mer [4]. The domain organization of HtrA1 is highly similar to that of HtrA3 and HtrA4, since it consists of a serine protease domain followed by a

PDZ domain. Certain additional domains at N-terminal regions such as signal sequence, insulin-like growth factor binding protein and Kazal type inhibitor motif render specificity to HtrA1 functions [51]. The protease domain of HtrA1 is formed by two β -barrel lobes (β 1– β 6 and β 7– β 12) with helical N-terminal and C-terminal regions. For activity, the catalytic triad including His220, Asp250, and Ser328 (located in a crevice between two barrel lobes) is very important. The importance of PDZ for enzymatic activity was more highlighted as PDZ domain deletion (HtrA1_ Δ PDZ) did not change enzymatic activity, the IGFBP/Kazal tandem is nonessential for catalytic activity and did not influence the equilibrium state. It was observed that the N-terminal tandem, kazal-like motif and PDZ domain has no effect on its enzymatic activity [51].

HtrA2 is a complex trimeric pyramidal serine protease which is expressed as a 49kDa proenzyme that is primarily targeted for its localization on the mitochondrial inner membrane space through its N-terminal transmembrane anchor. A monomeric structure of mature HtrA2 (ranging amino acid residues 134-458) comprises a trimerization motif (a.a. 146-151), a central serine protease domain (a.a. 150-343) and a C-terminal PDZ domain (a.a. 364-445). The mature HtrA2 after cleavage of first 133 amino acids from N terminus, with 7 α helices and 19 β sheets, has a short N-terminus, exposed tetrapeptide IAP binding motif (AVPS), a well defined serine protease and PDZ domains. The short N-terminal region holds the oligomers together and forms a pyramidal architecture through Van der Waals interactions involving three aromatic residues (Y14, F16 and F123) and extensive intermolecular hydrophobic interactions. The PDZ and SPD domains are covalently linked through a flexible interface linker sequences [52]. In SPD domain His-198,

Asp 228, and Ser-306 residues form catalytic triad as a conserved active site [4]. In case of HtrA2, SPD along with N-terminal domain is involved in the formation of a pyramid-shaped functional homotrimer while PDZ regulates its activity.

The modular architecture of the predominant long isoform of HtrA3 is composed of an N-terminal Mac 25 domain (21-128 a.a.), a conserved chymotrypsin like protease domain (175-340 a.a.) and one PDZ domain (359-444 a.a.). As in case of HtrA1, the Mac25 domain contains a signal sequence, insulin like growth factor binding motif and Kazal type inhibitor. Mac25 is required for the localization of protein in the mitochondria and is regulated by the protease function of HtrA3 [32]. The protein sequence of the short HtrA3 isoform is identical to that of the long except for the absence of a C-terminal PDZ domain where it instead has a seven amino acids (APSLAVH), which is encoded by a separate exon and is unique for this isoform. The crystal structure is not available for full length HtrA3 [53]. Studies carried out by Barbara et al. showed that HtrA3, with the PDZ removed and a N-terminal truncation were completely active over a wide temperature range and the absence of PDZ did not affect its proteolytic activity, suggesting that PDZ is dispensable for activity, as in HtrA1. However, HtrA3 forms a monomer in the absence of PDZ suggesting that PDZ influences trimer formation. The role of the C-terminal domain still needs to be understood. Δ N-HtrA3 formed stable trimers while both Δ N-HtrA3- Δ PDZ and Δ N-HtrA3S were monomeric [53]. This suggests that the presence of the PDZ domain, unlike in HtrA1 and HtrA2, influences trimer formation.

2.5 Allostery, activation and cleavage mechanism of HtrAs

Due to their structural complexity, multi-domain proteins require different levels of regulatory mechanisms for efficient execution of cellular functions. One such mechanism is allosteric modulation which often helps a protein to regulate a functional behavior such as for an enzyme to attain an active functional state upon ligand or substrate binding. In allostery, large conformational changes are required for significant rotations of individual domains at microsecond to millisecond timescales. While in some cases, minimum structural changes helps in signal transmission in an energy efficient way to the structurally restricted functional domains [54]. PDZ (postsynaptic density-95/discs large/zonula occludens-1) domains in HtrA family proteins are mainly involved in protein-protein interactions and exhibit structural changes during allosteric changes [55, 56].

Among human HtrA homologues, HtrA1 and HtrA2 activation and cleavage mechanisms are well characterized [36]. The human secreted serine protease HtrA1 exhibits endo-proteolytic activity, including autocatalytic cleavage [57, 58]. The crystal structure in both active and inactive forms of HtrA1 was solved by Erhmann and co-workers to understand its mode of activation and the structural changes and dynamics involved in the process. After binding to a substrate, HtrA1 switches to an active conformation where the catalytic triad is properly positioned for catalysis of the proteolytic reaction [59]. Based upon the substrate unbound structure which represents the resting form of HtrA2, Li et al. developed a model of HtrA2 activation. According to this model, in the basal state, the PDZ domains keep the protease activity of HtrA2 in check. Substrate or ligand binding at YIGV groove induces a huge

conformational change at the PDZ-protease interface which removes the inhibitory effect of PDZ from the active-site. This structural rearrangement leads to significant increase in activity, emphasizing intramolecular PDZ-protease cross talk to be pivotal in HtrA2 activation [60]. Recently our group revisited the model for HtrA2 activation and highlighted the importance of PDZ domain in not only interface dynamics and initial substrate binding but also in intermolecular cross-talk for efficient substrate hydrolysis [61, 62].

In HtrA family proteases substrate binding induces conformational changes which result in formation of active proteases, can be termed as substrate-induced activation. The oligomeric status of HtrA proteases tend to change in presence of substrate for e.g. *E. coli* DegP which is a close ortholog of human HtrAs is converted from 6-mers to the 12- and 24-mers in presence of substrate [63]. Temperature is also known to induce such conformational changes. In 2013, Chaganti et al., with a combination of in silico, enzymology and biophysical studies, demonstrated the complexity of conformational changes and dynamics that regulate HtrA2 functions. Their experimental data suggested that as a function of temperature interface movements occur between SPD and PDZ. In the same year, another group, Zurawa-Janicka et al. recorded the temperature-induced structural changes using different HtrA2 mutants and concluded that upon increase in temperature the HtrA2 structure relaxes, the PDZ-protease interface becomes more exposed to the solvent and significant conformational changes involving both domains (SPD & PDZ) occur at and above 30 °C. Both the groups observed that HtrA2 activity markedly increases with temperature, they have also given a model of HtrA2 activation and provided insights into the mechanism of temperature-induced changes in HtrA2 structure which lead to increased activity above 30 °C[61, 64].

Various literature reports highlighted different models of substrate cleavage by HtrA family proteases. In a hold-and-bite model, C-terminus of substrates is bound by the PDZ domain, and this facilitates the cleavage of an upstream sequence at a distant active site [65, 66]. In the hold-bite-and-rebind model, peptide binding sites of the PDZ and catalytic domains exhibit strikingly similar substrate specificities; both sites can anchor the substrate or ligand. After cleavage by protease domain, PDZ domain captures released peptide fragments from the proteolytic sites via their newly generated C-termini and prepares them for the next degradative cycle. This process generates multiple shorter fragments. In this model PDZ acts as an allosteric switch, upon binding to substrates, it propagates the signal to the protease domain through neighboring regulatory loops [67–70].

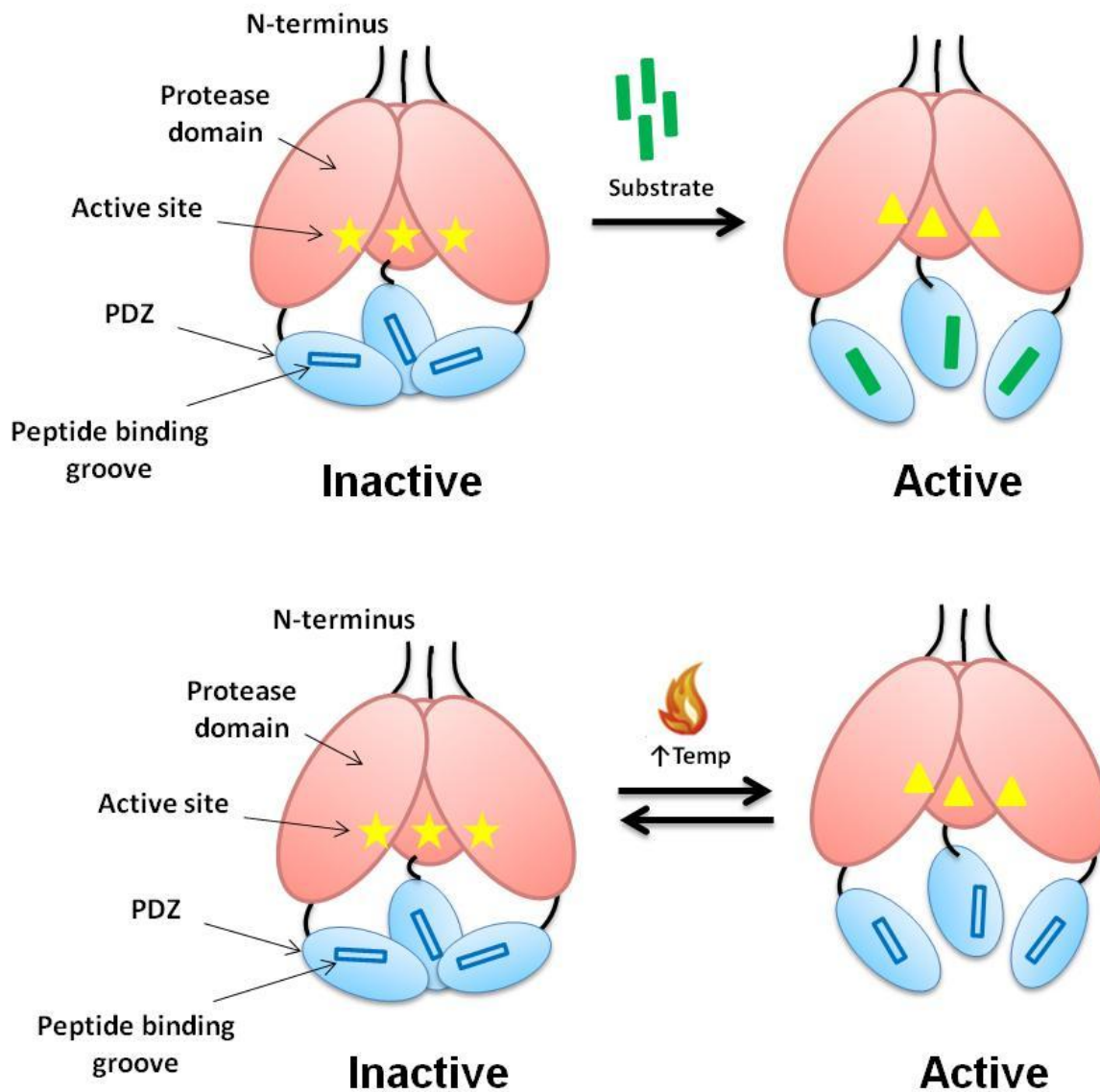


Figure 2.3: allosteric activation models for HtrA2 protease: According to the classical model, a conformational changes after binding of an allosteric peptide to the peptide binding groove of PDZ domain can expose the catalytic site for a substrate, an increase in temperature has similar effects on the HtrA2 structure which can also displace the PDZ domain and allow access to the catalytic site.

2.6 HtrA4 overview

Among the four human HtrA family members, HtrA4 is the least characterized protein in terms of structure and functions and shown to be up-regulated in PE, altered in many cancers like glioblastoma, breast carcinoma, pancreatic and prostate cancers [46, 71]. Recent reports suggested that it can be bio-marker of PE [33]. HtrA3 and HtrA4 proteins are found to be associated with pre-eclampsia (PE), which is a pregnancy-specific syndrome and it accounts for 15-20% of the pregnancy-associated mortalities [35]. PE is not a simple complication of pregnancy, but rather a syndrome involving multiple organ failure. Precise underlying mechanisms have remained elusive [72]. The pathophysiological role and cellular functions of HtrA4 has recently started emerging. Meta-Analysis and gene expression profiling of PE patients' placentae have resulted in identification of over expressed HtrA4 [73–75]. HtrA4 protein was also detected in the sera of normal pregnant women, the circulating levels were significantly elevated and high levels of HtrA4 cause endothelial dysfunction [33, 45]. Studies revealed that HtrA4 interacts with syncytin-1 and suppresses cell-cell fusion [47]. HtrA1 and HtrA3 suppress HtrA4-mediated trophoblast invasion by degradation of HtrA4 [47]. Mice homozygous for the HtrA4^{-/-} allele were appeared to be normal and fertile. These mice can be used as tool for study of HtrA4 role in development of coronary heart disease, and PE [50].

Certain physiological functions of HtrA4 are known which are as follows:

HtrA4 is involved in Human Placental development- The expression of HtrA4 is relatively high as pregnancy is established especially during post implantation and placentation. Along with GCM1 transcription factor it helps in the development of placenta. Down regulation of HtrA4 is associated with hypoxia and other pregnancy complications which indicate its importance in pregnancy [33].

HtrA4 suppresses the syncytin-1 fusogenic activity – Glial cells missing 1 (GCM1) is a transcription factor critical for placental development. GCM1 regulates the expression of syncytin-1 and -2 fusogenic proteins for syncytiotrophoblast differentiation and placental growth factor (PGF) for placental vasculogenesis. HtrA4 binds to syncytin-1, decreases the surface level of syncytin-1 and thereby suppresses syncytin-1-mediated cell-cell fusion [47].

HtrA4 promotes trophoblast invasion – A complicated process of trophoblast invasion into maternal uterine tissue involves multiple intrinsic and extrinsic factors like GCM1. This protein can trans activate serine protease HtrA4 and regulate invasion of placental cells. Thus, HtrA4 might cleave the extracellular matrix (ECM) fibronectin for placental cell invasion [47].

HtrA4 and pre-eclampsia

Pre-eclampsia (PE) is a pregnancy-specific syndrome that accounts for 15-20% of pregnancy-associated mortalities. It is one of the commonest and most serious pregnancy-related disorder which is a leading cause for maternal and prenatal morbidity [35]. The clinical

manifestation of pre-eclampsia suggest that the disorder can manifest as a maternal syndrome causing hypertension, proteinuria and multiple organ failure or as a prenatal syndrome causing fetal growth restriction, reduced amniotic fluid and abnormal oxygenation. The placenta plays a vital role in the etiology of this disorder because its removal normally alleviates the symptoms. According to the degree of placental involvement, PE can be classified as early onset and late onset [45]. Early onset is believed to be of primarily placental origin and it is often associated with severe disease and requiring premature delivery. On the other hand, late onset PE is associated with less placental abnormalities and occurs when maternal system fails to adapt to pregnancy. Early diagnosis of pre-eclampsia would be favorable to provide optimal care for these women and their fetuses. A number of promising candidate biomarkers for the early detection of preeclampsia is currently under investigation. Literature suggests that HtrA4 can be used as a potential biomarker for diagnosis of pre-eclampsia so, it is necessary to understand the different biochemical and biophysical characteristics of HtrA4. Therefore, an intricate dissection of HtrA4 structure with understanding of its functional reciprocity becomes imperative to harness its properties with desired characteristics.

2.7 HtrA2 overview

The HtrA family of serine proteases appears to be involved in the biological mechanisms of apoptosis and cancer. The primary function of HtrA2 is mitochondrial homeostasis maintenance. Under normal physiological conditions, it promotes cell survival and acts as a quality control factor. In response to apoptotic stimuli such as cellular stresses, UV exposure, oxidative stress, and death receptor activation, it transforms from being protective to a pro-apoptotic.

As in case of bacterial HtrA, HtrA2 also shows an increase in proteolytic activity during heat shock or stress. Like Smac/Diablo, human homologs of serine proteases are also involved in the inactivation of IAP's. HtrA2/ Omi is a well characterized human serine protease able to bind and neutralize IAP, and as a result induces apoptosis in human cells both in caspase-independent manner through its protease activity and in a caspase dependent manner. The following section highlights both these signaling mechanisms in detail.

Apoptosis

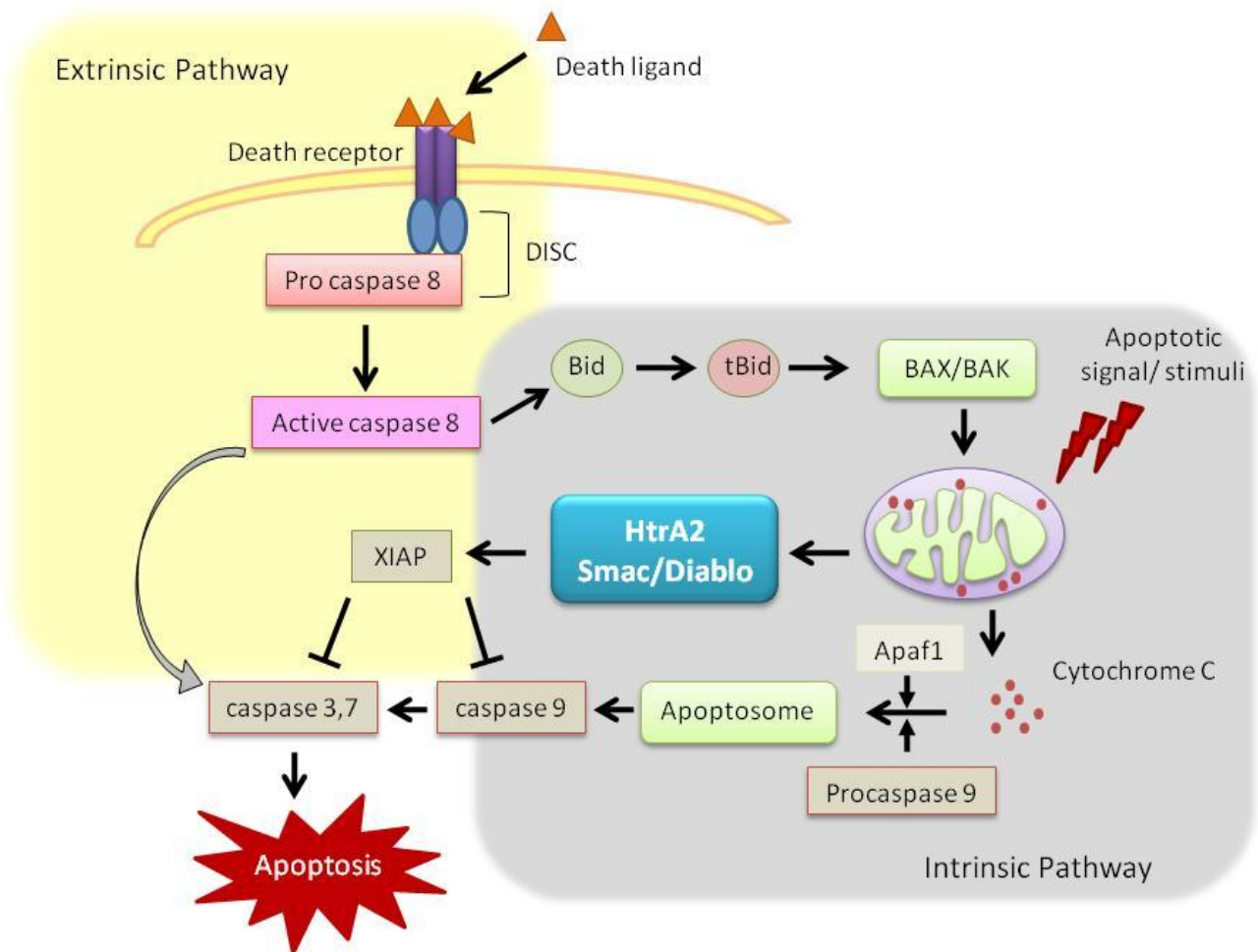


Figure 2.4: Apoptotic pathways. A) The extrinsic apoptotic pathway is initiated by the ligation of death receptors with their ligands, leading to the recruitment of adaptor molecules such as FAS-associated death domain protein (FADD) and then caspase 8. This results in the dimerization and activation of caspase 8, which can then directly cleave and activate caspase 3 and caspase 7, leading to apoptosis. B) Intrinsic apoptotic stimuli, such as DNA damage, activate B cell lymphoma 2 (BCL-2) homology 3 (BH3)-only proteins leading to BCL-2-associated X protein (BAX) and BCL-2 antagonist or killer (BAK) activation and mitochondrial outer membrane permeabilization (MOMP). Anti-apoptotic BCL-2 proteins prevent MOMP by

binding BH3-only proteins and activated BAX or BAK. Following MOMP, the release of various proteins from the mitochondrial intermembrane space (IMS) promotes caspase activation and apoptosis. Cytochrome c binds apoptotic protease-activating factor 1 (APAF1), inducing its oligomerization and thereby forming a structure termed as apoptosome that recruits and activates an initiator caspase, caspase 9. Caspase 9 cleaves and activates executioner caspases, caspase 3 and caspase 7, leading to apoptosis. Mitochondrial release of second mitochondria-derived activator of caspase Smac/Diablo and HtrA2 neutralizes the caspase inhibitory function of X-linked inhibitor of apoptosis protein (XIAP). C) Crosstalk between the extrinsic and intrinsic pathways occurs through caspase 8 cleavage and activation of the BH3-interacting domain death agonist (BID), the product of which (truncated BID; tBID) interacts with BAX and BAX and induces MOMP.

Apoptosis is a cellular process wherein death of the cell happens in a programmed way which is usually seen in multicellular organisms. The process of apoptosis is very much essential, since any disruption to this process can lead to diseases. Once it has begun, apoptosis cannot be stopped and so it is a tightly regulated process. Tumor maintenance, progression and resistance to chemotherapy are associated with decreased expression of pro-apoptotic protein and over-expression of anti-apoptotic protein. Future strategies to exploit our insights into tumor resistance mechanisms are to down regulate anti-apoptotic molecules and increase the regulation action of pro-apoptotic proteins. One such protein is IAP which belongs to anti-apoptotic family and helps to halt the apoptosis process. The apoptotic signaling pathway can be restored by targeting IAPs which have the potential to cure cancer. HtrA2 regulates apoptosis in both caspase-dependent and caspase-independent manner [76].

Caspase-dependent pathway

Although caspases are recognized as the main players in the initiation and execution of apoptosis, several reports have substantiated the role of HtrA2 in the apoptotic cascade. It can

induce cell death in both caspase-independent and caspase-dependent manner. It accomplishes the former by means of neutralizing anti-apoptotic proteins such as Inhibitor of Apoptosis Proteins (IAPs) and the latter by serine protease activity. In cytoplasm, HtrA2 interacts with XIAP through the N-terminal tetrapeptide and relieves the inhibition of IAPs on active caspases thus propagating caspase cascade and hence cell death. The precursor form of HtrA2/Omi protein contains a N-terminal signal peptide that directs localization to the mitochondria. Due to its auto-proteolytic activity, cleavage of the N-terminal 133 residues (containing the transmembrane segment) exposes an IAP binding motif which results in mature HtrA2 [11, 42, 43]. IAPs consists of XIAP, cIAP1, cIAP2, surviving, BIRC1. The IAPs inhibit apoptosis by binding to caspases like processed caspase 9 and caspase 3 [77–80]. To regulate anti-apoptotic activity of these IAPs, HtrA2 bind to the BIR domains of IAPs via a N-terminal conserved tetrapeptide AVPS motif or IAP-binding motif (IBM) [81].

Caspase-independent pathway

In caspase-independent pathway, and cancer promoting pathway HtrA2 can cleave substrates mostly anti apoptotic proteins such as Hax-1, peal5, actin, tubulin- α/β and vimentin and trigger cell death [19, 82]. In the cytosol HtrA2 digests ped/peal5 and the proteolytically modified ped/peal5 fails to block apoptotic signal initiated by FasL or TNF- α . Translocation of HtrA2 into the nucleus results in digestion of p73, which facilitates expression of Bax. Bax contributes to the release of proapoptotic proteins from the mitochondria. Additionally, at very early stages of cell death HtrA2 induces apoptosis by degradation of the mitochondrial protein Hax-1. HtrA2 also may contribute to cell death by degradation of several proteins such as components of translation machinery (eIF-4G1, EF-1 a) and cytoskeletal elements (tubulin, actin, vimentin) [71]

Following are some of the well characterized substrates of HtrA2:

IAP

Inhibitor of apoptosis proteins (IAPs) originally found in baculoviruses is conserved from insects to humans [83]. The structures of XIAP, cIAP1 and cIAP2 are characterized by three tandem repeats of the Baculoviral IAP repeat (BIR) domain at its N-terminus and a RING finger domain towards its C-terminus. The BIR domains of IAP are responsible for inhibiting caspase activity. Several studies indicated that HtrA2 mediated caspase independent apoptosis is mainly elicited due to proteolytic cleavage of IAPs [84].

Ped/Pea15

The DED domain containing anti-apoptotic protein Ped/Pea-15 is a substrate of recombinant HtrA2 and confirmed with *in vitro* experiments [13]. The presence of HtrA2 inhibitor Ucf-101 prevented Ped/Pea-15 degradation in 293T and HeLa cells (UV-irradiated condition). Cellular Ped/ Pea-15 levels modulate the ability of HtrA2 to relieve XIAP-mediated inhibition of caspases which suggests, in part, that the caspase independent cell death by HtrA2 is linked to the degradation of this anti-apoptotic molecule [13].

FLIP

Like Pea-15/PED, cytosolic HtrA2 also interacts with the DED domain of cellular Fas-associated death domain like interleukin-1 β -converting enzyme-inhibitory protein (cFLIP) and activate apoptosis by promoting degradation of the substrate FLIP. It was also found that HtrA2 inhibitor Ucf-101 enhanced cFLIP expression in myocardial ischemia/reperfusion induced injury [14, 85].

Others

Besides these targets, recently PAG 1 (Phosphoprotein associated with glycosphingolipid-enriched microdomains 1), a potential candidate to act as an apoptotic factor through protein – protein interaction has been found to interact with HtrA2. The C-terminal region of PAG specifically interacts with the PDZ domain of HtrA2, which causes an increase of the protease activity [86]. Suzuki et al. suggested that HtrA2 indirectly regulates the translocation of Bax by cleaving Bmf, an endogenous inhibitor of Bax normally sequestered within the actin cytoskeleton-based myosin V motor complex [8]. Moreover, upon induction of apoptosis, HtrA2 is translocated to the nucleus where it cleaves p73. Proteolytically modified p73 thereby stimulates transcription of the BAX gene, whose protein product exhibits proapoptotic function [87]. Furthermore, caspase-independent proapoptotic property is manifested by its ability to cleave important cytoskeletal proteins such as actin, α -tubulin, and vimentin culminating into cell destruction [19].

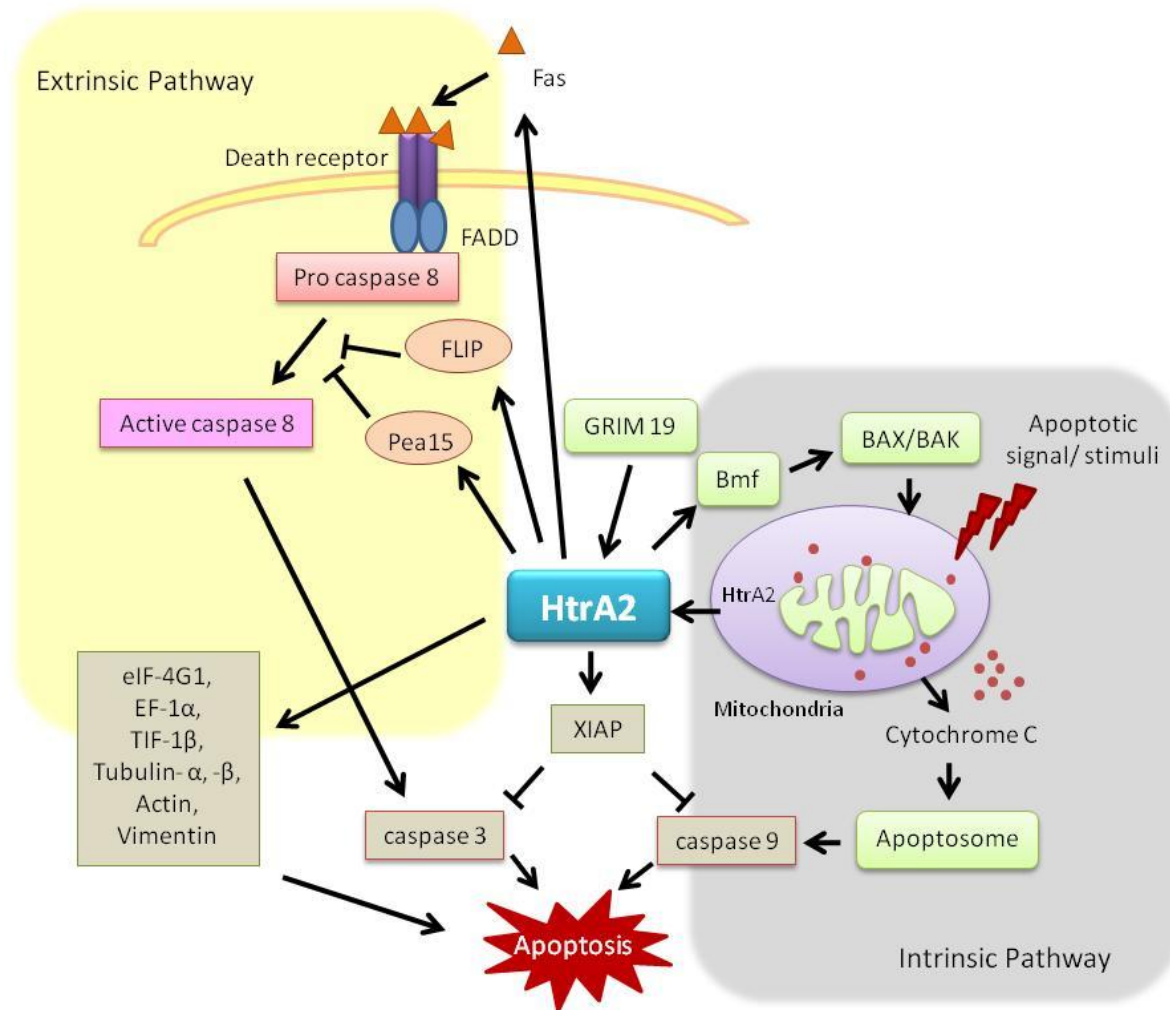


Figure 2.6. HtrA2 mediated cell death pathway. A) After receiving apoptotic signal, mature HtrA2 is released from the mitochondrial intermembrane space into the cytosol. HtrA2 interacts with the anti-apoptotic protein, XIAP thus relieving its inhibitory action on caspases, thereby facilitating caspase-dependent apoptosis. Homotrimeric HtrA2 interacts with Fas with its PDZ domain and initiates death-receptor pathway of apoptosis. It also induces caspase-independent cell death by binding and cleaving anti-apoptotic proteins FLIP, Pea15 and HAX1. GRIM-19 modulates HtrA2 protease activity. B) HtrA2 promotes apoptosis by proteolytic activation of pro-apoptotic p73 and WT1 (Wilms tumorsuppressor1) proteins. The proteolytically degraded p73 and WT1 result in elevated expression of BAX, c-myc and JunB. HtrA2 regulates the translocation of BAX into mitochondria by cleaving Bmf. It also cleaves many other cytoskeleton proteins like tubulin, actin, and vimentin in a caspase-independent manner leading to cell death.

Table 2.1: List of HtrA2 interacting partners

Interacing proteins	Functions	
XIAP [80], cIAP1 & cIAP2 [84], Apollon/BRUCE [88]	Inhibitor of apoptosis proteins	Anti-Apoptotic proteins
Ped/pea15 [13]	Antiapoptotic function, Cytoplasmic protein	
Hax-1 [15]	Antiapoptotic function, mitochondrial protein	
APP, APLP1& APLP2 [89]	Precursors of β -amyloid senile plaques	Amyloid proteins
HADH2 [90]	β -amyloid interaction protein	
Several kinases [91, 92] and phosphatases [93]	Phosphorylation and dephosphorylation	
TIF-1 β [16], eIF-4G1 [94], EF-1 α [16]	Transcription & translation factors	

P73 α [87]	Tumor suppressor, members of the p53 family	
NDUFV1 [95], Presenilin-1 [96]	Negative regulation of neuron apoptotic process	Negative regulators of apoptosis
PARL [97]	Negative regulation of intrinsic apoptotic signalling pathway	
GRIM19 [98]	Cell death- regulatory protein	

2.8 GRIM-19 Overview

GRIM-19 (Gene-associated with retinoid-IFN-induced mortality 19) gene is known to be regulated by cytokines-like interferons and retinoic acid [99, 100]. It is expressed ubiquitously in various human tissues and at a high level in the heart and skeletal muscle and to a lesser extent in liver, kidney, and brain. GRIM-19 has its localization in cytoplasm where it interacts with NOD2 and regulates antibacterial responses while in nucleus it regulates the genetic level of STAT-3 [101]. GRIM-19 is an essential subunit of the mitochondrial respiratory chain (MRC) complex I or mitochondrial nicotinamide adenine dinucleotide phosphate (NADPH): ubiquinone oxidoreductase complex I [102, 103]. GRIM19 comprises four domains including a non-cytoplasmic domain (from 1 to 29 amino acids), a transmembrane helix (from 29 to 51 amino acids), a coil region (from 74 to 95 amino acids) and a cell-death inducing domain (from 102-

144 amino acids). The prediction of domains was analyzed from InterPro family and domain database [104]. The residues from 20 to 60 in GRIM-19 are identified as mitochondrial targeting sequence and a motif in the N-terminal region of GRIM-19 is necessary for its function as a tumor suppressor. The motif is formed of 4 amino acids viz. Glutamic acid, Aspartic acid, Methionine and Proline (QDMP) which has structural similarity with some viral RNA proteins. Interferons (IFN) a family of cytokines along with retinoic acid (RA) is shown to enhance the pro-apoptotic interactions between HtrA2 and GRIM-19. However, the viral oncoprotein (vIRF1) interrupts this pro-apoptotic interaction to prevent cell death induced by GRIM-19 [105].

Functions of GRIM-19 and alterations in cancer

Several studies strongly indicate that GRIM-19 functions as non-canonical tumor suppressor by suppressing various oncoproteins, loss of GRIM-19 or its deregulation is directly involved in cancer development [106–109]. GRIM-19 inhibits cell motility, metastasis and cell proliferation by suppressing the expression of several responsible genes. With the help of proteomic analysis, it was discovered that GRIM-19 also interacts with CDKN2A (p16^{Ink4a}) which is an inhibitor of cell cycle and deletion of the gene causes embryonic lethality [109].

GRIM-19 was found to inhibit the stimulatory activity of STAT-3 [110]. Signal transducer and activator of transcription 3 (STAT3) has oncogenic role in carcinogenesis and inflammation-associated diseases [110]. It has been identified as a therapeutic target for human gastric cancer (GC) as aberration of this gene has been found in most of the cases. GRIM-19 suppresses the transcriptional activation of STAT3 and affects its downstream targets [109]. Accelerated GC cell growth was observed after knocking down GRIM-19 which resulted in activation of aberrant

STAT3 [111]. Yi Huang et. al. also highlighted the possibilities of mitochondrial GRIM-19 as prognostic biomarker and therapeutic target for STAT3 dependent gastric cancer [111].

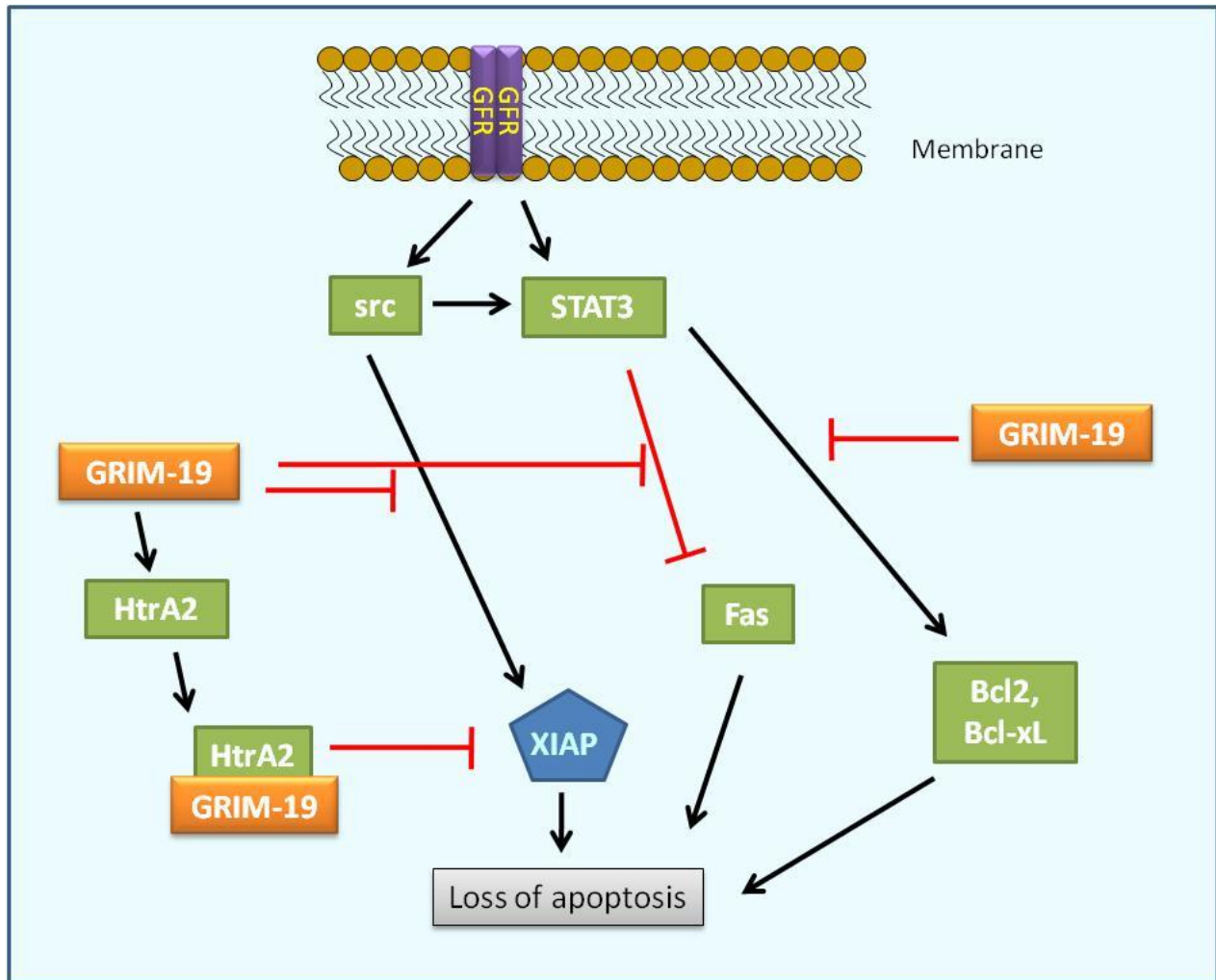


Figure 2.7: Anti-tumor mechanisms of GRIM-19. To promote pro-apoptotic gene expression and apoptosis induction, GRIM-19 targets STAT3 and Src. By associating with HtrA2, it adds to the proteolytic cleavage of XIAP and thus promotes caspase activity. GRIM-19 inhibits Src-induced tyrosyl phosphorylation of adherence and prevents the metastatic behavior of tumor cells, independent of STAT3 [107].

Physiological relevance of HtrA2 and GRIM-19 Interaction

GRIM-19 was identified as an interacting partner of HtrA2 using yeast two hybrid (Y2H) system and subsequently validated through Immunofluorescence studies [112]. The interaction further enhanced by Interferon (IFN)/Retinoic acid (RA) to inflate the cell death [112]. The mitochondrial localization signal (MLS) of HtrA2 is not essential for this interaction. The percent cell death was high in the cells where GRIM-19 and HtrA2 overexpressed simultaneously. Reduction in cell death was observed when they were overexpressed individually, indicating the mutual dependency of both proteins for induction of apoptosis [112].

CHAPTER – 3

MATERIALS AND METHODS

CHAPTER 3: MATERIALS AND METHODS

3.1 MATERIALS

3.1.1 Bacterial Strains

Different *E. coli* competent cells were used as cloning (*E.coli* DH5 α) and expression (BL21-DE3, BL21-pLysS and Rosetta-DE3) hosts.

Host/ Strain	Origin	Antibiotic resistance	Features
<i>E. coli</i> DH5 α (Cloning host)	New England Biolabs (NEB), Ipswich, USA	No resistance	
<i>E. coli</i> BL21 (DE3) (Expression host)	NEB	No resistance	High level expression. Contains T7 polymerase inducible by addition of IPTG
<i>E. coli</i> BL21 (DE3) pLysS (Expression host)	NEB	Chloramphenicol	Reduction of basal level expression

Rosetta (DE3) pLysS	Novagen	Chloramphenicol	It carries tRNA genes decoding seven rare codons and alleviates codon bias for expressing heterologous proteins
C41(DE3)	Novagen	Chloramphenicol	Effective for toxic and membrane proteins expression. The strain was derived from BL21 (DE3) and has one mutation for cell death prevention associated with toxic proteins.
Lemo21 (DE3)	Novagen	Chloramphenicol	It has some features of BL21 (DE3) with variation of natural inhibitor of T7 RNA polymerase, lysozyme (LysY) level (modulated by adding L-rhamnose) which allow tuneable expression of difficult proteins.

3.1.2 Plasmids used for cloning

Plasmid / Vector	Tag	Source
pET 20b (+)	C- terminal His6 tag	Addgene (Cambridge, MA, USA)
pMAL c5E-TEV	N-terminal MBP tag (Maltose binding protein) with TEV protease site	NEB
pGEX4T	N-terminal GST tag	GEHealthcare

3.1.3 Resins used for protein purification

Resin	Tag	Source
Ni-IDA	His6 tag	Biotex, Houston, USA
Amylose	MBP tag	NEB
Superdex 200	For gel filtration	GE healthcare, Healthcare, Bjorkgatan, Uppsala, Sweden
Glutathione	GST tag	NEB

3.1.4 Kits used

Kit	Purpose	Source
Plasmid miniprep kit	Plasmid isolation	Sigma chemicals, St. Louis, MO
Gel extraction kit	DNA extraction from agarose gel	Sigma
pJET 2.1 blunt end cloning kit	Blunt end cloning	Fermentas, Waltham, Massachusetts, USA
Quick change site directed mutagenesis kit	Mutagenesis	Stratagene, Cedar Creek, TX, USA

3.1.5 Specialized instruments

Instrument	Purpose	Source
Jasco J815 CD spectrophotometer	Secondary and tertiary structure of proteins	JASCO, Easton, MD, USA
Fluorolog-3 spectrofluorimeter	Fluorescence emission studies, enzyme kinetics	HORIBA scientific, Edison, NJ, USA
Mithras multiwell plate reader	Enzyme kinetics	Berthold technologies, Wildbad, Germany
AKTA purifier	Gel filtration	GE Healthcare, Buckinghamshire, United Kingdom

3.1.6 Buffers and Reagents

3.1.6.1 Antibiotics

a) Ampicillin sodium salt (Sigma A-9518)

Stock concentration: 100 mg/ml (Filter sterilized using 0.22 µm membrane), dissolved in deionised water and stored at -20°C.

Working concentration: 100µg/ml in LB media, stored at 4°C.

b) Chloramphenicol (MP Biomedicals)

Stock concentration: 34 mg/ml (Filter sterilized using 0.22µm membrane), dissolved in deionised water and stored at -20°C.

Working concentration: 34 µg/ml in LB media, stored at 4°C.

c) Kanamycin sulfate (Sigma K4378)

Stock concentration: A solution of 50 mg/ml was made in deionised water (filtered through a 0.22 µm filter).

Working concentration: 34µg/ml kanamycin was used in LB media.

3.1.6.2 Bacterial culture media

a) 2% Luria-Bertani (LB) medium (for 1 L)

20 g of LB powder (Himedia, Mumbai India) was dissolved in 1 L (final volume) of Milli Q (MQ) water and sterilized by autoclaving at 15 lbs for 20 min.

b) 2% LB- Agar Plates (for 1 L)

20 g of LB agar powder (Himedia) was dissolved in 1 L of MQ water and autoclaved. It was cooled to about 50 °C and 1 ml of respective antibiotic was added from stock. The media was poured into petri dishes (~25 ml/100 mm plate) and stored at 4 °C (dry place).

3.1.6.3 For cloning and site directed mutagenesis

a) Polymerase Chain Reaction (PCR)

25mM MgCl₂, dNTPs mix (2mM), 10X Pfu Turbo buffer from Stratagene, High fidelity DNA polymerase – Pfu Turbo from Chem-agilent

Primers

PCR primers were commercially synthesized from Sigma Genosys as a lyophilized pellet. The primer was centrifuged at 10,000 rpm for 1 min and then reconstituted in autoclaved deionised water to obtain final concentration of 1000 ng/ul. A working dilution of 125 ng/ul was prepared for further experiments.

b) Restriction Digestion and Ligation

Fast Digest DpnI, BamHI, EcoRI, NdeI, XhoI enzymes along with 10X fast digest buffer were obtained from Fermentas and T4 DNA ligase, 10X ligase buffer from NEB.

c) 0.5 M EDTA, pH 8 (for 1 L)

With 148 g of EDTA, ~30-40 g of NaOH pellets were added, pH was adjusted to 8 and volume was made to 1 L. Adjustment of pH using NaOH is essential for its solubility.

d) Tris-EDTA (TE) Buffer (for 50 ml)

Tris 60.66 mg (10 mM)

EDTA 14.62 mg (1 mM)

pH was adjusted to 7.5 with 10 N NaOH and autoclaved.

e) Tris Acetate EDTA (TAE) running buffer for agarose gel electrophoresis (for 1 L)

Stock concentration: 50X TAE (2 M Trisacetate, 50 mM EDTA, pH 8)

Working concentration: 1X TAE (0.04 M Trisacetate, 1 mM EDTA, pH 8)

Tris base 242 gm

Glacial acetic acid 57.1 ml

0.5 M EDTA (pH 8.0) 100 ml

f) 6X Gel Loading Buffer for DNA (for 100 ml)

(0.25% bromophenol blue, 0.25% Xylene cynol, 30% glycerol)

Xylene Cyanol FF 0.25 g (migrates at 4160 bp with TAE)

Bromophenol blue 0.25 g (migrates at 370 bp with TAE)

Glycerol 30 ml

Autoclaved Milli Q 70 ml

g) Ethidium Bromide (EtBr) (Sigma E-8751)

Stock concentration: 10 mg/ml (20000X) in deionised water

Working concentration: 0.5 µg/ml

3.1.6.4 Buffers for protein expression and purification

a) 1M Isopropyl-β-D-thiogalactopyranoside (IPTG) (for 5 ml)

IPTG (sigma-I5502) 1.19 g

Autoclaved Milli Q water 5 ml

Filter sterilized (0.2µm) and stored at -20°C.

b) Phosphate buffer, pH 8

Stock concentration: 10X (200 mM NaH₂PO₄/Na₂HPO₄, 1000 mM NaCl, pH 8)

Working concentration: 1X (20 mM NaH₂PO₄/Na₂HPO₄, 100 mM NaCl, pH 8)

Monobasic or monosodium phosphate (NaH₂PO₄) 59.99 g for 500 ml (1M)

Dibasic or disodium phosphate (Na_2HPO_4)	0.98 g for 500 ml (1M)
NaCl	35.6 g for 1L (1M)

To 200 ml of 1M dibasic solution, 1M monobasic solution was added and pH was adjusted to 8. Later 1M NaCl was added, volume was made to 1L using Milli Q. Buffer was filtered using 0.2 μm filter and autoclaved.

Ni -IDA Column Purification buffers

a) Lysis buffer (for 1 L)

(20 mM $\text{NaH}_2\text{PO}_4/\text{Na}_2\text{HPO}_4$, 100 mM NaCl, pH 8, 0.1% triton X 100)

10X Phosphate buffer (pH 8)	10 ml (1X)
1M imidazole	10 ml (10 mM, reduces non-specific binding of proteins)
TritonX-100	10 ml (0.1%)
10X Protease inhibitor	1X
BME (14.3 M)	0.34 ml (5 mM)

b) Ni-IDA Binding/Washing Buffer (for 1 L)

(20 mM $\text{NaH}_2\text{PO}_4/\text{Na}_2\text{HPO}_4$, 100 mM NaCl, 10 mM imidazole, pH 8)

10X stock Phosphate buffer (pH 8)	10 ml (1X)
1M Imidazole stock	10 ml (10 mM, reduces non-specific binding of proteins)
14.3M BME stock	0.14 ml (2 mM)

pH was adjusted to 8 , filtered (0.22 μm) and autoclaved

c) Ni-IDA Elution Buffer (for 100ml)

(20 mM $\text{NaH}_2\text{PO}_4/\text{Na}_2\text{HPO}_4$, 100 mM NaCl , 20-250 mM Imidazole, pH 8, 2 mM BME)

10X stock Phosphate buffer (pH 8) 10 ml (1X)

1M Imidazole stock 2ml (20 mM), 10ml (100 mM), 25ml (250 mM)

BME (14.3 M) 0.14 ml (2 mM)

pH was adjusted to 8, total volume was made to 100 ml, filtered (0.22 μm) and autoclaved.

Amylose column purification buffers

a) Binding buffer or column equilibration buffer

1X phosphate buffer

b) Elution buffer for 100 ml

(20 mM $\text{NaH}_2\text{PO}_4/\text{Na}_2\text{HPO}_4$, 100 mM NaCl , pH 8, 10 mM maltose, 2 mM BME)

10X stock Phosphate buffer (pH 8) 10 ml (1X)

0.5 M Maltose (stock) 2 ml (10 mM)

Milli Q 88 ml

Note: Filtered using 0.22 μm

Urea denaturation buffers

a) Dialysis buffer

20mM Sodium phosphate

100mM Sodium chloride

pH 8.0

10% Glycerol

b) Binding buffer

10mM Imidazole

20mM Sodium phosphate

100mM Sodium chloride

8M Urea

1% Glycerol

pH 8.0

c) Elution buffer

1M Imidazole

20mM Sodium phosphate

100mM Sodium chloride

8M Urea

1% Glycerol

pH 8.0

d) Lysis buffer

20mM Sodium phosphate
100mM Sodium chloride
8M Urea
0.1% TritonX
pH 8.0

e) Refolding buffer/Complicated buffer (For 200 ml)

50mM Tris.HCl (pH 8.5)	1.214g
1mM Sodium EDTA	0.0745g
0.05% PEG	0.1g
0.5% Triton X	1 ml
0.1mM L-arginine	4.213g
2mM Magnesium chloride	0.0813g
2mM Calcium chloride	0.0443g
10mM Potassium chloride	0.14919g
240mM Sodium chloride	2.8g

f) Wash buffer composition to remove MBP from GRIM-19 protein

1.5 % Glycerol
0.1% Triton
0.05% SDS
0.5M Urea

3.1.6.5 5X SDS sample loading buffer (10 ml)

(250 mM Tris-HCl pH 6.8, 10% SDS, 0.5% BME, 30% glycerol)

1M Tris-HCl (pH 6.8)	2.5 ml from stock 1M
SDS	10g
Glycerol	3 ml
BME	0.5 ml from stock 14.3M
Bromophenol blue	0.02 g
Milli Q	4 ml

3.1.6.6 30% acrylamide

(29.2% Acrylamide, 0.8 % N'N'-bis-methylene-acrylamide)

Acrylamide	29.2 g (29.2%)
N'N'-bis-methylene-acrylamide	0.8 g (0.8%)

3.1.6.7 SDS-PAGE Running Buffer (for 1 L)

(25mM Tris, 192mM glycine, pH 8.3, 1% SDS)

Tris Base	3.02 g (25mM)
Glycine	14.4 g (192mM)
Milli Q	1 L

No need to adjust pH

3.1.6.8 Staining / Destaining solution (for 1L)

(50% water, 40% methanol, 10% acetic acid, 0.1% Coomassie blue R-250)

Methanol 400 ml

Acetic Acid (glacial) 100 ml

Milli Q 500 ml

Coomassie blue R-250 1g

Destaining solution is the same, minus the Coomassie blue.

3.1.6.9 Tris-Tricine SDS-PAGE buffers

a) 10X cathode Buffer (upper buffer)

(1 M Tris, 1 M Tricine, 10% SDS)

Tris base 121.1 g

Tricine 179.2 g

SDS 10 g

Milli Q 1 L

b) 10X anode buffer (lower tank buffer)

(2 M Tris-HCl, pH 8.9)

Tris base 242.2 g

pH was adjusted to 8.9 and volume made to 1 L with Milli Q

c) Tris-Tricine gel buffer

(3M Tris-HCl, 0.3% SDS, pH8.45)

Tris base 182 g

SDS 0.9 g

pH was adjusted to 8.9 and volume made to 300 ml with Milli Q

3.1.6.10 1X Transfer Buffer (for 1 L)

(25 mM Tris, 192 mM glycine, pH 8.3, 20% methanol)

Glycine 14.4 g (192 mM)

Tris Base 3.02 g (25 mM)

Milli-Q 0.8 L

Methanol 200 ml (20%)

3.2 Methods

3.2.1 Primer reconstitution

All the primers used were synthesized from Sigma and were received as a lyophilized nucleic acid pellets (not visible with naked eyes). The primer pellet was centrifuged at 10,000 rpm for 1 min. Primers were suspended in 10mM Tris, pH 7.5 or autoclaved Milli Q water, pH 7 to obtain stock concentration of 500 µg/ml. Reconstituted primers were stored at -20° C. The working concentration of 125ng/µl was prepared.

Table 3.1: List of HtrA4 and GRIM-19 primers

HtrA4 domains	Primer sequence 5'- 3'
HtrA4 (F.P.)	GATGCTAGCCATATGGCCGTGCCTGTGCAGTGGG
HtrA4 (R.P.)	AAGCTTTAACTCGAGATTGATTGTTTCAGGTATGACTGTCAGG
SPD-PDZ (F.P.)	CAGCTAGCCATATGGGCTCTGGGTTCATAGTG
SPD-PDZ (R.P.)	AAGCTTTAACTCGAGATTGATTGTTTCAGGTATGACTGTCAGG
N-SPD (F.P.)	GATGCTAGCCATATGGCCGTGCCTGTGCAGTGGG
N-SPD (R.P.)	AAGCTTTAACTCGAGTGCCAAGAACTGCCTAAC
SPD (F.P.)	CAGCTAGCCATATGGGCTCTGGGTTCATAGTG
SPD (R.P.)	AAGCTTTAACTCGAGTGCCAAGAACTGCCTAAC
PDZ(F.P.)	GCTAGCCATATGCTGCAAATGCTGTCCCTCACTG
PDZ (R.P.)	AAGCTTTAACTCGAGATTGATTGTTTCAGGTATGACTGTCAGG
HtrA4 mutants	Primer sequence 5'- 3'
HtrA4 inactive (S326A) F.P.	GCCACAATTA ACTATGGGAATGCTGGTGGT CCTCTGGTG
HtrA4 inactive (S326A) R.P.	CACCAGAGGACCACCAGCATTC CCATAGTTAATTGTGGC
HtrA4 Δ AVPV (F.P.)	CGGCTAGCCAGTGGGGGAACTGCGGGGATAC
HtrA4 Δ AVPV (R.P.)	AAGCTTTAACTCGAGATTGATTGTTTC AGGTATGACTGTCAGG
Y167A (F.P.)	CCCGCTCAGGAGGAATGCTAACTTCATCGCCGCGGTGGTG

Y167A (R.P.)	CACCACCGCGGCGATGAAGTTAGCATTCCTCCTGAGCGGG
Y167A,F169A (F.P.)	CCCGCTCAGGAGGAATGCTAACGCTATCGCCGCGGTGGTG
Y167A,F169A (R.P.)	CACCACCGCGGCGATAGCGTTAGCATTCCTCCTGAGCGGG
F276A (F.P.)	CTTCGGGCTGGAGAGGCTGTGGTGGCTTTGGGC
F276A (R.P.)	GCCCAAAGCCACCACAGCCTCTCCAGCCCGAAG
F169D (F.P.)	GGAGGAATTACAACGATATCGCCGCGGTG
F169D (R.P.)	CACCGCGGCGATATCGTTGTAATTCCTCC
GRIM-19	Primer sequence 5'- 3'
GRIM-19 in pGEX-6P-1 F.P.	TTATAGGATCCATGGCGGCGT
GRIM-19 in pGEX-6P-1 R.P.	CGCTACTCGAGCGTGTACCACATG
GRIM-19 in pET28a(+) F.P.	TTATAGGATCCATGGCGGCGT
GRIM-19 in pET28a(+) R.P.	CGCTACTCGAGCGTGTACCACATG
GRIM-19 Cell death inducing domain F.P.	CATCATGAAGGACGTGGGATCCCCCGACTGGAAGGTG
GRIM-19 Cell death inducing domain R.P.	CACCTTCCAGTCGGGGGATCCCACGTCCTTCATGATG
GRIM-19 in pMAL-c5E F.P.	TTATAGGATCCATGGCGGCGT

GRIM-19 in pMAL-c5E R.P.	CGCTACTCGAGCGTGTACCACATG
--------------------------	--------------------------

3.2.2 Determination of DNA concentration

The absorbance of the DNA samples was measured with UV-Vis spectrophotometer (NanoDrop, Model-ND 1000) at 260 nm and the concentration was calculated according to the Lambert Beer Law. According to the Beer-Lambert law: $A = \epsilon \times c \times l$, where A is the absorption at 280 nm, ‘ ϵ ’ is the molar extinction coefficient, ‘c’ the molar concentration of the protein solution and ‘l’ is the cell length of the cuvette. To assess the purity of the sample with respect to protein contamination, ratio of absorptions at 260 nm versus 280 nm was observed which should be around 1.8-2.0 for a pure nucleic acid sample.

3.2.3 Polymerase chain reaction (PCR)

All PCR amplifications were done using pfu turbo polymerase (Stratgene kit) with proofreading activity. For sub cloning, the gene of interest was PCR amplified using gene specific forward and reverse primers. For site directed mutagenesis (SDM) plasmid with gene of interest was amplified using the forward and reverse primer with the desired mutation. In all SDMs, reverse primer was complementary sequence of the forward primer. The primers were designed using ‘*primer-X*’ software and ‘*oligoanalyser*’ tools. The parameters taken under consideration for

designing primers are primer length: 18-24 nucleotides, GC content: 40-60%, T_m: 50-65 °C. A typical PCR reaction composition is as follows:

Reagents	Volume (µl)
Autoclaved Milli Q water, pH 7.0	15.5
10 X Pfu buffer	2
10 mM dNTPs	0.5
Template DNA (60 ng)	1
Forward primer (125 ng/µl)	0.5
Reverse primer (125 ng/µl)	0.5
Pfu enzyme (1unit)	0.5
Total Volume	20

Typical cycling steps for the PCR are

Initial denaturation	95 °C, 5 min
Denaturation	95 °C, 30 sec
Annealing temperature	53 °C, 55 sec
Elongation	71 °C, 10 min (elongation time depends on size of the DNA and processivity of polymerase)
Final extension	72 °C, 10 min
Repeat step 2 to 4 for 25 cycles	for gene specific amplification 25 cycles, and for SDM 18 cycles were considered

For SDM, amplified PCR products were treated with DpnI enzyme (Fermentas) at 37 °C to degrade the parental template. DpnI is an endonuclease which would specifically target the methylated parental DNA strands. The digested PCR product was then transformed in *E. coli* DH5 α cells. Plasmids were isolated from colonies and sequence of the desired mutation was confirmed using the automated DNA sequencing facility at ACTREC.

3.2.4 Agarose gel electrophoresis of DNA

0.8 – 1 % agarose was prepared in 1X TAE and boiled using a microwave oven. Solution was allowed to cool to ~50-60°C and ethidium bromide (0.5 μ g/ml) was added to enable fluorescent visualization of the DNA fragments under UV light. The agarose solution was mixed thoroughly and poured in a gel casting tray with comb. The gel was allowed to polymerize for 20-30 mins. The DNA samples as well as DNA size-ladder in the range of 250–10,000 bp (Fermentas) were loaded along with the 1X DNA loading dyes. The samples were resolved at 100 volts for 30-50 min. The DNA bands were analyzed under UV 365 nm followed by documentation (UVP, Bioimaging Systems) and visualization (LaunchVision Works LS software) for gel.

3.2.5 Restriction digestion reaction

Restriction digestion was performed using desired enzymes to prepare the vectors and inserts for cloning. All restriction digestion reactions were carried out at 37°C for 1-4 hours using the

supplied buffers (Fermentas). After restriction digestion of the insert and the vector, both were purified by gel extraction protocol (Gel Extraction Kit, Sigma). A typical restriction digestion reaction conditions are:

10X buffer (Tango/FD)	2µl (1X)
DNA template	10 µl (2-4 µg)
Restriction enzyme	1 µl
Autoclaved MQ water pH, 7.0	7 µl
Final Reaction Volume	20 µl

3.2.6 Cloning/Ligation

Ligation was set up using T4 DNA ligase supplied with 10X ligation buffer (Fermentas). For cloning blunt end PCR products, pJET cloning kit (Fermentas) was used and ligation was carried out according to the manufactures protocol. The vector and PCR product were mixed in 1:3 molar ratios and ligated at 22 °C for 30 min. For cohesive-end cloning, restriction digested vector and insert were gel eluted and mixed in molar ratios of 1:3 or 1:6 and ligated using T4 DNA ligase at 22 °C for 3 hrs or 16 °C for 12 hrs.

The vector to insert molar ratio was calculated using a formula:

$$\frac{\text{Vector concentration (ng)}}{\text{Vector size (bp)}} = \frac{\text{Insert concentration (ng)}}{\text{Insert size (bp)}}$$

$$\text{Insert concentration (ng)} = \frac{\text{Vector concentration (ng)} \times \text{Insert size (bp)}}{\text{Vector size (bp)}}$$

The above equation is for 1:1 molar ratio of vector: insert concentration. For 1:3 molar ratios, 3 times the insert concentration was taken.

Composition for the ligation reaction is as follows:

Vector DNA concentration	60-80 ng
Insert concentration	Calculated from the above formula
10X T4 DNA ligase buffer	2 µl
T4 DNA ligase	1µl
Autoclaved water	Adjusted to total volume of 20 µl

3.2.7 Plasmid construction

3.2.7.1 HtrA4 constructs

Human ORF sequence of *HTRA4* (1-476 amino acids) cloned in pBluescriptR was obtained from Mammalian Genome Collection (MGC, NIH, USA). Using the appropriate primer shown in table 3.1, different constructs of *HTRA4* i.e. SPD-PDZ, N-SPD, SPD and PDZ were PCR amplified by inserting Nde-1 and Xho-1 restriction sites and cloned into pET20b (+) expression vector (New England biolabs, MA, USA) with a C-terminal His₆ tag. All HtrA4 constructs were confirmed by sequencing.

3.2.7.2 GRIM19 constructs

GRIM-19 gene of size 454 base pairs was amplified by incorporating BamHI and XhoI as restriction sites from pLX304 vector (obtained from DNASU Plasmid Repository, Arizona State University, USA) and cloned in the intermediate vector pJET1.2, the intermediate clones containing GRIM-19 gene was confirmed with restriction digestion and with sequencing. The GRIM-19 gene was also cloned in GST and MBP tag containing vectors using the primers as shown in table3.1.

3.2.8 Transformation

1 µl of DNA (100 ng) of interest was added to 100µl of competent cells stored in -80°C thawed on ice, followed by incubation in ice for another 20 minutes. A heat shock at 42°C for exactly 90 seconds was followed by snap chilling on ice for about 10 minutes. Luria broth (700 µl) was added into the tube which was incubated at 37°C for 1hr on shaker at 180 rpm. Cells were centrifuged at 5,000 rpm for 10 minutes at 15°C. Supernatant was discarded and fresh 100 µl Luria broth was used to re-suspend the pellet which was then spread onto a Luria Bertini agar plate containing a suitable antibiotic. Plates were kept at 37°C incubator overnight for about 12-16 hours. The resultant colonies were checked and were observed for the colony characteristics.

3.2.9 Recombinant protein expression and purification

Single colony from a freshly transformed plate of the respective expression host containing the recombinant vector was inoculated into 10 ml of LB medium in a sterile snap cap tube containing appropriate selective antibiotics. Culture was grown at 37°C overnight (primary inoculation). Starter culture (10 ml) with appropriate antibiotics were inoculated in bulk (1L) and incubated under 37°C shaker conditions until the O.D (600nm) reaches to 0.6. Fresh LB medium was used for the blank check. The culture was kept at 4°C for 15min. Induction with 0.8mM IPTG concentration was done following sampling of an uninduced culture (1ml) and expression was allowed for appropriate time period. After an appropriate incubation the culture was centrifuged to collect the pellet using Beckman Coulter centrifuge (Rotor Id JA-10) at 4°C, 8000rpm for 8 minutes. A post induction sample was collected for the expression check. The pellet obtained can be directly used for purification or can be stored for further use at -80°C.

Rosetta (DE3) pLysS cells (New England Biolabs, MA, USA) were transformed with pET20b (+) plasmid containing HtrA4 variants. Cells were grown at 37 °C until the OD₆₀₀ reached 0.6 followed by induction with 0.6 mM IPTG. Cells were further cultured at 16°C for 18 hrs post induction. Cells were lysed by sonication in lysis buffer containing 20 mM Na₂HPO₄/NaH₂PO₄ and 200 mM NaCl at pH8.0 (buffer A) with 10 mM imidazole and 0.2 % (v/v) Triton X-100. Lysates were centrifuged at 14000 rpm for 30 min. Supernatants were incubated with His 60 Ni superflow resin (DSS Takara Bio India Pvt. Ltd, New Delhi, India) for 1 h at 4°C. Unbound protein was washed with wash buffer (buffer A with 10 mM imidazole and 2 % (v/v) glycerol). Using an imidazole gradient (20–500 mM) in elution buffer (buffer A with 2 % (v/v) glycerol)

the elution was performed and the eluted protein was dialyzed overnight with storage buffer (buffer A with 2 % (v/v) glycerol) (stored the aliquots at -80 °C).

Full length XIAP clone in pGEX-4T with GST-tag was obtained from Addgene (Cambridge, MA, USA). Proteins with GST-tag (GST-XIAP) were purified by affinity chromatography using GST-sepharose resin (Novagen, MA, USA) in buffer 20 mM Na₂HPO₄/NaH₂PO₄, pH 7.8 containing 100 mM NaCl, 25 mM β-mercaptoethanol (β-ME), and 50 μM ZnCl₂. All the fractions with highest percentage of purity were stored in aliquots at -80°C.

SDS-PAGE (for all domains of the protein except PDZ domain) and Tris-Tricine Gel (for PDZ domain) was run at 120V for about 90 minutes followed by staining with Coomassie Brilliant Blue (CBB) and destaining. The gel was viewed using Launch Vision Works LS software.

Sterilization

Bacterial culture media and solutions were sterilized by autoclaving by heating at 120°C with a pressure of 120 lbs for 20 min. For sterility, heat sensitive solutions were filtered with a 0.22 μm filter.

Growth conditions

All recombinant proteins were expressed either in *E. coli* BL21 (DE3) or BL21 (DE3) pLysS. These strains lacks the Lon and OmpT proteases and each carries a chromosomal copy of the T7 RNA polymerase under the control of lacUV5 promoter (inducible by IPTG) and therefore can conveniently express genes driven by the T7 promoter. Additionally, BL21 (DE3) pLysS was used for expression of toxic genes. The strain contains a chloramphenicol resistant pLysS

plasmid which encodes for T7 lysozyme to prevent basal or leaky expression. A single, transformed, isolated colony of expression host was inoculated in 10 ml LB medium and grown overnight at 37°C with constant shaking at 200-250 rpm. 10 ml inoculum was further inoculated in 1 litre LB broth in a ratio of 1:100. The culture was grown until the O.D600 reached 0.6-0.8. Cells were then induced with 0.3 mM isopropyl-D-thiogalactoside (IPTG) and incubated at 18°C for 16 hrs. Culture was harvested by centrifugation at 5,000 rpm for 10 min at 4°C. The bacterial pellets were stored at -80°C until further use.

3.2.10 General protocol for protein purification

3.2.10.1 Ni-NTA agarose affinity chromatography

High affinity Nucleo-pore® Ni-NTA (Nickel-Nitrilotriacetic acid) or Bio-Rad Ni-IDA (Nickel iminodiacetic acid) agarose was used to purify HtrA4 and its domains. (Reagents required mentioned in materials section). Ni-NTA affinity purification method was used to purify His₆ tagged proteins. Ni-NTA agarose beads of 2 ml were taken in 1X 10 cm econo column (Millipore). Beads were washed with 1X washing/equilibration buffer with at least three column volumes under native conditions. Equilibrated Ni-NTA beads were then incubated with protein lysate at room temperature (22°C) for about 30 min. After incubation, unbound lysate (flow through) was collected separately. Beads were washed with 3 column volumes of washing buffer. His₆ tagged proteins were eluted with elution buffer containing imidazole gradient (20-500 mM). The agarose beads in the column stored in 20% ethanol were washed with filtered autoclaved distilled water (DW). Stripping of the column was done using the stripping buffer

consisting of 50mM EDTA (1 column volume ~ 10 ml) followed by 5 column washes with autoclaved DW to remove excess stripping buffer. Further the column was incubated with 1 column volume of 100mM NiSO₄. One or more autoclaved distilled water washes were given and the column was equilibrated with pre-chilled binding buffer for 30 minutes.

3.2.10.2 Amylose affinity chromatography

Amylose affinity purification method was used to purify the protein tagged with MBP. Amylose beads (Novagen) of 2 ml were taken in 1X 10 cm econo column (Millipore). Beads were washed with 3 column volumes of 1X washing/column equilibration buffer. Equilibrated Amylose beads were incubated with protein lysate at room temperature (22 °C) for about 30 min on a rocker with gentle agitation. After 30 min, flow through was collected and beads were washed with 3 column volumes of wash buffer. Bound proteins were eluted using elution buffer containing 10 mM maltose.

Cell lysis

The cell pellet was completely dissolved in the lysis buffer forming a viscous mixture. This mixture was sonicated (5 cycles of 2 minutes with 2 minutes of respite after every cycle) and centrifuged at 20,000rpm for 30 minutes at 4°C (Beckman coulter JA-25.50 rotor). Filtered (0.45µm syringe filter) supernatant was loaded on the Ni-NTA column followed by gentle mixing by inverting the column several times. Then the column was kept on the rocker for binding for 45 minutes to 1hr at 4°C (Cold room).

3.2.11 Purification of HtrA2 variants

Mature HtrA2 with C-terminal His₆-tag in pET-20b (+) was expressed in *E. coli* strain BL21 (DE3) pLysS. Protein expression was induced by culturing cells at 18°C for 20 hrs in presence of 0.2 mM IPTG. Cells were lysed by sonication and the centrifuged supernatants of HtrA2 variants were incubated with pre-equilibrated Ni-IDA beads for 1 hr at room temperature. The flow through was collected and beads were washed with wash buffer (3 column volumes). Elution was performed using an imidazole gradient (20–300 mM) in elution buffer. Further eluted protein was purified using gel permeation chromatography. N-SPD was purified using amylose resin and the bound protein was eluted with 10 mM maltose. After that the protein was subjected to TEV protease cleavage to remove maltose binding protein (MBP). N-SPD was separated from MBP using Ni-affinity chromatography. For purity analysis, all purified proteins were analyzed by SDS-PAGE. The fractions with >95% purity were dialyzed against phosphate buffer and stored in aliquots at -80°C until use.

3.3.12 Purification of GRIM 19 and variants

Constructs with different domain combinations of GRIM-19 was cloned in bacterial expression vectors with his₆ tags and expressed in *E.coli*. Proteins were purified using standard protein purification protocols as mentioned above. The GRIM-19 and its domains were also cloned in pMALc5E and pGEX4T vectors with MBP and GST tag respectively and used for pull-down studies.

3.3.13 Urea denaturation protocols

In urea denaturation protocols all the steps were same except for the buffer composition. In this method binding and elution buffer contain 8M urea in addition to the regular salts and additives as mentioned in material section. After purification to remove urea the protein was dialyzed with refolding buffer followed by 1X dialysis buffer.

3.3.14 Urea denaturation modified protocols

In normal protocols after purification the protein transferred directly to refolding buffer. In modified protocol the protein shifted from 8M Urea to 6M, 4M, 2M and 0M and then shifted to refolding buffer. In modified protocol additives listed in materials part were also added for proper folding.

3.3.15 Concentration of the protein using millipore centricon

Millipore centricons were used to concentrate the purified protein. The filtrate vial was washed with autoclaved DW followed by equilibration with appropriate buffer. Elutes with highest concentration of the proteins were added to the vial and centrifuged at 3000 rpm until the desired concentration was achieved. The concentration was monitored using nanodrop. The protein was then injected into the analytical column for size exclusion chromatography.

3.3.16 Gel filtration chromatography

Molecular mass of HtrA4 variants were estimated by size exclusion chromatography. After purification, all HtrA4 variants were concentrated to 1 ml using Amicon Ultra centrifugal filter units (Ultra-15, MWCO 10 or 3 kDa, sigma, St. Louis, MO, USA) to 2-3mg/ml concentration. The protein samples were injected into Superdex 200 10/300 HR column (GE Healthcare, Uppsala, Sweden) pre-equilibrated with buffer containing buffer A.

With the same buffer, proteins were eluted at a flow rate of 0.6 ml/min. The standards used for calibration were Blue Dextran, Alcohol Dehydrogenase (ADH), Bovine Serum Albumin (BSA), Lysozyme and MBP (purchased from Sigma, St. Louis, MO, USA except Maltose-Binding Protein which was purified in lab). Elution volume (V_e)/void volume (V_0) versus log of molecular masses of standards were plotted to generate the calibration curve from which molecular masses of HtrA4 variants were calculated. Oligomerization status of HtrA4 in presence of generic substrate β -casein (Sigma, St. Louis, MO, USA) was analysed by pre-incubating inactive HtrA4 (S326A) and β -casein for 12hrs in 1:2 molar ratio respectively at 4°C. This HtrA4- β -casein complex subjected to analysis using size exclusion chromatography as described above.

3.3.17 Determination of Protein concentration

To measure the protein concentration of a given sample two distinct methods have been used.

3.3.17.1 Bradford protein assay

The Bradford protein assay is a spectroscopic analytical procedure used to measure the concentration of protein in a solution. It is based on the observation that for an acidic solution of coomassie brilliant blue G-250 the absorbance maximum shifts from 465 nm to 595 nm when binding to protein occurs. 5 µl of the BSA standards (1, 0.5, 0.25, and 0.125 mg/ml) were mixed with 200 µl of Bradford reagent (1:4 diluted, Bio-Rad) in triplicates in a 96- well plate. Readings were taken with ELISA plate reader (Spectra Max 790) at 595 nm using SoftMaxPro 4.6 software. A standard graph was plotted by taking absorbance on Y-axis and concentration of protein on X-axis. Concentration of protein of interest was extrapolated from the standard curve.

3.3.17.2 Absorbance at 280 nm

The Absorbance of a protein sample at 280 nm was measured with a Nanodrop and calculated the concentration. According to the Beer-Lambert law: $A = \epsilon \times c \times l$, where A is the absorption at 280 nm, 'ε' is the molar extinction coefficient, 'c' the molar concentration of the protein solution and 'l' is the cell length of the cuvette. Molar extinction of proteins was calculated according to the Edelhoch method. The equations to calculate the protein concentration are as provided below:

- 1) Protein concentration (mg/ml) = Absorbance 280/ $\epsilon \times$ Molecular weight of protein (Daltons)
- 2) Protein concentration (µM) = Absorbance 280/ $\epsilon \times 1000000$

3.3.18 SDS polyacrylamide gel electrophoresis (SDS-PAGE)

According to the method of Laemmli, SDS-PAGE was used for the electrophoretic separation of proteins. The stacking and the resolving (separating gel) were prepared as described in material section. The protein samples were mixed with 5x sample buffer, boiled for 5 min and loaded onto the gel. The electrophoresis was performed at 100 V for about 60 min. The gel was stained with coomassie brilliant blue for 10-15 min. The gel was then destained overnight in the destainer and finally preserved in 10% acetic acid and documented.

3.3.19 12% TRIS TRICINE- SDS PAGE

The tris-tricine gel system is most commonly used for the separation of low molecular weight proteins, with masses ranging from 1-100 kDa. It is preferred electrophoretic system for the resolution of proteins smaller than 30 kDa. The concentration of acrylamide used in these gels is lower than in other electrophoretic systems and it makes the use of tricine instead of glycine in the running buffer. Tricine is more negatively charged than glycine allowing it to migrate faster. These lower concentrations facilitate electro-blotting particularly for hydrophobic proteins. In addition, tricine has high ionic strength leading to more ion movement and less protein movement. This allows the separation of low molecular weight proteins in lower percentage of acrylamide gels. This system has low pH and tricine in the running buffer which results in sharper bands and higher resolution of proteins.

Table 3.2 : 12% Tris tricine SDS gel preparation

Contents	12% RESOLVING GEL	12% STACKING GEL
30%Acrylamide (ml)	3.2	0.67
D/W (ml)	1.2	2.7
Tris-Cl (ml)	2.7	0.5
70%glycerol (ml)	0.8	-
APS (μl)	100	40
TEMED (μl)	5	4
Total Volume	8ml	4ml

3.3.20 Biophysical studies

Biophysical techniques those have been used in this thesis to structurally characterize a given protein are:

3.3.20.1 Circular Dichroism (CD) spectroscopy

CD spectroscopy is used to determine the secondary and tertiary structural properties of biomolecules. Circular dichroism is the property of chiral molecules to absorb the right and left components of circularly polarized light to a different extent. Far UV CD spectra in the range (260-190 nm) was used to analyze different secondary structural components of the protein such as alpha helix, parallel and anti-parallel beta sheet, turn, and others. Absorption minima at 208 and 222 nm indicate α -helical structure, whereas a minimum at 218 nm is a characteristic of β -

sheets. Proteins with greater disordered secondary structural elements or random coil regions are characterized by a low ellipticity at 210 nm and negative band near 195 nm.

Far-UV CD scans of Htra4 and its variants were acquired using a JASCO J 815 spectropolarimeter (JASCO) using a quartz cell with 1-mm path length. Far-UV CD spectrum (260-190 nm) was recorded using a bandwidth of 1 nm and an integration time of 1s, with proteins of 10 μ M concentrations. Each spectrum was an average of 5 scans, with a scan rate of 20 nm/min. Thermal stability of proteins were assessed by monitoring the CD spectrum with increasing temperature. A Far-UV CD spectrum was collected in a temperature range of 20 °C-90 °C with an increment of 2 °C/min. At each data point, the sample was equilibrated for 3 mins. Ellipticity corresponding to 222 nm at different temperatures was obtained for calculation of melting temperature (T_m).

Data analysis

The CD data was represented in the form of the mean residual ellipticity (MRE or $[\theta]$) given as $\text{deg.cm}^2.\text{mol}^{-1}$. Ellipticity obtained from the CD spectra was converted to mean residue ellipticity using the formula:

$$[\theta]\text{MRE} = (\theta \times \text{MRW}) / (10 \times c \times d)$$

Where, MRW (Mean residue weight) = Molecular weight / (N-1)

'c' is concentration of protein (mg/ml), 'd' is the path length in cm and 'N' is the number of amino acids.

3.3.20.2 Fluorescence spectroscopy

Fluorescence is a phenomenon in which a molecule absorbs a lower wavelength photon, undergoes electronic excitation, and then emits longer wavelength. Fluorescence spectroscopy is used for studying dynamics, protein unfolding and biomolecular interactions. The intrinsic fluorescence of a folded protein is a combination of the signal from individual aromatic residues (Phe, Tyr, Trp) with the major contribution from tryptophan residues. Fluorescence emission of different constructs (2 μ M) were measured by Fluorolog-3 spectrofluorometer (Horiba Scientific) using a quartz cell with 3 mm path length cuvette. Fluorescence spectra of 2 μ M protein solutions were recorded with 295 nm excitation followed by emission between 310-400 nm using a 5 nm excitation and emission slit widths with an integration time of 0.1sec.

3.3.21 Biochemical studies

3.3.21.1 Affinity pull down studies

Affinity pull down studies help to understand protein-protein interaction in *in vitro* and *in vivo*. Recombinant MBP-fused GRIM19 was lysed in a lysis buffer containing (20 mM $\text{Na}_2\text{HPO}_4/\text{NaH}_2\text{PO}_4$, 100 mM NaCl, pH 8, 0.1% Triton X100). 10 μ g of GRIM19 lysate was incubated with 10 μ l of amylose beads (Invitrogen) for 1hr at 4 °C. Beads were then washed extensively with the phosphate buffer. After washes, 100 μ g of purified recombinant HtrA2 variants were incubated with amylose bound MBP fused GRIM19 proteins (~10 μ g), in a final

volume of 200 µl in wash buffer. After overnight incubation under agitation at 4°C, beads were extensively washed for four times with wash buffer and boiled in 30 µl Laemmli buffer. Samples were then analyzed by 15% SDS-PAGE and coomassie blue staining.

HtrA4 and XIAP binding studies were performed using *in vitro* pull down studies where GST tagged XIAP was used as bait and HtrA4 (S326A) as prey. 10 µg of GST-XIAP cell lysate was incubated with 20µl of GST sepharose resin (Novagen) for 3 hr at 4 °C. To prevent nonspecific protein binding to GST resin, beads were incubated with 5% BSA for 10hrs. Beads were then washed extensively with buffer A containing 0.5 mM DTT, 0.1% TritonX-100 (pH 7.2). After washes, 100 µg of purified recombinant HtrA4 was incubated with GST bound XIAP for 2 hours at 4 °C. Unbound HtrA4 was removed by washing the beads three times with buffer A and boiled in 30 µl Laemmli buffer. The bound proteins were separated on 12% SDSPAGE and were probed with anti-His antibody (Abcam, Cambridge, MA, USA) against HtrA4.

3.3.21.2 Western Blotting

Western blotting uses specific antibodies to identify proteins that have been separated based on size by gel electrophoresis. The gel is placed next to a membrane made of nitrocellulose or PVDF (polyvinylidene fluoride) and application of an electrical current induces the proteins to migrate from the gel to the membrane. The membrane is then incubated with labeled antibodies specific to the protein of interest.

Washing off the unbound antibody will leave only the bound antibody to the protein of interest. Then the bound antibodies are detected by developing the film. As only the protein of interest bind to the antibodies, only one specific band should be visible. The thickness of the band can be related with the amount of protein present; thus doing a standard can indicate the amount of protein present.

Procedure -

1. Loading and running the gel: Load equal amounts of protein into the wells of the SDS-PAGE gel, along with molecular weight marker. Load 10-100 ng of purified protein. Run the gel for 1–2 h at 120 V.
2. Transferring the protein from gel to PVDF membrane: The membrane can be either PVDF or nitrocellulose; each has its own advantages. Activate PVDF with methanol for 3 minutes. Equilibrate the gel and PVDF membrane in transfer buffer at room temperature for 10 minutes.
3. Prepare the stack as follows:



Carry out the transfer at 90 volts for 2 hours or by 45 volts for 16-18 hours at 4°C. Transfer of proteins to the membrane can be checked using Ponceau staining before the blocking step. The blot can be destained by giving washes with TBS till bands disappear.

4. Antibody staining

a. Block the membrane for 1 h at room temperature or 45 minutes at 30 °C using blocking buffer.

Wash the membrane thrice with TBST (tween20-0.1%) for 5 minutes each.

b. Incubate the membrane with 1:1000 dilution of primary antibody i.e. antimouse 6-His-tag antibody in blocking buffer. Incubate either at room temperature for 1 hour or at 4°C O/N.

c. Wash the membrane in TBST for 5 times, 5 minutes each.

d. Incubate the membrane with 1:6000 dilution of conjugated secondary antibody (antimouse antibody raised in goat) in blocking buffer at room temperature for 1 h.

e. Wash the membrane in TBST for 5 times, 10 minutes each. Change the membrane from TBST to only TBS after washes.

f. Acquire image using darkroom development techniques for chemiluminescence, or normal image scanning methods for colorimetric detection.

3.3.21.3 Serine protease enzymatic assays

Protease assays with β -casein as substrate:

To determine the protease activity of different constructs of HtrA4, generic serine protease substrate β -casein was used. For each 30 μ l reaction mixture, 6 μ g of β -casein was incubated with 4 μ g of different HtrA4 variants in a buffer A at 37°C for 10 hr. Protease assays were also performed at a temperature range of 30 to 45°C for 10 hrs using β -casein as substrate. The reaction was stopped by adding 2X SDS sample loading buffer and boiled for 5 min. All reaction products were analyzed on 12% Tris-tricine gel and bands were quantified using Image J (1.47V, NIH, USA). For all quantitative enzyme kinetic studies, fluorescein isothiocyanate-labelled (FITC) casein (sigma, St. Louis, MO, USA) was used, and assays were performed. Fluorescent substrate cleavage was determined by incubating 30 μ M of enzymes with increasing concentration (0–20mM) of β -casein at 37°C in cleavage buffer (buffer A with 0.1 mM DTT). Using excitation wavelength of 485 nm and emission at 545 nm, fluorescence was monitored in a multi-well plate reader (Berthold Technologies, Germany). Assays were done in triplicate. The steady-state kinetic parameters were obtained by fitting data to Michaelis-Menten equation using GraphPad Prism 7. To determine the optimal temperature of protease activity over a temperature range of 30 – 45°C with 5°C intervals; for each reaction mixture, 6 μ g of β -casein, 4 μ g of different constructs of HtrA4 in a buffer A were incubated for 10 hours. The reaction was stopped by adding 2X SDS sample loading buffer and boiled for 5 min. All reaction products were analyzed on 12% Tris-tricine gel and bands were quantified using Image J (1.47V, NIH, USA). Graphs were plotted using GraphPad Prism 7. Initial velocities were calculated at each

respective temperature using linear regression analysis. Assays are representative of at least three independent experiments done in triplicate. *Note:* FITC β -casein is photosensitive.

Data analysis:

Graph was plotted by taking time (min) on X-axis and increase in fluorescence intensity on Y-axis. Slope value for each substrate concentration was determined using linear regression analysis. Reaction rates v_0 ($\mu\text{M}/\text{min}$) of unquenched FITC at respective substrate concentration were determined by dividing the slope with 19422 (slope of free FITC standard curve). By fitting data to Michaelis-Menten equation using nonlinear least squares subroutine in *KaleidaGraph* program (Synergy software). The steady-state kinetic parameters were obtained from the reaction rates.

Protease assays with GRIM-19 as substrate:

HtrA2 protease activity was assayed by incubating 4 μg of recombinant HtrA2 variants with 2 μg of recombinant GRIM-19 constructs in an assay buffer (20 mM $\text{Na}_2\text{HPO}_4/\text{NaH}_2\text{PO}_4$, pH 8, 100 mM NaCl, 0.1 mM DTT) for 0-24 hrs at 37 °C. The reactions were stopped with SDS-sample buffer and boiled for 5 min. The reaction products were analyzed on Tris-Tricine SDS-PAGE at a constant voltage of 90 V followed by coomassie Blue staining.

3.3.21.4 N-terminal sequencing

To determine the substrate specificity of HtrA4, generic serine protease substrate β -casein was used. HtrA4 (4 μg) was incubated with β -casein (10 μg) in buffer A at 37°C for 10 hrs. The

reaction was stopped by adding 2X SDS sample loading buffer and boiled for 5 min. The proteolytic products were analyzed on 12% Tris-tricine gel and transferred onto PVDF membrane (Millipore Corporation, Billerica, MA, USA) using Biorad wet transfer apparatus in 1X transfer buffer (25 mM Tris, 192 mM glycine, 20% (v/v) methanol, 0.025–0.1% SDS, pH 8.3) at a constant voltage of 20V for 10 hrs. Transferred proteins were stained with 0.1% amido black, 25% isopropanol, 10% acetic acid solution, followed by destaining in 40% methanol and 10% acetic acid. The stained fragments were excised from the membrane and sent to protein sequencing facility at Tufts University, Boston, MA. Five to seven N-terminal amino acids identified using ABI 494 sequence proTM Protein sequencers.

3.3.22 Crystallization

A three-dimensional structural analysis of a protein is essential to understand the protein function and design small molecule effectors to modify its function. During crystallization, purified protein forms nucleation from an aqueous solution. Discreet arrangement of protein molecules in the form of lattice are held together by non-covalent interactions, and make up smallest "unit cells". Protein crystallography is used to determine protein's three-dimensional structure using X-ray diffraction method. The diffraction pattern can then be processed to derive the three-dimensional structure of the protein. To to produce a well-shaped crystal, appropriate uniformity with purity of the protein is required at an optimal pH condition[113]. For crystallization, protein should be present in suitable buffer system and precipitants. Several elements can affect crystallisation of proteins, which comprises protein purity, concentration, temperature, pH, ionic

strength, and volume of crystallization solution, etc. Process of crystallization is distinguished into two steps: Nucleation process and crystal growth.

Nucleation and growth can happen in the supersaturated regions as represented in phase diagrams (**Figure: 2.1**). The illustration mainly includes three regions; unsaturated region, saturated region, and supersaturated region. Crystal grows in saturated or supersaturated region while nucleation most habitually starts in supersaturated region. The major focus of crystallization process is to obtain diffraction quality crystals. The best method to get crystals is through organized exposure of the protein solution to a diverse range of buffers, which have different amalgamations of suitable precipitants, such as salts, polyethylene glycols. For better crystallization, the protein-precipitant mixture must reach to the nucleation phase gradually to deliver necessary time for crystal growth. Most commonly used precipitants in crystallization trial are salts of sodium, ammonium and potassium ($(\text{NH}_4)_2\text{SO}_4$, NaCl , KH_2PO_4), organic polymers (PEG) and alcohols (methanol, ethanol, propanol, acetonitrile). Salt generally preserve the ionic environment of the solution although organic polymers diminishes protein solubility by dropping the dielectric constant of solvent. Solubility of a protein is found lowest at its isoelectric point (pI) since protein carries a net zero charge.

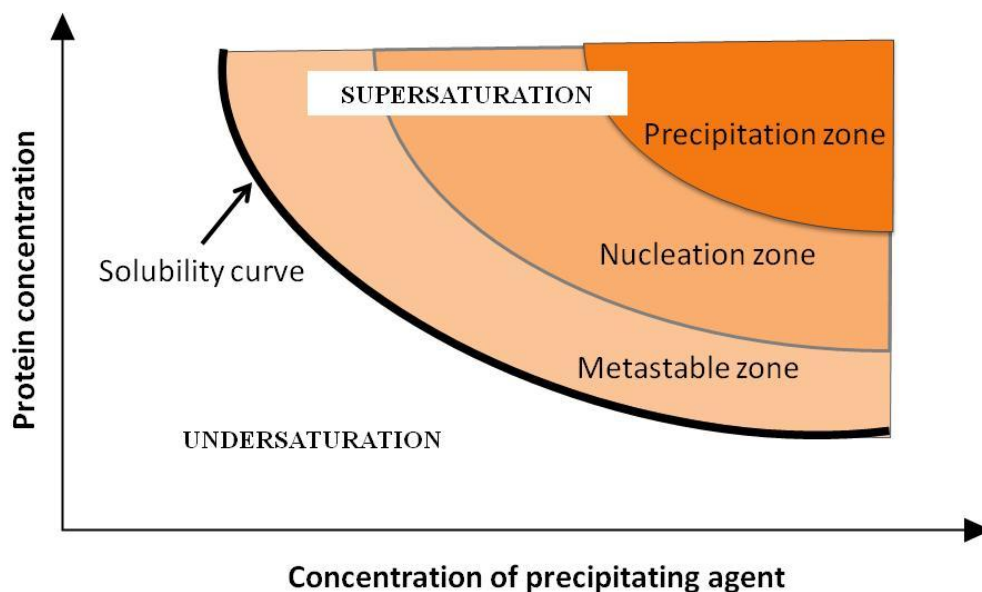


Figure 3.1: The phase diagram of crystallization

Methods of crystallization:

Different strategies have been established to grow crystals of functionally important proteins. Some of the more frequently used methods are vapour diffusion, micro-batch, dialysis and liquid–liquid diffusion technique.

1) **Vapour Diffusion method:** Subclasses into hanging drop and sitting drop method. In both the methods, a drop of purified protein mixed well with buffer and precipitant is present in a closed system and permitted to equilibrate with reservoir solution comprising the same precipitant. In the beginning, protein and precipitant concentration in the droplet is different, but as the system equilibrate the diffusion starts from higher concentration to lower concentration which in turn leads to nucleation, a level optimal for crystallization. Vapour diffusion is a simple but potent technique since it consumes less amount of protein, and several crystallization conditions can be

explored with a limited volume of protein. It is also appropriate for crystal growth monitoring, crystal manipulation and harvesting.

2) **Micro batch:** The micro batch method of crystallization is introduced to resolve the problem of microcrystal formation. In micro batch system a low density paraffin oil (~0.87 mg/ml) which float on the surface of protein-precipitant mixture, thus diminishes the rate of evaporation can be used [114]. In this process, a mixture of paraffin and silicon oil in combination can also be used. It is an excellent technique for filtering the known crystallization conditions to optimize the crystal growth [115].

3) **Dialysis:** The dialysis process is based upon the principal of slow diffusion of inorganic molecules through a semi permeable membrane, which leads to super saturation of protein solution. The system tries to maintain equilibration between precipitant and solute particles by permitting selective passage of water and precipitant. The dialysis bag is kept in a chamber containing the pool solution with a precipitant [116].

4) **Liquid–liquid diffusion method:** In this method, protein and precipitant solution keep a direct contact with the dense solution at the bottom. A concentration gradient is created due to the diffusion of protein and precipitant and thus crystallization may occur at suitable protein and precipitant concentration. Free interface diffusion is a method of choice for fine tuning the crystallization conditions.

3.3.23 Molecular modeling, docking, and simulation

3.3.23.1 HtrA4

Modeling, sitemap analysis and docking

Due to unavailability of a HtrA4 crystal structure, homology modeling was used to build the model of HtrA4. Human HtrA4 sequence starting from ¹⁴⁴AVPV (UniProt ID: P83105) was retrieved from UniProt database and submitted in I-TASSER server for 3D structure prediction [117]. This server prepares models either by comparative modeling or de novo threading methods depending on the availability of the templates for the particular model. The resultant HtrA4 model given by I-TASSER was built using other three HtrA homologs, namely, HtrA1 (PDB ID:- 3NUM) [51], HtrA2 (PDB ID:- 1LCY) [118] and HtrA3 (PDB ID:- 4RI0) [53] as templates. Quality of the predicted model was checked by Ramachandran plot [119], which showed few residues lying in the energetically disallowed regions of the plot. Those outlier residues were refined using ModLoop online server [120] and the refined structure was further validated using Ramachandran plot. The stability of the model was assessed using Molecular Dynamics Simulation (MDS) method to generate the best conformer. This final model was later used for SiteMap analysis and docking.

Using SiteMap (Sitemap, Schrödinger, LLC, New York, NY, 2018) binding sites of HtrA4 model were predicted and a list of five binding pockets was analysed as result. Based on their volume, hydrophobic and hydrophilic characters, degree to which ligand might donate or accept hydrogen bonds and exposure to solvent these pockets were scored. The top ranked site based on the site score was selected as the selective binding pocket (SBP_HtrA4) for further analysis.

Along with linker region residues, residues from both SPD and PDZ domain were included in SBP_HtrA4.

For docking analysis, beta casein which is a known substrate for HtrA4 was used. Domain signature peptide of beta casein (¹⁹⁹DMPIQAFLLYQEPVLGPVRGPFPIIV²²⁴) was extracted and divided into 23 heptamer peptides. As a negative control, an 11 mer peptide sequence LNQPKNPKNN that does not match with the consensus SBP_HtrA4 binding peptide pattern was used. All the peptides were built using 3D builder (Schrödinger, LLC, New York, 2018). After that, using protein preparation wizard (Schrödinger, LLC, New York, 2018) they were pre-processed and energy minimised and then docked with HtrA4. Using the protein structure and sitemap output (Sitemap, Schrödinger, LLC, New York, NY, 2018) energy minimised HtrA4 structure was prepared for docking and grid file was generated. Peptide docking tool from Bioluminate was used where glide performed the docking and a scoring pattern called MM-GBSA (Molecular Mechanics using Born and surface area continuum) was used [121]. Docking score was used to filter out energetically less favourable peptide poses and get a subset of best possible peptides for further studies.

Molecular dynamics simulation (MDS) and analysis

Using GROMACS 2018 MDS was run for the HtrA4- β -casein complex, which scored the highest in terms of binding affinity and glidescore [122]. The complex was surrounded by a cubic box of TIP4P water molecules with a buffer space of 10 Å to prepare the system for simulation [123]. To maintain charge neutrality of the system, adequate number of positive (Na⁺) ions was added as per requirement. For the simulation analysis, unbound HtrA4 structure was

also prepared to use it as a control. Neutralization was completed by adding 4 Na⁺ ions for unbound HtrA4 and three Na⁺ ions for HtrA4-peptide complexes. Two rounds of steepest-descent minimization [124] were performed for each system where using particle-mesh Ewald method (PME) the long range electrostatic interactions were treated [125]. For short range electrostatic and van der waals interactions, cut-off was kept at 10 Å. Throughout the simulation, to maintain constant temperature and pressure, a modified version of Berendsen thermostat, namely, V-rescale temperature coupling [126] and Parrinello-Rahman pressure coupling [126] were used, respectively.

After the energy minimization, the systems were equilibrated to establish a favourable orientation of water molecules and Na⁺ ions around unbound HtrA4 and HtrA4-peptide complexes. At first, the systems were subjected to equilibration performed under NVT or isothermal-isochoric ensemble [127] for 500 ps where the whole system was heated at 300 K with the solutes (protein and protein-peptide complexes). This was followed by NPT or isothermal-isobaric equilibration [127] for 2000 ps where pressure was kept constant at 1 atm with isothermal compressibility of solvent at 4.5e-5 atm⁻¹ and constant temperature of 300 K. For both phases of equilibration, LINCS constraint algorithm was used to apply position restraining force on all the heavy atom bonds in the protein [128]. Finally, 30000 ps MD simulations (production runs) were conducted under NPT ensemble where coordinates are saved in every 1 ps of time interval. The resultant trajectories from the MD simulations were analysed using energy, rms, rmsf, trjconv etc. packages from GROMACS 2018. MD quality analysis involved calculation of potential energy of the proteins and total energy of the systems. To conduct comparative analysis, the best structure was chosen from each simulation using clustering method [129]. Clusters were generated at 100 ps intervals throughout the 30 ns simulation which

gave a total of 300 structures for each simulation. Among them, the structure representing the largest cluster was taken as the best conformer for comparative analysis. Comparisons were based on their overall calculated RMSD and domain wise RMSD and were plotted using XmGrace (<ftp://plasma-gate.weizmann.ac.il/pub/grace/>).

3.3.23.2 GRIM-19

Molecular modelling of GRIM-19 and its docking with HtrA2

Due to unavailability of structural information for GRIM-19, its protein sequence (UniProt ID: Q9P0J0) was retrieved from UniProt [130]. The retrieved sequence was submitted to I-TASSER webserver, which generates models either by comparative modeling or *de novo* threading methods depending on the availability of the templates for the particular model [117]. The server generated a total of five GRIM-19 models which were ranked on the basis of their C-score value. C-score or confidence score is normally calculated based on the significance of threading template alignments (closeness of the homology templates with the final model) and the convergence parameters of the structure assembly simulations (averaging the largest cluster) where higher value indicates better model [117]. Quality of the best GRIM-19 model was further assessed by Ramachandran plot, which showed few residues lying in the energetically disallowed regions[119]. These outlying residues were subjected to refinement using ModLoop server, and the resultant refined structure was eventually analyzed using Ramachandran plot[120]. Final GRIM-19 model was given for blind protein-protein docking with HtrA2 (PDB ID: 1LCY) using Bioluminate software (Bioluminate, Schrödinger, LLC, New York, NY, 2018) and was scored using MM-GBSA (Molecular Mechanics using Generalized Born and surface

area continuum) scoring method[131]. The top 5 docked complex were analysed for the identification of interacting surface residues using PDBSum online server [132].

SiteMap analysis and induced-fit docking of GRIM-19 peptides with HtrA2

HtrA2 structure (PDB ID: 1LCY) lacks N-terminal residues (AVPSP) and two flexible regions (²¹¹RGEKKNSSSGISGSQ²²⁵ and ¹⁴⁹ARDLGLPQT¹⁵⁷)[118]. These regions were modelled using Prime 8.0 (Schrödinger, LLC, New York, NY, 2018) and the resultant structure was energy minimised using Desmond (Desmond, Schrödinger, LLC, New York, NY, 2018). Trimeric HtrA2 ensemble was generated using the crystal symmetry data given in the structure and was subjected to SiteMap (Schrödinger, LLC, New York, NY, 2018) analysis to generate putative binding sites. The best site was chosen on the basis of the site-score calculated on the basis of their overall volume and surface area, ratio between the hydrophobic and hydrophilic residues, the degree to which ligand might donate or accept hydrogen bonds and exposure to solvent.

The interacting residues identified from the rigid body protein-protein docking between GRIM-19 and HtrA2 indicated that cell death inducing domain of GRIM-19 was predominantly involved in the interaction. However, rigid body docking single-handedly cannot predict the effect of the bound ligand on the receptor, hence induced-fit docking was performed the using GRIM-19 peptides generated from the residues belonging to the cell death inducing domain of GRIM-19. The stretch of residues belonging to the aforementioned domain (¹⁰²PDWKVGESVFHTTRWVPPLIGELYGLRTTEEALHASHGFMWYT¹⁴⁴) were divided into stereochemically stable 44 heptamer peptides which were also of optimum size to be

accommodated into the binding site [133]. Using 3D builder and protein preparation wizard (Schrödinger, LLC, New York, 2018), these peptides were processed and energy minimized, prior to docking with HtrA2 trimer. The receptor structure (HtrA2 trimer), with the combination of the best SiteMap (Sitemap, Schrödinger, LLC, New York, NY, 2018) output was used for the generation of the docking grid file. Using induced-fit docking tool in Glide (Glide, Schrödinger, LLC, New York, NY, 2018), each peptide was docked into the receptor grid and scoring was done using MM-GBSA (Molecular Mechanics using Generalized Born and surface area continuum) scoring method[131].The best docked complex was taken for subsequent comparative analysis with unbound HtrA2 using MD simulation studies.

MD simulation analysis

Unbound HtrA2 and the best scored HtrA2_GRIM-19 complex were given for MDS run using GROMACS 2018[122], where AMBER99sb-ILDNP force field was used for the generation of the system topology parameters[134].TIP3P water molecules were added to each system during solvation, which was followed by neutralization using sufficient combination of positive (Na^+) and negative (Cl^-) ions[124]. One round of steepest- descent minimization was enough for each system to attain the lowest potential conformation where all the electrostatic and van der waalsinteractions were treated using the particle-mesh Ewald method (PME) [124, 125].Prior to MD run, systems were equilibrated under NVT (N=number of particles, V=system's volume, T= absolute Temperature)or isothermal-isochoric ensemblefor 1000 psand NPT (N=number of particles, P=system's pressure, T= absolute Temperature) or isothermal-isobaric ensemble equilibrationfor 2000 ps[127]. During equilibration, atom-wise position restraining forces were

applied on each system using LINCS (LINEar Constraint Solver) constraint algorithm [128]. These equilibrated systems were individually subjected to an 100 ns of MD simulation (production run) under NPT ensemble to generate trajectories at 2fs intervals. For comparative analysis, the best structure was retrieved from each simulation using clustering method[129]. Clusters were generated at 100 ps intervals throughout the 100 ns simulation with an output of 1000 structures for each simulation. Among them, for each simulation, the representative structure of the largest cluster was taken as the best conformer. Comparisons were based on their overall as well as domain-wise RMSD and were plotted using XmGrace (<ftp://plasma-gate.weizmann.ac.il/pub/grace/>).

3.3.23.3 Types of interactions

Different kinds of non-bonded interactions that are present in interacting molecules are described below:

1) Electrostatic interactions

Coulomb law: The attraction and repulsion between charged bodies is directly proportional to product of their charges and inversely to distance between them which is given as,

$$V_{\text{Ele}} = \sum_{i>j} \frac{q_i q_j}{4\pi\epsilon r_{ij}}$$

Where, ϵ represents dielectric constant (value 1 for vacuum, 4 - 20 for protein core and 80 for water), q_i and q_j are the charge on interacting bodies and r is the distance between them.

2) van der Waals interactions

It involves *attractive part* which exist due to induced-dipole/dipole and *repulsive part* due to Pauli's Exclusion Principle. It is usually represented by the Lennard-Jones potential which is obtained from the single atom parameter ϵ and σ .

3) Hydrogen bonds

Interaction of the type is $D-H \cdots A$. The origin of this interaction is a dipole-dipole attraction. Typical ranges for distance and angle: 2.4 - 4.0 Å (D-A) and 90°-180° (D-H \cdots A).

4) Hydrophobic interactions

This interaction exists due to combined effect of contact between water, polar medium and hydrophobic groups, and is usually present with in a distance of 4.7 Å.

3.3.24 Animal cell culture

3.3.24.1 Materials

- **Medium**

Powdered Dulbecco's modified Eagle's medium (DMEM) from GIBCO was dissolved in 1 litre of deionized water (3.7 g of sodium bicarbonate per litre was added and the pH of was adjusted to 7.4). The medium was filtered using millipore assembly – 0.22 µm membrane filter (Whatman). One ml of the filtered medium was added to the sterility test medium and incubated at room temperature for 6 days under observation. Sterility test medium (14.9 g of Fluid-thioglycolate was dissolved in ~250 ml of water. The volume was made up to 500 ml in measuring flask and boiled. After aliquoting 6 ml of the medium in glass tubes a pinch of CaCO₃ was added to each tube and autoclaved.)

- **Phosphate Buffered Saline (PBS) –**

150 mM NaCl

2 mM KCl

8 mM Na₂HPO₄

1 mM KH₂PO₄

- **0.4% Trypan Blue solution** - Prepared in 0.81% NaCl and 0.06% KHPO₄, dibasic

- **Trypsin-EDTA** (0.025% Trypsin, 0.2 mM EDTA)

- **Complete medium**

DMEM with 10% Fetal bovine serum and 1% antibiotic solution (Amphotericin B 20 µg/ml, Penicillin 2500 Units/ml, Streptomycin 800 µg/ml)

- **Freezing mixture** (90% Fetal bovine serum, 10% DMSO)

- **Cell lines** – Human Embryonic Kidney (HEK) 293, HeLa, MCF7, SiHa and A549

3.3.24.2 Protocols

a) Revival of cells

Revival of frozen cell cultures was carried out by thawing the freezing vials with the cells into a glass beaker containing water at 37 °C. Immediately the thawed cell suspension was added drop wise into a sterile centrifuge containing 5 ml of complete medium. The cell suspension was centrifuged for 10 min at 1,000 rpm. The supernatant was discarded and the cell pellet was washed with 1X PBS twice for complete removal of freezing mixture. Finally, the cell pellet was re-suspended in 3 ml of complete medium. The cell suspension was mixed gently with a Pasteur pipette to remove any clumps and finally transferred in a culture plate or flask. The cells were incubated in a humidified CO₂ (5%) incubator at 37 °C and their growth was observed each day under inverted microscope.

b) Trypsinization and Subculture

Cells with 70-80% confluency were washed with 1X PBS twice and 1 ml of trypsin-EDTA was added to the culture plate. Excess trypsin-EDTA was discarded and the plate was incubated till the cells partially detached. Complete medium was added into the plate and the resulting cell suspension was mixed with pipette to make a single cell suspension. Total cell count and the percent viability were calculated by dye exclusion method using Trypan Blue dye on a haemocytometer using an inverted microscope. Appropriate amount of cells depending upon cell type were seeded in culture plates. The plates were further incubated in humidified CO₂ incubator at 37 °C.

c) Freezing and cryopreservation

For freezing the cells, 70-80% confluent culture flask or dish was subjected to trypsinization. After noting the total cell count, the cell suspension was spun at 1,000 rpm for 10 min. The supernatant was discarded and the pellet was dislodged by tapping the tube gently. One ml of freezing mixture was added drop wise and mixed gently with pipette. The cell suspension was then transferred to freezing vials. The freezing vials were labelled and suspended in a cylinder with liquid nitrogen vapour and cooled gradually before plunging it into liquid nitrogen for long term storage.

d) Preparation of whole cell lysate

Reagents: SDS lysis buffer (5 mM EGTA, 5 mM EDTA, 0.4% SDS and protease inhibitor cocktail in 25 mM Tris-HCl pH 7.2) and non-denaturing lysis buffer (20 mM Tris-HCl pH 8.0, 137 mM NaCl, 0.5% Nonidet P-40, 1 mM EDTA)

Protocol: Post 30 h of transfection, the cells were spun at 1,000 rpm for 10 min at 4 °C. Cells were suspended in SDS or denaturing lysis buffer and incubated on ice for 40 min. The cell suspension was then subjected to ultra-sonication for 1 min, followed by centrifugation at 13,000 rpm for 15 min to separate cell debris. The supernatant and pellet were loaded on SDS-PAGE followed by Western blot analysis using respective antibodies.

e) Protein estimation using Bradford method

This assay is optimized for a microtitre plate. BSA standards were prepared from a BSA stock of 1mg/ml by serial dilutions and 5 µl of each of the serially diluted BSA standards was added to each well in triplicates along with a blank (i.e. no BSA). 1 µl of the cell lysate (i.e. unknown protein sample) was added to each well in triplicates. 100 µl Bradford reagent was added to each well and absorbance was recorded on a microplate reader at 595 nm. The mean absorbance of each standard (blank corrected) was used to draw a scatter plot and a straight line equation was deduced from the trendline. The absorbance of the unknown samples was extrapolated onto the graph and concentrations of the unknown samples were thus derived.

CHAPTER – 4

DISCERNING THE MECHANISM OF ACTION OF HTRA4 AND FUNCTIONAL REDUNDANCY

CHAPTER 4: DISCERNING THE MECHANISM OF ACTION OF HTRA4 AND FUNCTIONAL REDUNDANCY

4.1 Introduction

High temperature requirement protein A (HtrA) is a family of oligomeric serine proteases that are conserved from prokaryotes to humans. The *E coli* counterparts DegP, DegQ and Deg S have dual regulatory functions; they act as molecular chaperones at lower temperatures while exhibit proteolytic activity with increase in temperature. There are four homologous HtrA proteins in human cells: HtrA1, HtrA2/Omi, HtrA3 and HtrA4 [23, 31, 32]. Loss or dysfunctions of these proteins can results into development of severe pathologies or diseases, including oncogenesis, neurodegenerative diseases and arthritic disorders. In eukaryotic organisms HtrA proteins play important roles including function under normal and stress conditions, and participate in regulation of cell death, cell signalling and motility, maintenance of mitochondrial homeostasis, embryo implantation and other processes.

These proteins share a common domain architecture that comprise an N-terminal region, serine protease domain (SPD) for enzymatic activity, PDZ domain (postsynaptic density of 95 KDa, disk large, and zonula-occludens 1 domain) for protein-protein interactions [135, 136] Apart from these common domains, all except HtrA2 harbour a Kazal like domain that acts as an inhibitor for serine protease activity, Insulin-like growth factor binding protein domain (IGFBP) and a signal peptide. While, HtrA1, HtrA3 and HtrA4 share very similar domain organizations,

the uniqueness of HtrA2 is manifested through absence of Kazal and IGFBP domains and existence of a distinct N-terminal region, which includes a prominent IBM (IAP binding motif) and a transmembrane domain [135, 136]. Available literature suggests that these serine proteases form functional oligomeric assemblies that are primarily mediated through their N-terminal region. While, hexameric and higher order oligomeric complexes are observed in bacterial HtrAs, their human counterparts are mostly trimeric in nature. For example, in *Escherichia coli* HtrA (DegP), the trimeric units further oligomerize to form higher order oligomers upon substrate binding ranging from trimeric to 24-mer [4]. Therefore, despite overall structural conservation, subtle conformational differences and distinctness in oligomeric assembly define diversity in HtrA cellular and pathophysiological functions. In humans, these proteases are involved in numerous cellular processes ranging from maintenance of mitochondrial homeostasis to cell death, deregulation of their normal functions leads to various diseases that include neurodegeneration, neuromuscular disorders, arthritis, age-related macular degeneration, pregnancy-specific pre-eclampsia and cancer [18, 20, 22, 33, 137–139]

Among human HtrA homologues, HtrA1 and HtrA2 are well characterized with available high-resolution crystal structures. The secreted trimeric HtrA1 exhibits endo-proteolytic activity, including autocatalytic cleavage [38, 57]. It binds, cleaves and activates a variety of targets, which are involved in important physiological processes such as maintenance of cell death and cell signaling. HtrA2, the most elaborately studied family member, has the unique characteristic of being allosterically activated both through its N-as well as C-terminal regions [140, 141]. It is a mitochondrial serine protease that has been associated with both caspase-dependent as well as independent apoptosis. The latter is believed to be achieved by cleavage of important cellular proteins directly through its serine protease activity. Upon

apoptotic induction, the first 133 residues that include the mitochondrial localization signal get cleaved, forming the active mature form of HtrA2 with the exposure of the tetrapeptide IBM (IAP-binding motif) that comprises AVPS residues at the N-terminus. This IBM motif is critical for binding antiapoptotic IAPs (inhibitor of apoptosis proteins) and relieves their inhibition on caspases. Therefore, involvement of HtrA2 in apoptosis and other cellular processes has implicated it in various diseases including neurodegeneration and cancer. Although, some studies have been done on HtrA3, its partial low-resolution structure might not be sufficient for providing a detailed snap-shot of its intricate structural complexities [53]. Among the four human HtrAs, HtrA4 is the least characterized protein with respect to both structure as well as its functions. It has been found to be up-regulated in pre-eclampsia (PE) and hence has been suggested to be used as a bio-marker of PE [33]. It has also been altered in many cancers such as glioblastoma, breast carcinoma, pancreatic and prostate cancers making it as emerging potential therapeutic target [22, 71]. Therefore, an intricate dissection of HtrA4 structure with understanding of its functional reciprocity becomes imperative to harness its properties with desired characteristics. In this study, *in silico*, biochemical and biophysical characterizations of HtrA4 have been performed to delineate the role of different domains (individually and in different combinations) in defining substrate specificity, oligomerization, stability and allostery of HtrA4. Our studies highlight the importance of the short N-terminal region in enzyme catalysis and oligomerization. The observation that PDZ positively influences protease activity suggests requirement of allosteric modulation and intricate inter-molecular interaction network in HtrA4 functions. This information coupled with functional enzymology studies would help decipher the mechanism of activation of HtrA4.

4.2 Results

4.2.1 Sequence alignment of HtrA4 with other family members

Human HtrA family members have similar domain organizations. Therefore to understand the sequence similarity among these proteases, we aligned the sequence of HtrA4 with other family members, Figure 4.1 shows the sequence alignment of HtrA4 with its family members. ClustalW software was employed to obtain alignment of HtrA4 with other human counterparts. Sequence identity and similarity obtained after aligning the individual HtrA1, HtrA2 and HtrA3 sequences with HtrA4 using EMBOSS stretcher pairwise sequence alignment program (https://www.ebi.ac.uk/Tools/psa/emboss_stretcher/), and results were shown in Table 4.1.

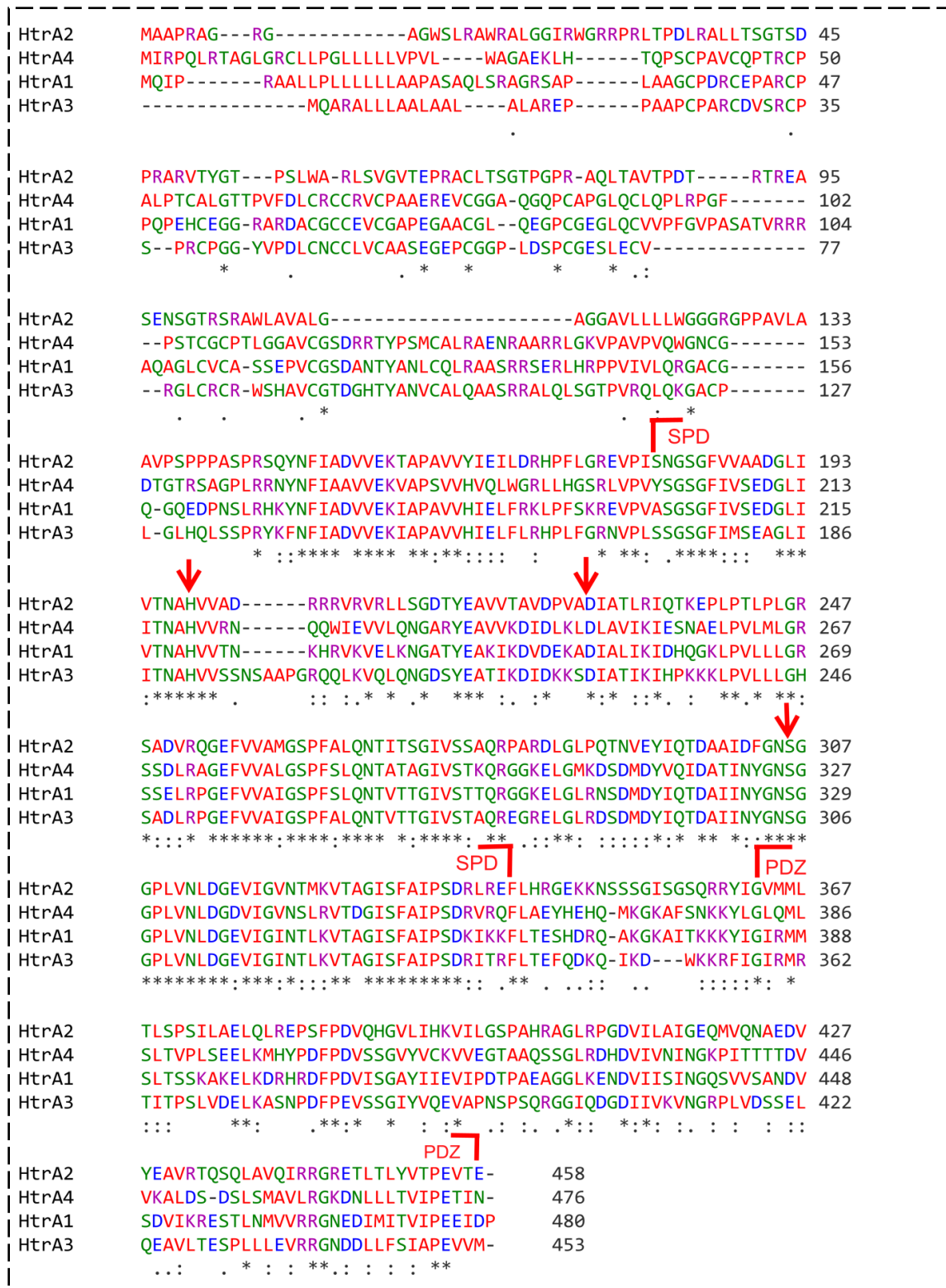


Figure 4.1: Multiple sequence alignment (MSA) analysis of HtrA proteins. Full length sequences of HtrA1, HtrA2, HtrA3 and HtrA4 are aligned using Clustal Omega

(<https://www.ebi.ac.uk/Tools/msa/clustalo/>) [142]. Catalytic triad residues (H218, D248, and S326) are denoted by red inverted arrows. Domain boundaries are indicated above where SPD denotes Serine Protease Domain, and PDZ indicates postsynaptic density protein (PSD95), *Drosophila disc large tumor suppressor (Dlg1)*, and *zonula occludens-1 protein (zo-1)*. Identical amino acids are depicted by (*), conserved amino acids are depicted by (:) and semi-conserved amino acids are depicted by (.).

Table 4.1: Comparison of HtrA4 with other family members

Sequence identity and similarity obtained after sequence alignment with EMBOSS Stretcher program.

	With HtrA1	With HtrA2	With HtrA3
Sequence similarity	67.2%	54.5%	65.0%
Sequence Identity	51.5%	37.4%	48.9%

4.2.2 Endogenous level of HtrA4 in different cell lines

Several *in vitro* and *ex vivo* studies along with site-directed mutagenesis experiments with full length (52kDa) and truncated versions (~36kDa) of HtrA2 revealed that HtrA2 is autocatalytically processed at a particular site in an intermolecular manner results in 36-kDa mature protein fragment which starts from AVPS. Seong, Y.M. *et al.* identified the site and amino acids where the autoproteolytic cleavage was occurring, this autocatalytic processing results in exposure of an inhibitor of the apoptosis protein (IAP) binding motif in its N-terminus [143]. Various literature sources suggest that the autocatalytic processing of HtrA2 is crucial for

regulating HtrA2 mediated apoptotic cell death [144]. The serine protease HtrA2 is released from mitochondria during apoptosis has AVPS sequence [79, 145, 146]. Our extensive search for conservative motifs and consensus sequence resulted in identifying the N-terminal AVPV residues which are similar to HtrA2 AVPS motif (IAP binding motif); furthermore, when we analyzed the endogenous levels of HtrA4, we could observe a ~36kDa band along with the full-length form (51kDa) (Figure 4.2). Expression of the endogenous level of HtrA4 was analyzed in various cancer cell lines. Using Trypan blue staining and hemocytometer, an equal number of cells of MCF7, HeLa, A549, SiHa, and HEK 293 (normal) were calculated and seeded. The cells were grown in complete media, were lysed, and protein concentration was estimated by Bradford's method. Purified HtrA4 expressed in Rosetta™(DE3)pLysS cells was used as a positive control for HtrA4. The bacterial cell lysate was used as a negative control for antibody specificity in the study. From our results, it is clear that all of the above-mentioned cell lines showed almost similar protein levels of HtrA4, we could also observe a 36kDa band indicating that HtrA4 also has a maturation process similar to that of HtrA2. However, this needs to be confirmed with additional experiments.

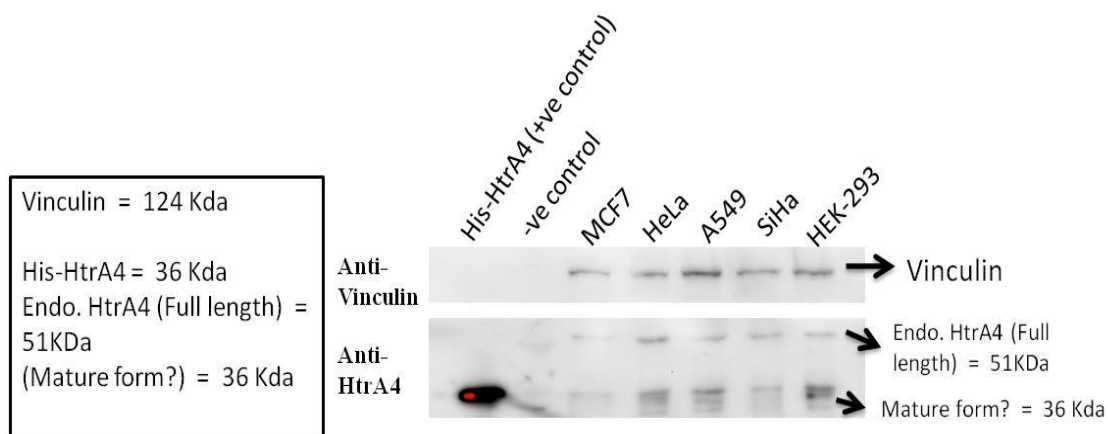


Figure 4.2: The endogenous level of HtrA4 in various cancer and normal cell lines:

The top bands indicating expression of Vinculin in all different cell lines were observed to have equal intensity, indicating an equal amount of protein (20µg) loaded in the analysis. Bands of HtrA4 in lane 3,4, 5, 6, and 7 indicate the endogenous level of HtrA4 full length (51kDa) in the MCF7, HeLa, A549, SiHa, and HEK293 (normal) cell lines. All cell lines showed expression of HtrA4 and ~36 kDa band of HtrA4 also observed in all the cell lines.

4.2.3 Cloning of different domains, expression, and purifications

Different variants of HtrA4 were generated using polymerase chain reaction and site-directed mutagenesis to understand the role of different domains and their combinations in regulating HtrA4 stability and functions (Figure 4.3). Previously it has been reported that N-terminal aromatic residues are crucial for maintaining oligomeric architecture and functions of prokaryotic and human HtrAs [60]. Since HtrA4 also has this conserved N-terminal ¹⁴⁴AVPV (IAP binding motifs) and ¹⁶⁷Y, ¹⁶⁹F and ²⁷⁶F (Trimerization motifs) residues similar to that of HtrA2 (sequence alignment with mature HtrA2 given in figure 4.4). The endogenous level of HtrA4 in different cell lines also showed a ~36kDa band. Based on these observations, we assumed that maturation site and processing of HtrA4 is similar to that of HtrA2; we cloned HtrA4 starting from AVPV residues, and we referred this construct as HtrA4. We generated N-terminal deleted construct (SPD-PDZ) to understand the role of N-terminal in oligomerization, stability, and functions of HtrA4. Similarly, PDZ deleted variant (N-SPD) was made to understand the regulation of protease activity by PDZ domain. It was reported in the literature that in DegP, DegS, and HtrA2, PDZ inhibits the protease activity by restricting the substrate accessibility to the active-site [147]. Similarly, only the SPD variant was also generated for understanding the role of the N-terminal region and PDZ inhibition in enzyme catalysis. Inactive

HtrA4 was generated by mutating the serine 326 to alanine which acted as a control for all enzymatic and other studies. The different domains were PCR amplified and cloned in the pET20b (+) vector and confirmed. Confirmed clones were transformed into different expression strains of E.coli and screened for the expression. The expression was observed in Rosetta™(DE3)pLysS and confirmed with mass spectrometry as well as western blot analysis using anti-His antibody. After expression analysis, HtrA4 active and inactive (S326A), SPD-PDZ, N-SPD, and SPD proteins were purified by Ni-IDA affinity chromatography (Figure 4.5).

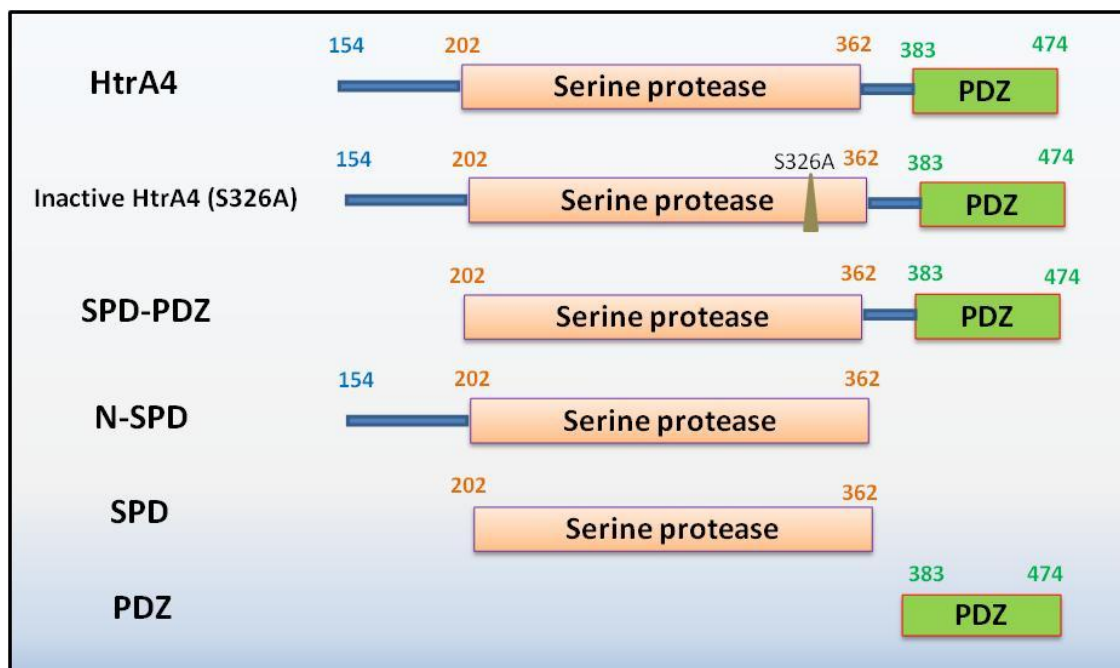


Figure 4.3: Schematic representation HtrA4 and various other different sub domains generated for the study. Domains are color-coded: light orange boxes indicate the protease domain (202 –362 residues); dark green boxes indicate PDZ domain (383 –474 residues); solid lines indicate N-terminal region (154–202 residues) and linker region (362–383 residues).



Figure 4.4: Sequence alignment of mature HtrA2 and HtrA4: mHtrA2 (mature HtrA2) aligned with HtrA4. alignment performed using online software ClustalW2. (HtrA2-UniProtKB ID: O43464 and HtrA4-UniProtKB ID: P83105). IAP binding and trimerization motifs are highlighted.

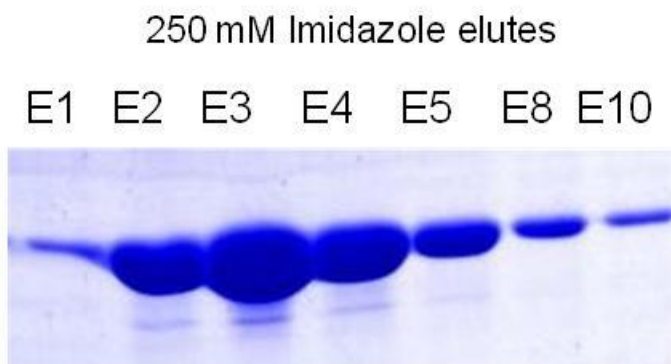


Figure 4.5: Purification of HtrA4 protein expressed in Rosetta (DE3) pLysS expression system. HtrA4 was purified with Ni-NTA resin, approximately ten fractions analyzed on 12% SDS-PAGE gel and stained with Coomassie blue. E1-E10 are different elutes of the protein. E1 represents Elute1, which was collected after adding 250 mM concentration of imidazole as a competitive binder to elute the His-Tagged protein. The theoretical molecular weight of HtrA4 is 36 kDa.

4.2.4 Secondary and tertiary structural characterization of HtrA4

To check for structural perturbation, if any, in the S326 HtrA4 variant, the secondary structural analyses of the inactive mutant, as well as the HtrA4 protein, were performed using far UV CD. The similarity in secondary structure for S326A and HtrA4 as observed (Figure 4.6) and calculated using K2D2 software ($84.2 \pm 0.8\%$ and $82 \pm 0.7\%$ helical content, respectively) demonstrate that the mutation is not structurally perturbing [148]. Melting curves of HtrA4 and inactive HtrA4 suggest that the proteins have same thermal stability with a $T_m \sim 58^\circ\text{C}$ as shown in Figure 4.6. We could not calculate the T_m for the rest of the domains as they started precipitating after 45°C . Fluorescence emission of HtrA4 and denatured HtrA4 was measured using Fluorolog-3 spectrofluorometer. Trp and Tyr have absorption maxima at 280 nm, 277 nm respectively (extinction coefficients $5563 \text{ cm}^{-1}/\text{M}$ and $1220 \text{ cm}^{-1}/\text{M}$, respectively). Trp absorbs 5

times more than the Tyr at 280 nm. At 280 nm both the Trp and Tyr will be excited. At 295 nm only tryptophan is excited. The extinction coefficient of Trp at 295 is $1614 \text{ cm}^{-1}/\text{M}$ and of Tyr is only $56 \text{ cm}^{-1}/\text{M}$, i.e., at 295 nm Trp absorbs ~30 times more than the Tyr at 295 nm. In HtrA4 amino acid sequence there are three Trp and nine Tyr. Fluorescence spectra recorded with 280, 295nm excitation followed by emission between 310-400 nm. Purified HtrA4 protein showed a blue shift ($>10 \text{ nm}$) in emission maxima when compared to unfolded, suggesting that the protein might have folded properly (Figure 4.7).

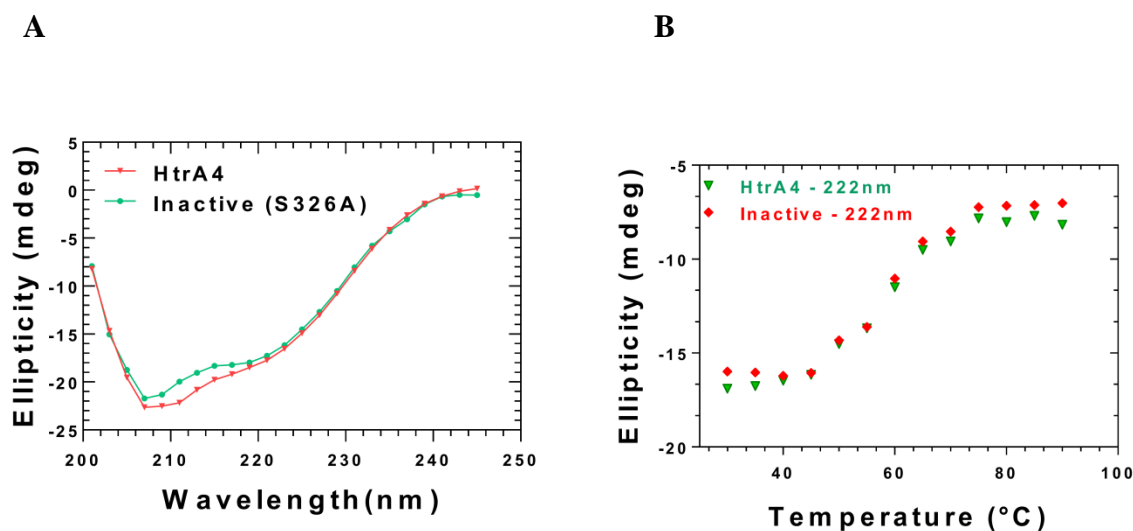


Figure 4.6: A) Comparison of secondary and tertiary structural properties of HtrA4 and its variant: Far-UV CD of HtrA4 and its variants at 25°C. These spectra are representative of three sets of experiments, averages of three scans were baseline-subtracted, and the α -helical percentage was calculated. B) Thermal denaturation curves for HtrA4 and its variant within the temperature range of 30–90°C. Variation of the CD signal at 222nm recorded within a temperature range of 30-90°C with a heating rate of 2°C/min.

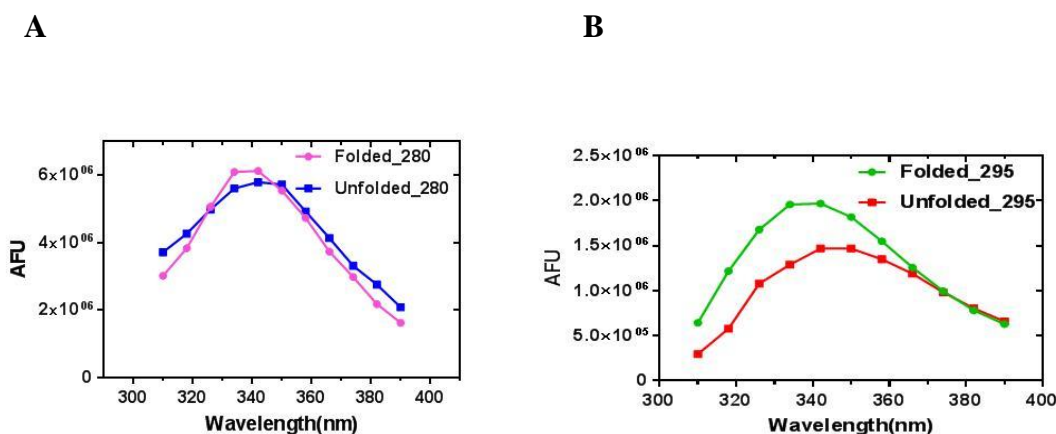


Figure 4.7: Fluorescence emission spectra of HtrA4 protein. Fluorescence emission spectra of urea denatured and renatured HtrA4 at A) 280, B) 295nm and excitation at 310 to 400 nm emission wavelengths. The refolded proteins have low emission maxima and show considerable blue shift indicating that bacterially expressed and purified HtrA4 protein is well folded. (Emission max 295 folded: 337nm, emission max 295 unfolded: 349nm, emission max 280 folded:339nm and emission max 280 unfolded: 351nm)

4.2.5 Native oligomerization status of HtrA4 and its domains

It has been reported that the functional unit of HtrA family protein appears to be a trimer, which is stabilized exclusively by residues of the protease domains. Moreover, it has been shown that, in HtrA1, HtrA2, and HtrA3 N-terminal aromatic residues are prerequisite for maintaining their trimeric architecture through intermolecular van der Waals interactions [36]. Prokaryotic HtrAs family members are capable of forming pyramidal 3-mers to higher-order complexes consisting of up to 24 molecules have been reported [149, 150]. DegS_{EC} is a stable trimer whereas active DegQ_{EC} forms a higher-order oligomer comprising 12 monomeric subunits and active DegP_{EC} forms 24- mer [34, 150]. Human HtrA1, HtrA2 and HtrA3 forms 3-mers [53, 59, 60].

Therefore to understand the oligomerization status of various HtrA4 domains, gel filtration chromatography was performed using superdex 200 gel filtration column. Elution profiles of all HtrA4 variants were monitored, and their respective molecular weights were calculated from the calibration curve generated from protein standards (Figure 4.8 and Table 4.2). The estimated molecular weights of the proteins are shown in Table 4.2, which demonstrates that HtrA4 and N-SPD are trimers with intact N-terminal regions. In case of HtrA4, we could observe a small fraction of monomeric population along with the dominant trimeric population. Further to understand the role of N-terminal in trimerization of HtrA4, gel filtration chromatography was performed with constructs devoid of N-terminal region such as SPD, and SPD-PDZ and they eluted as monomers reiterating the importance of N-terminal in homotrimerization as suggested within the literature.

Previous literature reports suggested that three residues Y147, F149, located in the N-terminal domain and F256 in the protease domain are crucial for maintaining the oligomeric architecture of HtrA2 [60, 151]. Pairwise sequence alignment showed that HtrA4 also has identical aromatic residues at the respective regions (Figure 4.4). Therefore, to understand the role of these residues for HtrA4 trimerization, we have performed gel filtration chromatography with a series of mutations mentioned in Table 4.2. However, unlike HtrA2, a single mutation of F169 to either A or D did not alter its oligomerization status. Moreover, the double mutant HtrA4 (F169A, Y167A) also could not bring any change to the oligomerization status of the serine protease. Mutation of all the three residues in HtrA4 (Y167A, F169A, F276A) however led to protein aggregation and subsequent elution in void volume during gel filtration. Overall these observations suggest that single or double mutation alone might not be sufficient for disruption

of HtrA4 trimerization and mutation of all the three residues might have led to structural perturbation and hence protein aggregation.

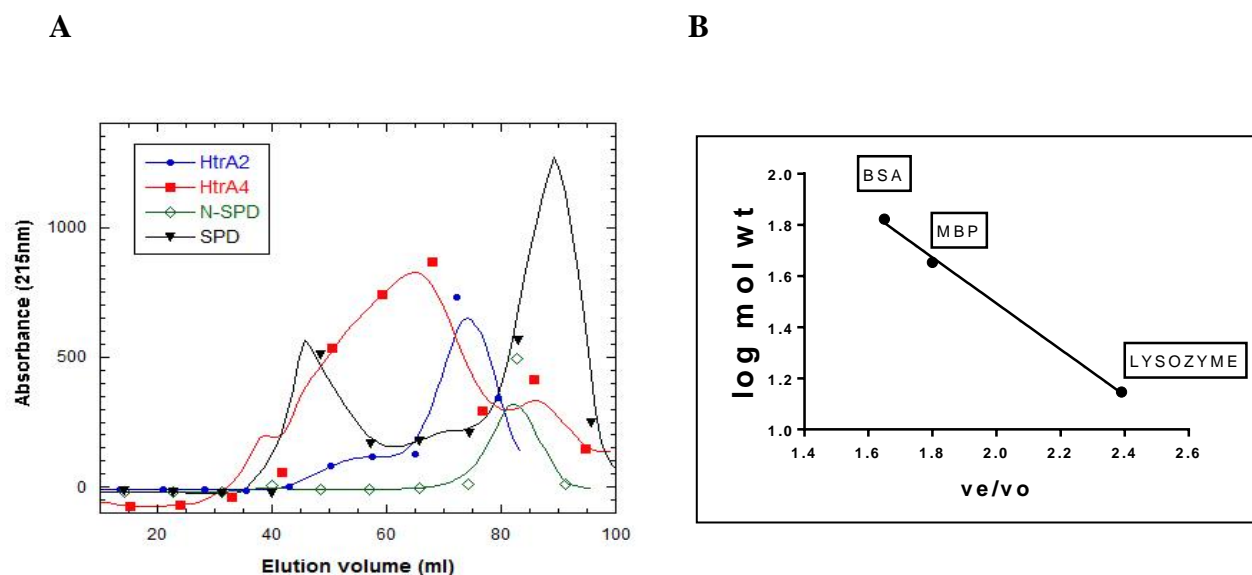


Figure 4.8: Gel filtration results of HtrA4 and its domains. **A)** Recombinant HtrA4 and sub-domains purified using Ni NTA chromatography and further subjected to gel filtration chromatography (Superdex 200 10/300 HR column). **B)** The standards used for generating the calibration curve were Bovine Serum Albumin (BSA), Maltose Binding Protein (MBP) and Lysozyme.

Table 4.2: Oligomeric properties of different HtrA4 constructs

	Protein	Theoretical molecular mass (kDa)	Calculated molecular mass (kDa)	Oligomeric status
1	HtrA4 (N-SPD-PDZ-Inactive- S326A)	109	120±10 36±8	Trimer(~80%) monomer(~20%)
2	N-SPD	71.4	66±5	Trimer
3	SPD	19	24±8	Monomer
4	HtrA4 (N-SPD-PDZ-Inactive- S326A) + β casein	NA	140±10	Trimer
5	Y167A/D	NA	120±10 36±8	Trimer(~80%) monomer(~20%)
6	Y167A, F169A	NA	120±10 36±8	Trimer(~80%) monomer(~20%)
7	Y167A, F169A, F276A	NA	NA	Aggregated
8	HtrA2	109	108±2	Trimer
9	Blue dextran	2000	NA	NA
10	BSA	66	NA	NA

11	MBP	43	NA	NA
12	Lysozyme	14.4	NA	NA

4.2.6 Oligomerization status of HtrA4 in the presence of substrate

It is known that the majority of the HtrA family proteases upon substrate binding are converted from lower-order oligomers to form higher-order oligomers with enhanced protease activity. For example, *E. coli* DegP, which is a close ortholog of human HtrAs, is converted from 6-mers to the 12- and 24-mers in the presence of substrate [63].

Therefore to identify whether the oligomerization status of HtrA4 is affected in the presence of substrate, we incubated proteolytically inactive HtrA4 (S326A) with the generic substrate β -casein and analyzed the samples using gel filtration chromatography. Further, the peak fractions were collected and analyzed on SDS-PAGE. In the presence of β -casein, only one peak was observed, and the peak fraction contained HtrA4 as well as β -casein (Figure 4.9 and Table 4.2). The observed mass of HtrA4- β -casein co-eluted fraction was found to be ~140 kDa, which suggests that one trimeric HtrA4 (110 kDa) might be bound with one molecule of β -casein (25 kDa). However, if HtrA4 would have been transformed into higher-order oligomer (>trimer) in the presence of β -casein, then the calculated mass should have been higher than 240 kDa. Since the eluted HtrA4 in the presence of β -casein appears to be equivalent to the trimer, suggest that under these experimental conditions, HtrA4 does not form large multimers similar to other bacterial HtrAs. However, upon incubation of inactive HtrA4 with its generic substrate β -casein, only the trimeric peak was observed with complete disappearance of the monomeric population.

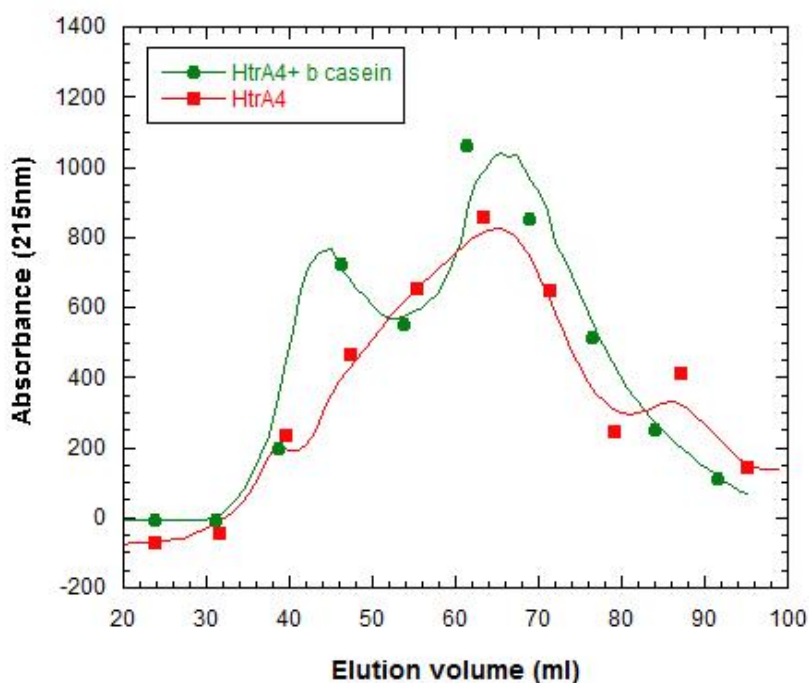


Figure 4.9: Gel filtration results of HtrA4 in presence and absence of substrate. HtrA4, β -casein mixture was loaded on to a Superdex 200 10/300 HR column and eluted with buffer containing 20 mM $\text{Na}_2\text{HPO}_4/\text{NaH}_2\text{PO}_4$ and 200 mM NaCl at pH8.0. Elution was followed by monitoring the absorbance at 215 nm.

4.2.7 Protease assays to understand the role of different domains and the effect of temperature on catalytic activity

We want to study the kinetics of HtrA4 and its subdomains to understand the role of different domains in enzymatic activity. Protease assays of HtrA4 and its domains were performed using generic substrate β -casein. After purification of different HtrA4 domains, they were incubated

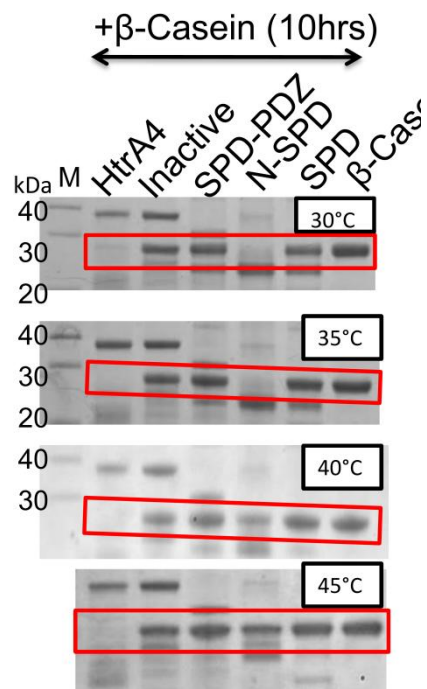
with β -casein. The cleaved β -casein after 10hrs was semi quantified using Image J software (Figure. 4.10 A and B). From the graphical data, it is evident that the active HtrA4 and the N-SPD domain of HtrA4 showed significant activity, while the constructs lacking the N-terminal domain, i.e., SPD-PDZ and SPD were found to be completely inactive and did not cleave the β -casein. These observations highlight the importance of the N-terminal region for HtrA4 enzymatic activity.

In 2013, two independent groups (Chaganti et al., and Zurawa-Janicka et al.) observed that HtrA2 activity markedly increases with temperature, they also gave a model of HtrA2 activation and provided insights into the mechanism of temperature-induced changes in HtrA2 structure which lead to the increased activity above 30°C [152, 153]. So, to understand the effect of temperature on HtrA4 catalytic efficacy, we incubated different domains of HtrA4 with β -casein at different temperatures ranging from 30 °C to 45 °C for 10 hours and analyzed using Tris-tricine gels and semi quantified using Image J software (Figure 4.10 A and B). From the results, it is evident that an increase in temperature leads to a gradual increase in activity above 30 °C, continuing up to 45 °C. We confined all temperature based assays to 45 °C because we could not see any increase in activity above 45 °C from the gel-based assay (Figure 4.10 C). As per our observations, active HtrA4 could cleave β -casein extensively (>95%) at 35 °C and 40 °C. N-SPD did not cleave β casein at higher temperatures (>35 °C); this might be possible because it lacks the PDZ domain at the c-terminus and more susceptible to denaturation at higher temperatures. These experimental data highlight the importance of the effect of temperature on HtrA4 catalytic efficacy.

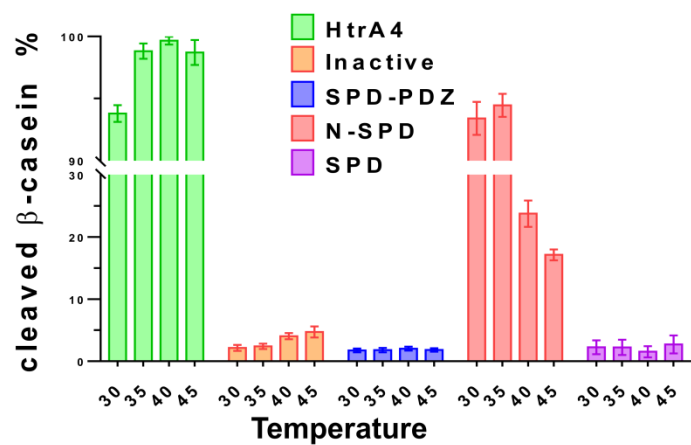
Kinetics of active HtrA4 was measured using FITC casein (Figure 4.10 D). From the quantitative enzymatic study of active HtrA4, the observed V_{max} (1.9×10^{-12} M/s) and k_{cat} (0.06×10^{-6} s⁻¹)

were relatively low which indicates lower enzymatic reaction and turnover when compared with the other family members [53, 61] (Table 4.3). The Hill coefficient value of HtrA4 found to be 1.3 which indicates HtrA4 also shows allosteric activation like other members, while the K_m value found to be almost similar to HtrA2 suggesting the similar affinity for binding with the substrate. Similar findings were observed in gel-based assays also, the time taken to cleave the same amount of β -casein and XIAP is much higher for HtrA4 when compared with HtrA2 in similar conditions. HtrA2 cleaves 6 μ g of β -casein into two small fragments completely in 5 minutes while HtrA4 cleaves 80% β -casein in 6 hours into six different size fragments, similarly HtrA2 cleaves ~8 μ g of GST-XIAP in approximately 1 hour while HtrA4 cleaves 85% XIAP in 24 hours. For the representative purpose, assay gels are shown in figure 4.11 were incubated for 3hrs and 37°C (Figure 4.12 and Figure 4.13).

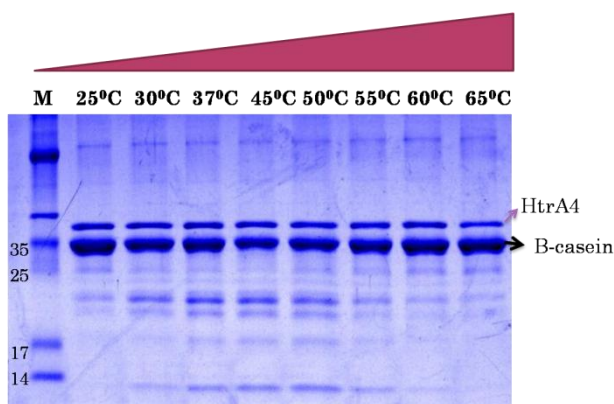
A



B



C



D

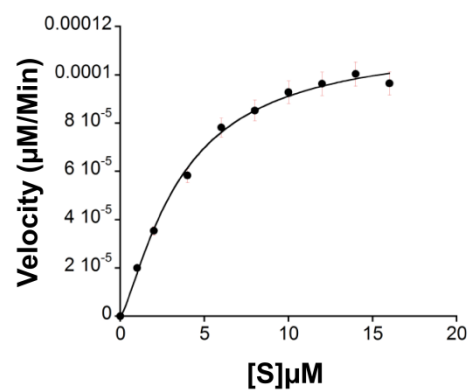


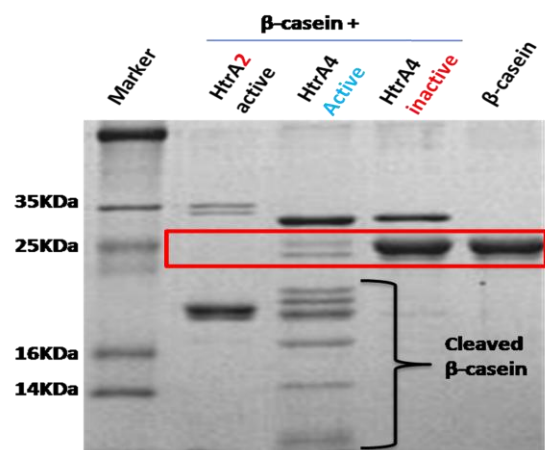
Figure 4.10: Proteolytic activity of HtrA4 and its variants with β -casein as a substrate. A) Different constructs of HtrA4 were incubated with β -casein at 37 °C for 10 hrs. Reaction

samples were resolved by 15% Tris-tricine SDS-PAGE and visualized with coomassie brilliant blue staining. B) The intensity of the substrate remained after 10 hrs was semi-quantified using Image J software and the cleaved β -casein percentage was calculated and plotted. (The error bars are the representation of SEM, n=3). C) HtrA4 incubated with β -casein at different temperatures for 35 minutes and resolved on 15% SDS-PAGE, highest protease activity found at 45°C. D) Steady-state kinetic parameters of HtrA4. The steady-state kinetic parameters were calculated from the reaction rates by fitting the data to the Hill form of the Michaelis–Menten equation. Results are represented as mean \pm SEM, n=3.

Table 4.3: Kinetics of HtrA family proteins.

	HtrA2 [61]	HtrA3 [53]	HtrA4 (N-SPD-PDZ)
$K_m(\mu\text{M})$	4.60 ± 0.5	0.958	4.84 ± 0.8
$V_{\max} (\text{M/s})$	4.08×10^{-9}	-	1.9×10^{-12}
$k_{\text{cat}} (\text{s}^{-1})$	0.02 ± 0.004	0.029	$0.06 \times 10^{-6} \pm 0.01$
$k_{\text{cat}}/K_m (\text{M}^{-1} \text{s}^{-1})$	4.5×10^3	30271	0.0123
Hill coefficient	2.8	-	1.3

A



B

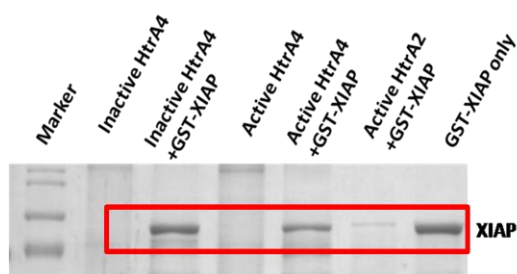


Figure 4.11: Proteolytic assays of HtrA2 and HtrA4 with substrates. HtrA4 and HtrA2 incubated with β -casein and with XIAP at 37°C for 3 hrs. Reaction samples were resolved by 15% SDS-PAGE and visualized with coomassie brilliant blue staining.

4.2.8 Substrate specificity of HtrA4

Cleavage specificity of HtrA1, HtrA2, and HtrA3 has been well documented in the literature [59, 154–157], therefore, to understand whether HtrA4 shares similar substrate specificity as its the other isoforms we determined the substrate specificity of HtrA4 using the generic substrate β -casein. Proteolytically cleaved fragments (~23KDa, 19KDa, 13KDa, 7KDa and less than 5KDa) of β -casein were subjected to N-terminal sequencing by Edman degradation. The specificity profile of N-terminal sequence analysis of these fragments identified three preferred cleavage sites on β -casein (Figure 4.15 A and B). The first cleavage site is between 15A-16R, second

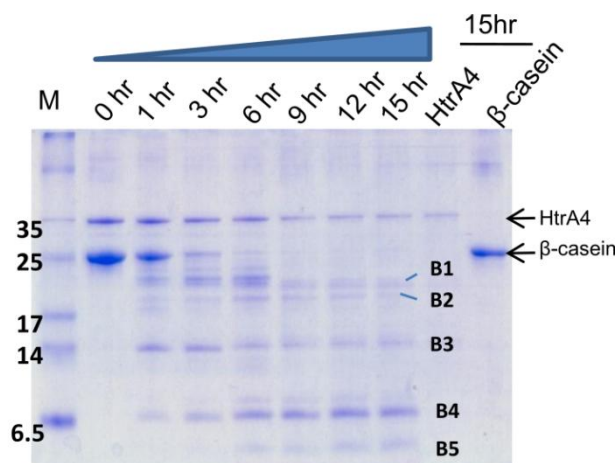
between 108M-109G and third cleavage site is between 170V-171M amino acids respectively. Cleavage at single or multiple sites resulted in a combination of different peptide fragments as shown in Figure 4.15 C.

Our observations suggest that HtrA4 has a strong preference for aliphatic residues at P1 (A, V, and M) position. Interestingly, this preference order for aliphatic residues at P1 position very well matches with the other three human HtrA homologs. The P2 position is occupied by aliphatic (L and V) and polar (T) residue, HtrA1, and HtrA2 also preferred similar aliphatic residues (L) at this position. At P3 and P4 positions, HtrA4 preferred aliphatic (A and L), polar (P and E), which also matches with HtrA1 and HtrA3 preferences. At P1' position, HtrA4 preferred aliphatic (G and M) and polar amino acids (R), at similar position other family members preferred the same amino acids. At P2' position like other family members, HtrA4 also preferred aromatic (F) and aliphatic (V) residues. At P3' position, HtrA4 preferred polar (S and P) and aliphatic (L) residues. At the same position, HtrA2 and HtrA3 showed preference to similar polar residues (S and P) only. At P4' position, other family members showed preference to mostly aromatic (F, Y, and W) and polar (S), while HtrA4 preferred polar (P, E and K) residues [16, 51, 59, 158]. Overall, these results suggest that HtrA family members mostly prefer similar kind of amino acids at the cleavage site (Table 4.4).

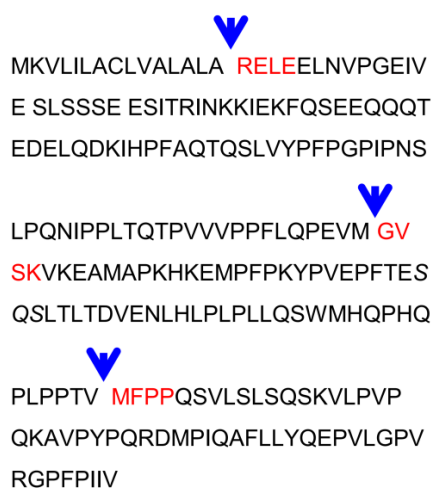
We also tried to evaluate the HtrA4 activity against different artificial substrates like malic dehydrogenase, citrate synthase, lysozyme, bovine serum albumin and ribonuclease A. These artificial substrates used in understanding the substrate specificity, oligomerization status of HtrA3 by Glaza, P. *et al.* and also implemented to understand oligomerization status, activation and substrate specificity of HtrA1 by Truebestein, L. *et al.* [53, 59]. HtrA4 did not cleave these artificial substrates, activity against malic dehydrogenase was present but negligible to get

cleaved products. From our data, it is clear that, although these family members have similar substrate specificity they might not share the same substrates suggesting that additional structural elements might be required to identify and bind to a particular substrate. Identifying its natural substrates will help us understand more about HtrA4 substrate specificity as well as functions.

A



B



C

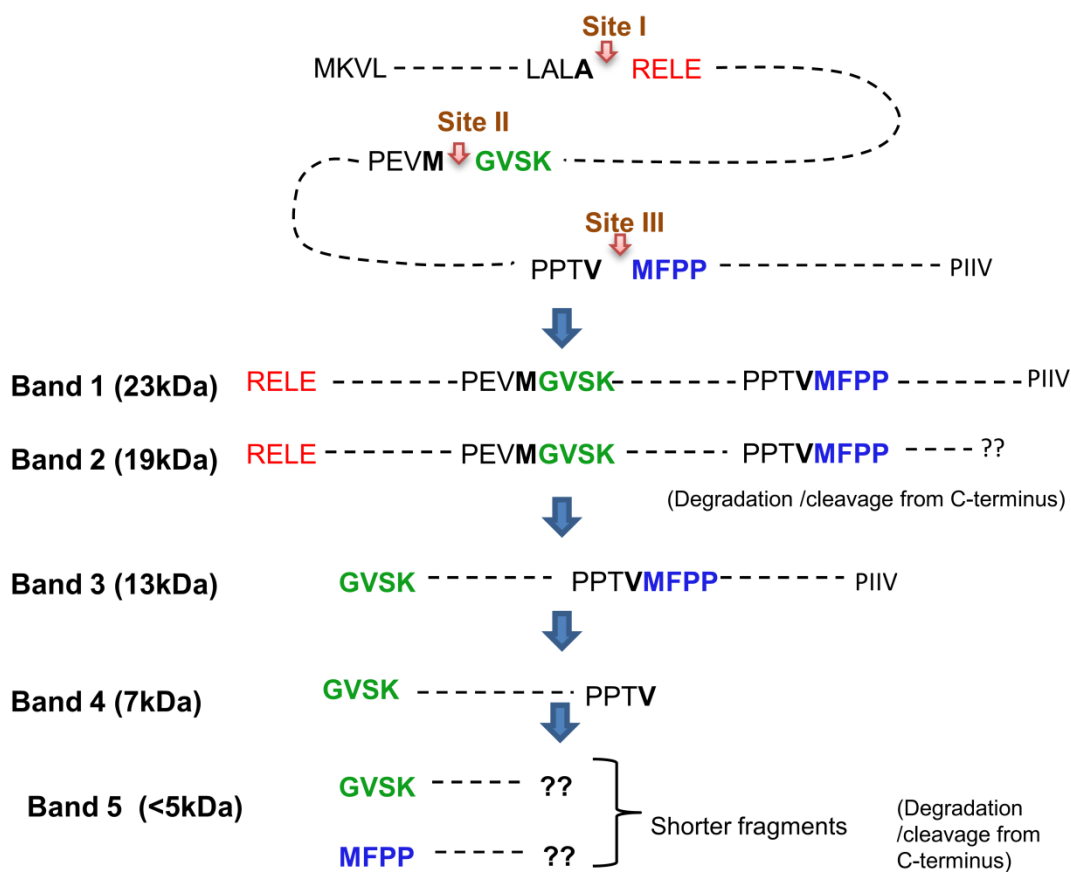


Figure 4.12: Generic substrate β -casein cleavage by HtrA4. A) Protease assays of HtrA4 with β -casein: peptide fragments sent for N-terminal sequencing are indicated as B1, B2, B3, B4, and B5. B) Residues identified by N-terminal sequencing are highlighted in red. Blue arrows indicate preferred cleavage sites. C) Schematic representation of cleavage products observed on the gel after proteolysis. The 25 kDa β -Casein is cleaved into various fragments after incubating with HtrA4, initially, cleavage at site one generated fragments B1 (~23kDa) and B2 (~19kDa), upon further incubation, cleavage at site two generated B3 (~13kDa). Further incubation, cleavage at site three generated B4 (~7kDa) and B5 (<5kDa) bands.

Table 4.4: Substrate specificity of HtrA family members:

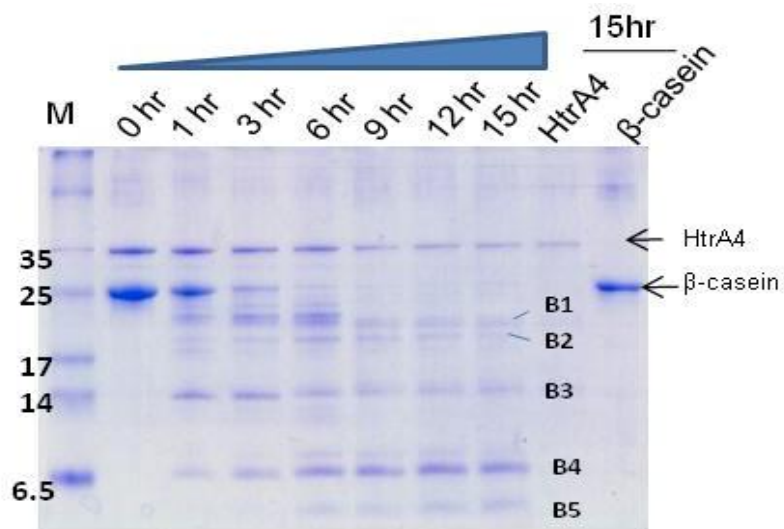
Positions	HtrA1 [51, 59]	HtrA2 [16, 158]	HtrA3 [53]	HtrA4
P1	A, M, I, V, L	M, I, V	A, I, V, L	A, M, V
P2	L, T	L, R	E, S, Q, P	L, V, T
P3	Q, L	K, R, Y	E, P, L, S, V	E, A, P
P4	A, P	L, P, I	L, P, Q	L, P
P1'	R, S, T	S, A	S, A, E	R, G, M
P2'	L, P, W	Y, F	V, Q, L, G	E, V, F
P3'	V, M, D	S, P, Y	S, P, V	S, P, L
P4'	F	F, Y, S	L, G, W, S	E, K, P

4.2.9 Mechanism of cleavage and the role of PDZ in substrate cleavage:

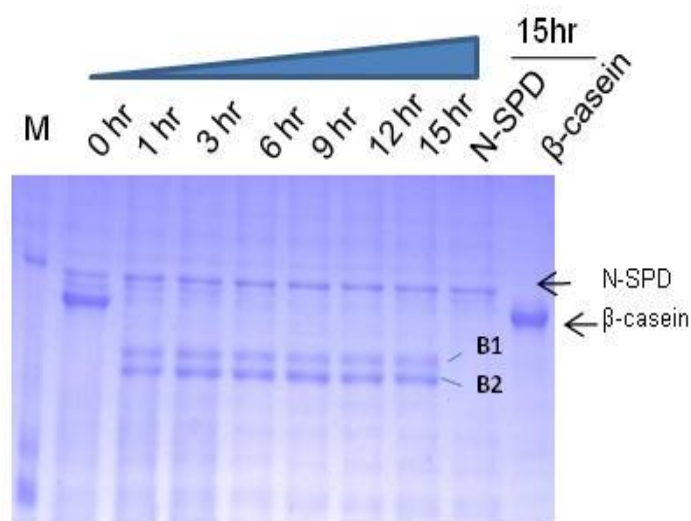
HtrA family members mostly recognize consensus sequence in substrates and cleave them at a particular position. Mitochondrial HtrA2 regulates the levels of misfolded proteins in a manner very similar to its bacterial counterparts, DegP and DegS [159]. In our study, we used β -casein as substrate and identified cleavage specificity of HtrA4. Because of its unstable secondary structure, β -casein cannot form a well-defined three-dimensional structure, indicating that no other well defined structural elements required for binding and cleavage of β -casein by HtrA4 other than amino acid sequence [160]. Various literature reports highlighted different models of substrate cleavage by HtrA family of proteases. In hold-and-bite model, C-terminus of substrates is bound by the PDZ domain, and this facilitates the cleavage of an upstream sequence at a distant active site. In hold-bite-and-rebind model, peptide binding sites of the PDZ and catalytic domains exhibit strikingly similar substrate specificities; both sites can anchor the substrate or ligand. After cleavage by protease domain, PDZ domain captures released peptide fragments from the proteolytic sites via their newly generated C-termini and prepares them for the next degradative cycle. This process generates multiple shorter fragments (Figure 4.13 C). In this model PDZ acts as an allosteric switch, upon binding to substrates, it propagates the signal to the protease domain through neighboring regulatory loops [67–69]. From our data, it is clear that full-length HtrA4 cleaved substrate (β -casein) into multiple fragments, whereas Δ PDZ-HtrA4 (N-SPD) generated only two large fragments (Figure 4.13 A and B) reiterating the importance of the PDZ domain in hold-bite-and-rebind processive mechanism. It is well known that interplay between PDZ and protease domain is essential for cleavage of substrates and PDZ helps in subsequent translocation of the ligand into the catalytic cavity [161]. Δ PDZ-HtrA4 (N-SPD)

might be, unable to leave the cleaved substrate from the protease site, and fail to rebind the new cleaved substrate as PDZ is missing. In case of HtrA2, full-length HtrA2 and Δ PDZ-HtrA2 (N-SPD) cleaved β -casein into two fragments suggesting that it might follow a hold-and-bite model (Figure 4.13 D). However, this mechanism needs to be well explored with more artificial and natural substrates.

A



B



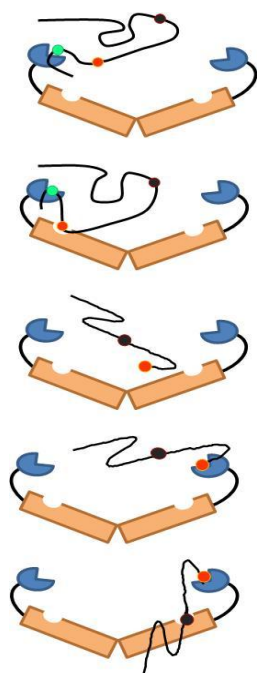
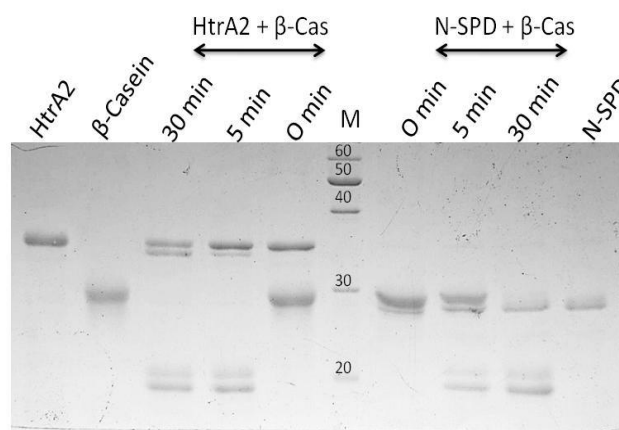
C**D**

Figure 4.13: Mechanism of cleavage and the role of PDZ in substrate cleavage. Cleavage assay of HtrA4, Δ PDZ-HtrA4 (N-SPD) and HtrA2, Δ PDZ-HtrA2 (N-SPD) with β -casein. **A)** Cleavage assays of HtrA4 with β -casein, peptide fragments generated after cleavage indicated as B1, B2, B3, B4, and B5. Five different size fragments were generated. **B)** Cleavage assay Δ PDZ-HtrA4 (N-SPD) with β -casein, only two peptide fragments generated after cleavage indicated as B1 and B2. **C)** Cartoon representation of hold-bite-and-rebind processive mechanism. This model shows how PDZ and protease domains cooperate to degrade substrate proteins in a processive manner. Illustrated is a schematic side view of one HtrA4 trimeric form showing only two subunits (protease, light orange; PDZ, blue). A substrate protein with several potential cleavage sites (colored spheres) is first bound and cleaved by one subunit. As the cleavage (protease) and docking (PDZ) sites obtain similar binding specificities, the introduced cut generates a substrate for the next digestive cycle that can bind to a nearby PDZ domain (the red sphere illustrates possible binding to the adjacent subunit). **D)** Cleavage assay of HtrA2 and N Δ PDZ-HtrA2 (N-SPD) with β -casein; only two peptide fragments generated after cleavage with both HtrA2 and Δ PDZ-HtrA2 (N-SPD).

4.2.10 Crystallization of the PDZ domain of HtrA4 protein

After purifying the PDZ protein, it was concentrated and injected into gel filtration chromatography to remove aggregated protein and imidazole. Eluted peak fractions were collected and further concentrated to 100 μ l using Millipore centricon (Figure 4.14 A and B). Concentration was checked by nanodrop, from the O.D, further concentration was calculated using Beer Lambert's Law and was found to be 10.6mg/ml, the concentration was satisfying enough to proceed to crystallization. Hanging drop and sitting drop methods were followed, where the PDZ protein was added to the crystallization buffer acting as a precipitant in several ratios to screen optimum possibility for crystal formation (Figure 4.14 C and D). A 50mm crystal plate was taken, with 50 wells. In case of hanging drop the protein drops were kept with crystallization buffers (Hampton crystal screen 1& 2 and Molecular dimensions structure screen 1 & 2) obeying, 1: 1.5 ratio (1part buffer, 1.5 parts of protein) whereas in sitting drop method the protein drops were kept with crystallization buffers following the ratio 1:1:0.5 for buffer and 0.5:1:1 for protein (Figure 4.14 E and F). The screening was done to identify the best buffer condition favoring crystallization. A few crystals were observed in one of the wells of the hanging drop set-up, which was further confirmed by dye absorption test using Izit crystal dye and trial on fire test and it was found to be salt crystal. The sitting drop set up showed the presence of precipitation might be due to the high concentration of the PDZ domain protein or the salts present in the buffer (Figure 4.14 F). Screening for other conditions (different buffers, pH and temperatures) with varying concentrations of protein to buffer ratios might give us the leads for crystallization.

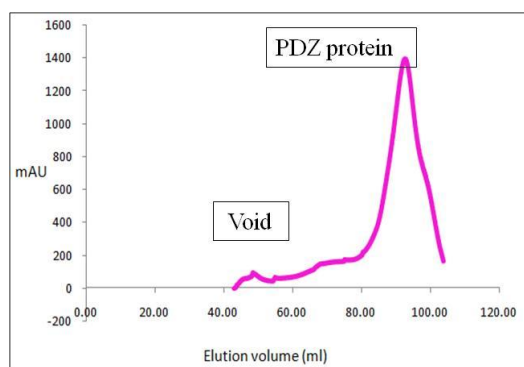
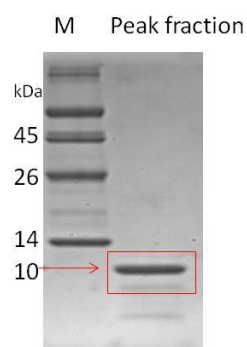
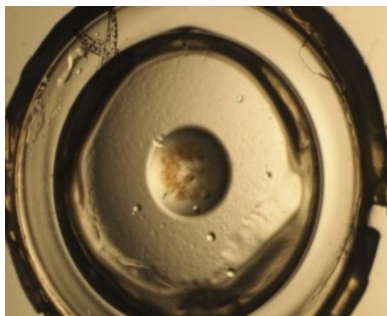
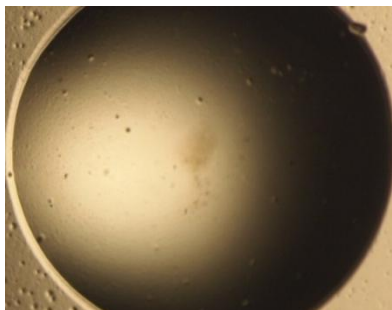
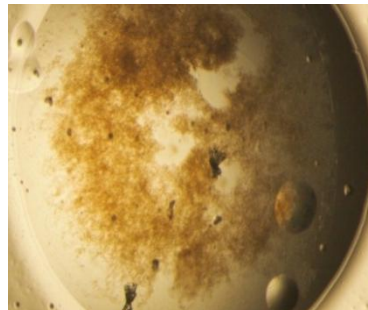
A**B****C****D****E****F**

Figure 4.14: Crystallization of PDZ domain. A) Peaks obtained at $\lambda 1$ (215nm) from superdex-200 showing the PDZ domain of HtrA4 protein peak at the monomeric position. B) Tris-Tricine gel showing a concentrated sample kept for crystal trials C) Basic setup of crystallization methods hanging drop and D) sitting drop method. Hanging drop well consisting of concentrated protein mixed with crystallization buffer showing E) a clear drop and F) well with salt crystals.

4.2.11 Functional analysis: Binding and cleavage analysis with X-Linked Inhibitor of Apoptosis:

In humans, the first homolog to baculoviral inhibitors of apoptosis (IAPs) identified was neuronal apoptosis inhibitor protein (NAIP) [162]. Two motifs were identified in baculovirus IAPs: the baculovirus IAP repeat (BIR) and the RING domain. Human X-linked Inhibitor of Apoptosis Protein (XIAP) has three BIR domains and one RING finger domain [163]. RING finger domain is responsible for self-degradation and not essential for apoptosis, whereas BIR domains are responsible for apoptosis [164, 165]. XIAP is an extremely potent suppressor of apoptosis [166], inhibits apoptotic cell death that is induced by diverse stimuli [167]. Caspases are the enzymes primarily responsible for apoptosis [168]. Caspase regulation is achieved either by controlling zymogen activation or by inhibition of nascent active caspases; inhibition is achieved through IAPs [169]. XIAP binds to and inhibits caspase 3, 7 and 9 but gets inhibited by two other proteins DIABLO (Smac) and HtrA2 (Omi) which are pro-apoptotic proteins and negative regulators of XIAP [146, 170–172]. HtrA2 interacts with XIAP through its amino-terminal Reaper-like motif, the effect of HtrA2 binding to XIAP on its ability to block caspase

activation [42, 173]. Stretch of amino acids (i.e., IAP binding motif /AVPS motif) involved in the interaction with XIAP has been identified by experiments with full length and truncated versions HtrA2 [12, 42, 79]. The AVPS motif in HtrA2 is responsible for binding to XIAP [60, 143]. Active HtrA2 can cleave XIAP in a dose-dependent manner both *in vitro* and *ex vivo*; indicating that IAPs are physiological substrates for HtrA2 protein. The IAP binding motif of HtrA2 seems to enhance its ability to cleave XIAP [60]. HtrA2 plays a direct role in the degradation of IAPs during cell death.

HtrA4 shares more than 55% sequence similarity with other human HtrA family members. Therefore, to identify functionally conserved motifs, we performed *in silico* sequence analysis of HtrA4 with well-characterized XIAP binding partners. Sequence alignment showed that HtrA4 has a conserved N-terminal AVPV similar to AVPS (IAP binding motif) motif of HtrA2 (Figure 4.15 A). Based on these observations, we hypothesized that HtrA4 might also bind to XIAP similar to HtrA2 and shows functional redundancy with HtrA2 in the cellular milieu. To test our hypothesis, we performed *in vitro* binding and proteolytic assays of HtrA4 with XIAP. For pull-down studies, GST fused XIAP used as a bait protein and HtrA4 as prey. The interaction was confirmed with western blot analysis using anti His antibody. The observed result suggests that HtrA4 interacts with XIAP (Figure 4.15 B). No pull-down was detectable using GST control alone.

Further to understand whether XIAP acts as a substrate for HtrA4, cleavage assays were performed with GST-XIAP as putative substrate. Interestingly, HtrA4 cleaved XIAP, and no proteolysis was observed with GST alone as a substrate, suggesting that XIAP could be a novel substrate for HtrA4 (Figure 4.15 C). Further to investigate the rate of protease activity, time-based degradation of XIAP was monitored. The rate of hydrolysis was quantitated by analyzing

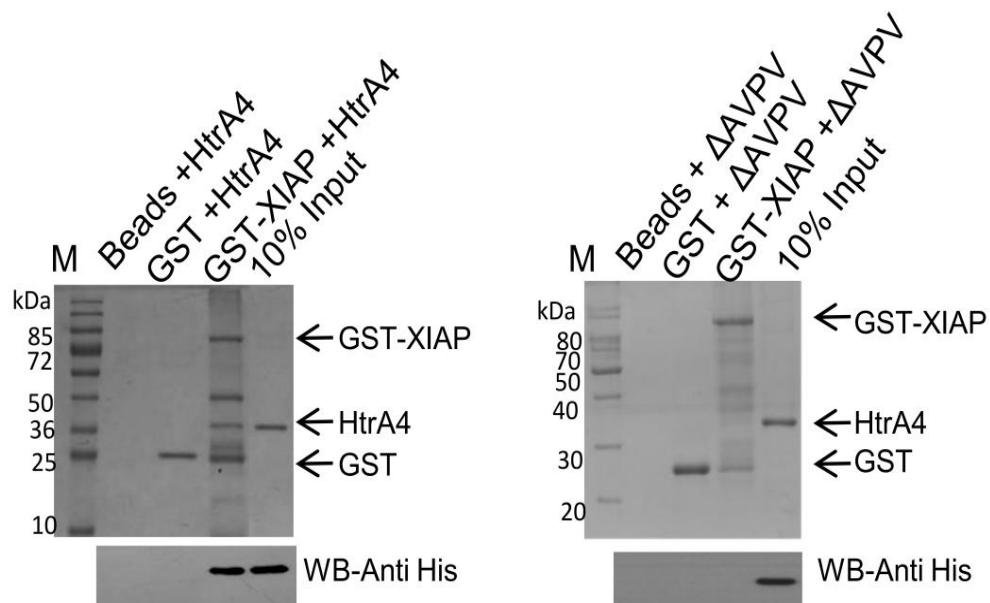
the intensity of proteolytically degraded XIAP band at 24 hr relative to the uncleaved XIAP using *Image J* software. HtrA4 cleaved XIAP in a time-dependent fashion, and 80% of the XIAP was hydrolyzed in 24hr. It was also observed that the cleavage rate increased with time, showing a significant difference when compared 0-hour sample with 24 hours ($p=0.0002$) (Figure 4.15 D). Results suggest that XIAP cleaved in the reaction mixtures containing active HtrA4 but not in case of inactive HtrA4 (S326A). GST protein was used as control; we did not observe any cleavage of GST protein by active HtrA4. Hence, from the pull-down assay, it is evident that HtrA4 interacts with XIAP while enzymatic assays clearly show the cleavage of XIAP in a time-dependent manner, indicating XIAP as a novel HtrA4 substrate.

To determine the role of the N-terminal 144 AVPV in binding to XIAP if any, we performed pull-down studies with Δ AVPV construct of HtrA4. The absence of AVPV abrogated the interaction, thus highlighting its importance in HtrA4–XIAP complex formation (Figure 4.15 B). Further to corroborate our binding studies, we performed protease assays with Δ^{144} AVPV construct (Figure 4.15 C), no cleavage of GST-XIAP was observed with this deletion construct of HtrA4 as expected. These observations suggest 144 AVPV might be a pre-requisite for binding and subsequent cleavage of XIAP by HtrA4. In all the protease assays inactive HtrA4 (S326A) was used as a negative control.

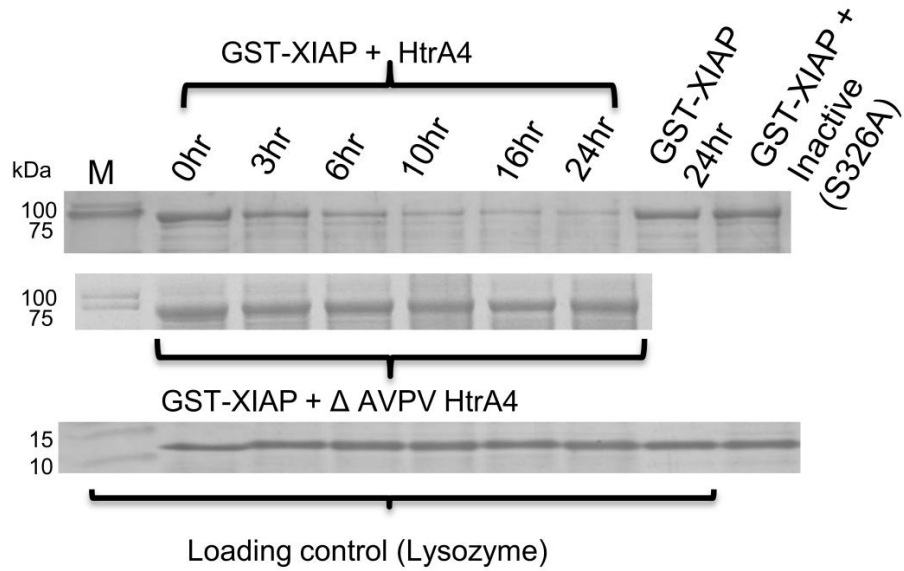
A

Mouse casp-9 p12	A V P Y	Q E G P R P L D Q
Human casp-9 p12	A T P F	Q E G L R T F D Q
Mouse DIABLO/Smac	A V P I	A Q K S E P H S L
Human DIABLO/Smac	A V P I	A Q K S E P H S L
HID	A V P F	Y L P E G G A D D
GRIM	A I A Y	F I P D Q A Q L L
REAPER	A V A F	Y I P D Q A T L L
SKL	A I P F	F E E E H A P K S
Mouse HtrA2	A V P A	P P P T S P R S Q
Human HtrA2	A V P S	P P P A S P R S Q
Human HtrA4	A V P V	Q W G N C G D T G

B



C



D

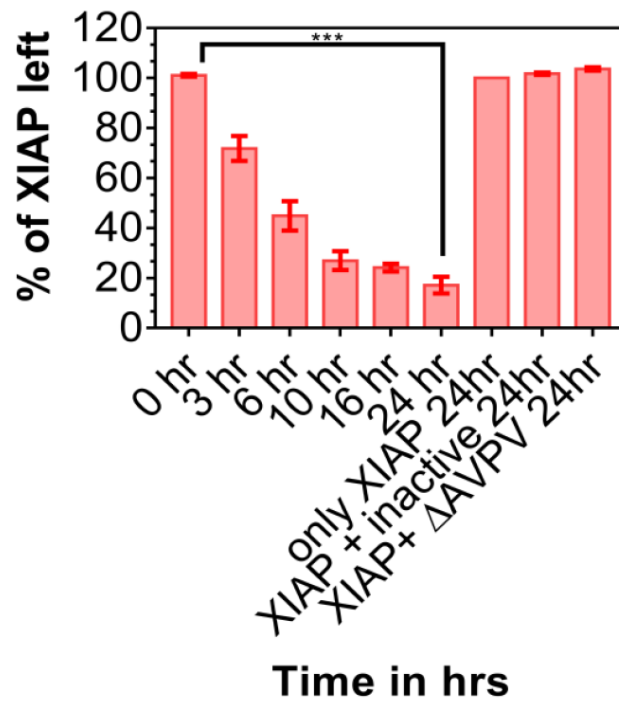


Figure 4.15: Binding and protease assays of HtrA4 using GST-XIAP as a putative binding partner and substrate. **A)** Sequence alignment of HtrA4 with Other IAP binding proteins: Collinear alignment of N-terminal sequences of mouse casp-9, human casp-9, mouse DIABLO/Smac, human DIABLO/Smac, *Drosophila* HID, GRIM, REAPER, SKL, mouse HtrA2, human HtrA2, and human HtrA4. The IAP binding motif (IBM) is highlighted in the box. **B)** GST pull-down assay. Pull down was performed using GST-XIAP as bait and HtrA4 as prey. The interaction was further validated by western blotting using anti-his antibody. **C)** Protease assays of HtrA4 and Δ^{144} AVPV with GST-XIAP. GST-XIAP incubated with HtrA4 at 37 °C for 0-24 hrs. Reaction samples were resolved by 15% SDS-PAGE and a decrease in the intensity of the full-length GST-XIAP was observed as a function of time. **D)** Quantitative analysis of GST-XIAP cleavage calculated from the intensity of the full-length protein band as a function of time. The intensity of the residual substrate after 24 hrs was quantified using Image J software. Error bars represent mean \pm SEM of four independent experiments. P-Value (0.0002) was calculated using a paired t-test.

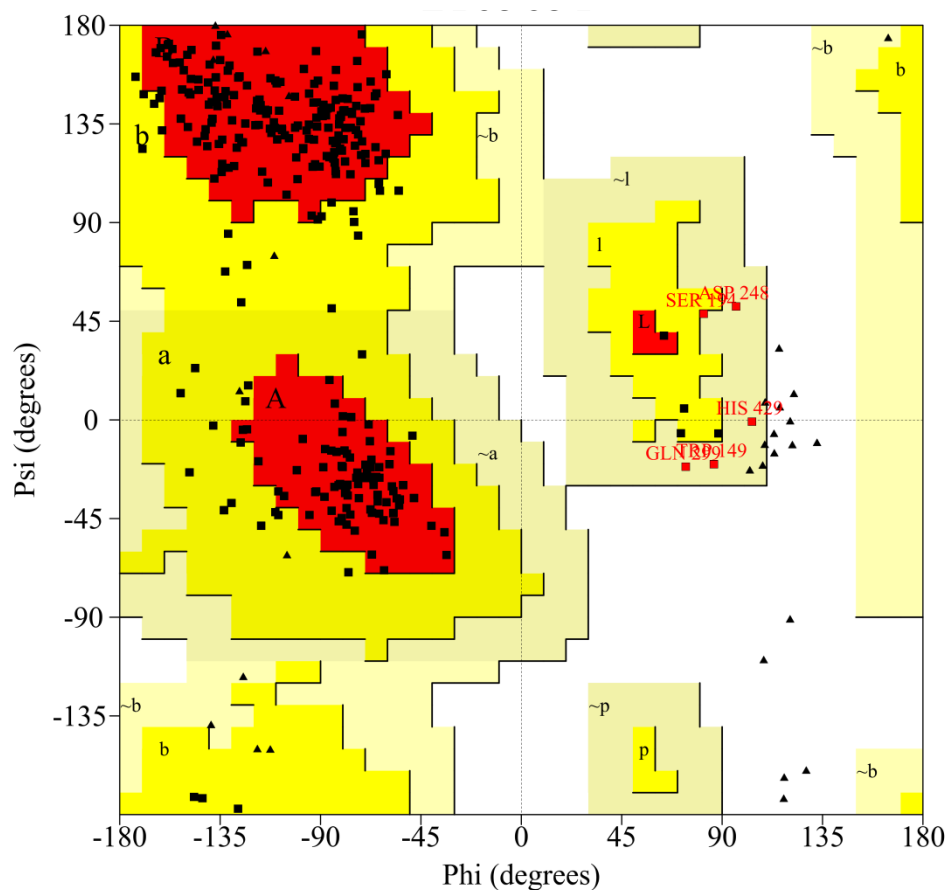
4.2.12 Selective binding pocket identification in HtrA4 and structural changes associated with peptide binding

4.2.12.1 Structural analysis and identification of binding pocket of HtrA4

HtrA4 model generated from the I-TASSER server. Quality of the predicted model was checked by the Ramachandran plot, which showed few residues lying in the energetically disallowed regions of the plot [119]. Those outlier residues were refined using ModLoop online server, and the refined structure was further validated using the Ramachandran plot (Figure 4.16 A) [120]. Refined model was submitted to an online server, protein model database (PMDb) with id: PM0081859. The model was further analyzed to understand the orientation of the secondary

structures using PSIPRED tool [174]. PSIPRED showed a total of five α helices, twenty β -strands and eight major loops traversing throughout the SPD and PDZ domain of HtrA4 model. Helices and β -strands were numbered sequentially starting from the N-terminus towards the C-terminal end of the model (Figure 4.16 B). SPD contains twelve β -strands (β 1- β 12) connected by evolutionarily conserved loops which were named according to the chymotrypsin nomenclature [175]. Among these loops, LB (β 3- β 4), LC (β 6- β 7), and L1 (β 9- β 10) accommodate the catalytic triad residues His218, Asp248, and Ser326, respectively. These loops synergistically interact with LA (β 1- β 2), LD (β 7- β 8), and L3 (β 8- β 9) loops, which are found to be essential for proteolytic activity and its regulation for various serine proteases (Figure 4.16 C) [36, 151].

A



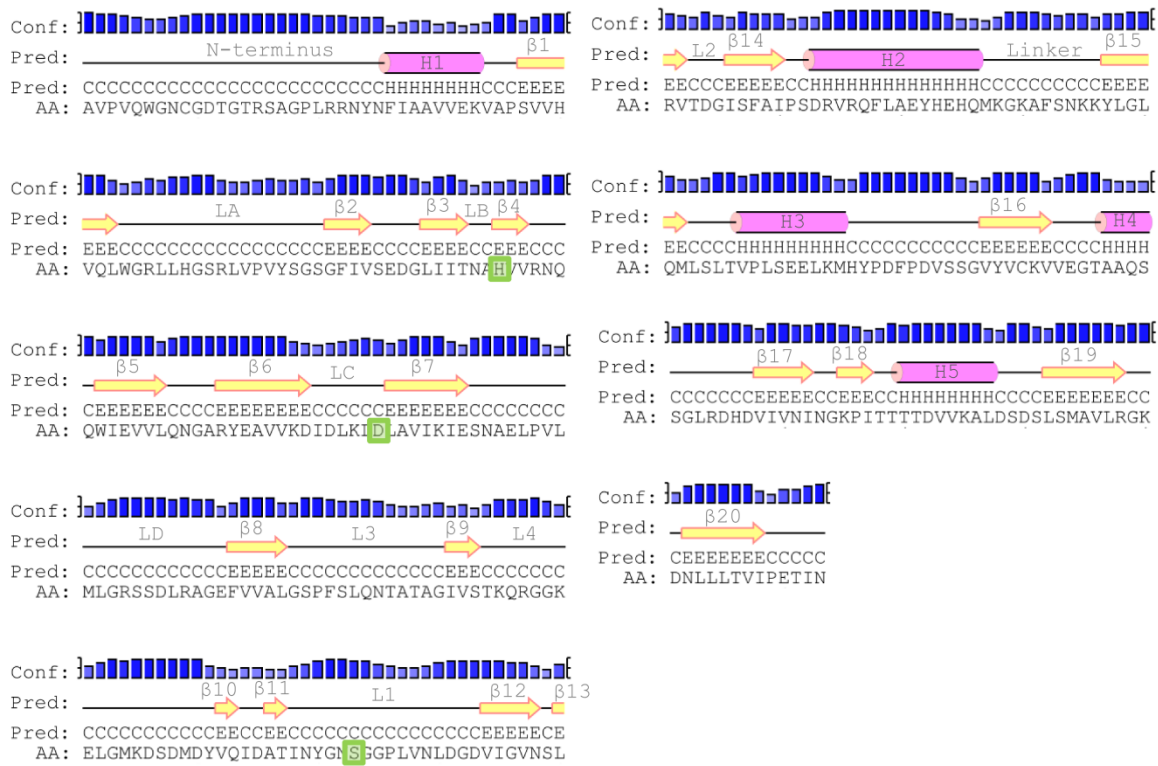
Plot statistics

Residues in most favoured regions [A,B,L]	242	84.0%
Residues in additional allowed regions [a,b,l,p]	41	14.2%
Residues in generously allowed regions [~a,~b,~l,~p]	5	1.7%
Residues in disallowed regions	0	0.0%

Number of non-glycine and non-proline residues	288	100.0%
Number of end-residues (excl. Gly and Pro)	2	
Number of glycine residues (shown as triangles)	30	
Number of proline residues	13	

Total number of residues	333	

B



C

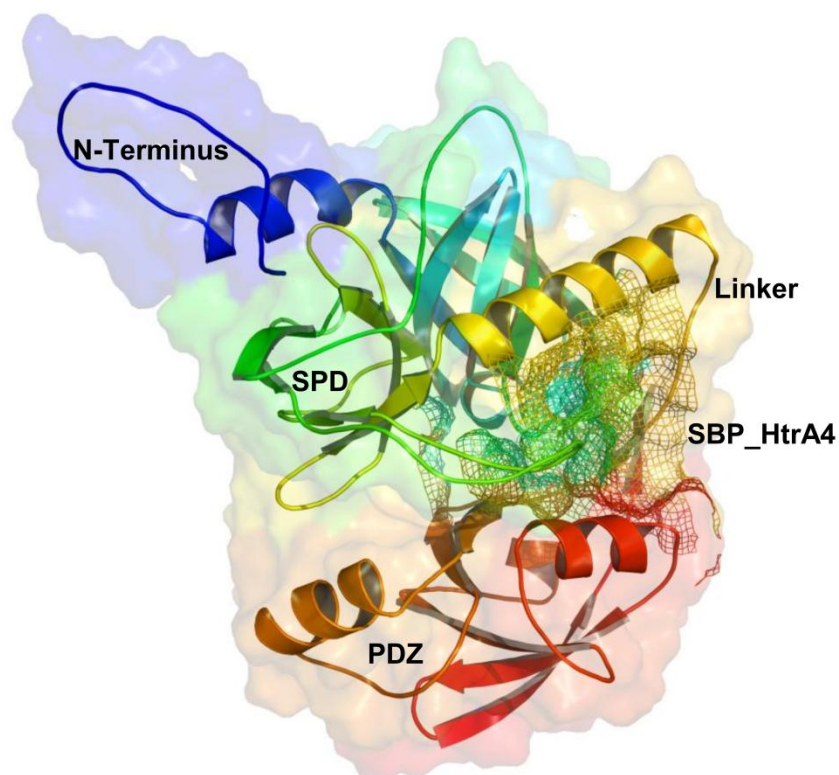


Figure 4.16: In silico modeling of HtrA4 protein: A) Ramachandran plot validation of HtrA4 model. Ramachandran plot analysis of HtrA4 model is done using PROCHECK [176]. It shows 84.0% of residues are in energetically most favored regions, 14.2% in additional allowed regions and 1.7% in generously allowed regions. No residues are there in the disallowed regions. B) Secondary structure prediction of HtrA4 model. PSIPRED results of HtrA4 model showing secondary structures in ribbon representation; helices (pink), β strands (yellow) and loops (black). The numbering of the secondary structures is done sequentially starting from the N-terminal. Green colored boxes highlight catalytic triad residues. C) In silico model of HtrA4 protein.

Prior to docking analysis of the HtrA4 with its binding partners, the binding pocket was identified using SiteMap. The best binding pocket (named as SBP_HtrA4) was selected based on site score which is calculated using parameters like effective volume, solvent accessible surface area (SASA) and nature of residues in terms of a donor to acceptor ratio. SBP_HtrA4 has the

maximum number of available hydrogen donor and acceptor groups that are essential for interacting with the peptides. It is also generously proportioned enough to accommodate the heptameric peptides generated from the peptide library analysis. Among the top five resulted sites, SBP_HtrA4 was the only site to represent residues from both SPD and PDZ domain (Table 4.5). Moreover, with stronger hydrophobicity when compared to the other four sites, SBP_HtrA4 was considered as the best interaction site and was chosen for further docking and MDS studies (Figure 4.17 A). The residues belonging to the SBP were conserved across the family (Figure 4.17 B).

A



B



Figure 4.17: Selective binding pocket identification (SBP) and Multiple sequence alignment (MSA) analysis of HtrA proteins A) Cartoon representation of HtrA4 model generated by I-

TASSER. Important regions such as N-terminal, SPD, linker, YLGL motif, and PDZ are labeled. A mesh surface marks selective binding pocket. B) Multiple sequence alignment (MSA) analysis of HtrA proteins. Full length sequences of HtrA1, HtrA2, HtrA3 and HtrA4 are aligned using Clustal Omega. Red inverted arrows denote catalytic triad residues (H218, D248, and S326). Orange-colored boxes highlight residues belonging to the SBP_HtrA4. Domain boundaries are indicated above where SPD denotes Serine Protease Domain, and PDZ indicates postsynaptic density protein (PSD95), *Drosophila disc large tumor suppressor (Dlg1)*, and zonula occludens-1 protein (*zo-1*).

Table 4.5 : SiteMap analysis of putative binding sites in HtrA4.

Putative binding sites along with their residues are ranked based on the Site score. Site score is provided by SiteMap tool in which scoring is done based on volume, hydrophobicity, hydrophilicity, and solvent accessible surface area (SASA).

SiteMap number	Residues present in the site	Site score*
Site 1	A217, H218, R221, N222, Q223, Q224, V239, V240, K241, D242, I243, D244, L245, K246, L247, D248, S296, T297, K298, Q299, R300, G301, G302, K303, E304, L305, G306, D313, Y314, V315, Q316, Q360, F361, H368, Q369, K373, Y380, L381, G382, L383, Q384, V410, V416, T442, D445, V447, K448, L450, D451, I475	1.048
Site 2	V199, Y200, S201, G202, N216, H218, D248, L286, I321, N322, Y232, G324, N325, S326, N341, S342, L343, R344	0.974
Site 3	V174, V177, A178, P179, V181, V182, H183, V229, L230, Q231, N232, G233, L280, G281, S282, P283, F284, N288, T289, A290	0.862
Site 5	G266, R267, S268, S269, D270, L271, R272, E275, N332, D334, D336, I338	0.680
Site 4	I206, E209, D210, G211, I213, K253, I254, S256, N257, A258, E259, L260, P261, V262	0.653

4.2.12.2 Docking analysis reveals the important interacting residues in SBP_HtrA4

To find leads toward critical interacting residues, the affinity of the interaction and the allosteric changes associated upon peptide binding, we prepared peptide library of β -casein (library preparation and docking discussed in the Methods section) and docked them with HtrA4. Among 23 β -casein peptides present in the library, $^{199}\text{DMPIQAF}^{205}$ (β -casein peptide- $^{199}\text{DMPIQAFLLYQEPVLGPVRGPFPIIV}^{224}$) showed the highest binding affinity with a docking score of -10.126 kcal/mole. The negative control peptide LNQPKNNPKNN, as expected, did not dock at the SBP_HtrA4 site. Interaction analysis showed residues L245, D248, D309, L383 and S394 of HtrA4 forming hydrogen bonds, whereas, A217, K308, F361, K379, V447, and D451 making van der Waals contacts with DMPIQAF peptide. A217 and L245 belong to the LA and LB loops respectively where the catalytic triad residues, H218, and D248 reside. Apart from that, L383 that is present in the conservative YLGL motif (corresponding to GLGF motif in PDZ domain of HtrA family) formed hydrogen bond with the DMPIQAF peptide [150]. V447 and D451 that are located at the SPD-PDZ interface of SBP_HtrA4 also showed van der Waals interactions with the same peptide (Figure: 4.18). Hence, the complex formed by β -casein (DMPIQAF) peptide after binding with HtrA4 was chosen for further analysis using Molecular Dynamics Simulation.

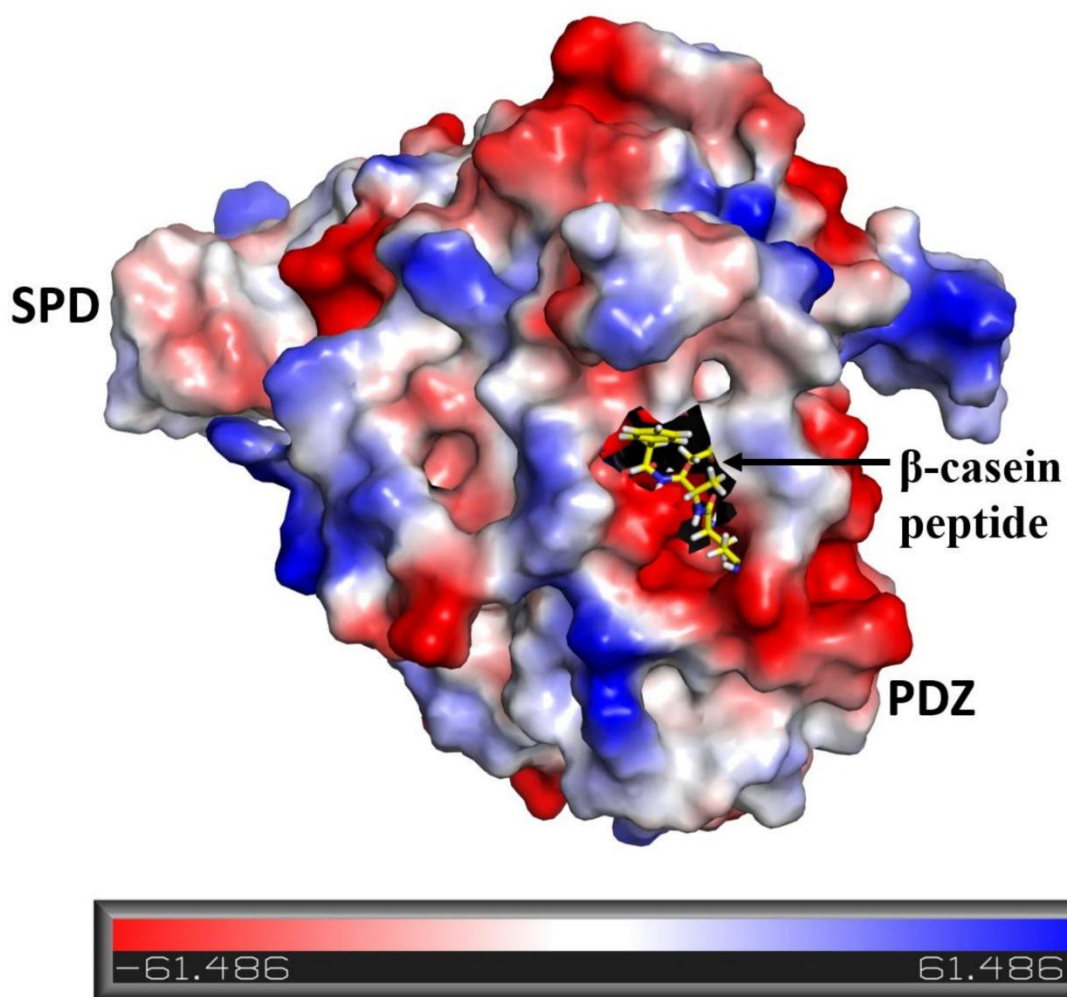


Figure 4.18: Electrostatic potential map of peptide-bound HtrA4 model. Electrostatic potential map of peptide-bound HtrA4 is generated using the APBS plugin of PyMol visualizing software [177]. Extreme red region indicates the minimum or negative potential, whereas the extreme blue region shows maximum or positive potential. SBP_HtrA4, where the peptide binds, comprises a balanced combination of both negatively- and positively-charged residues.

4.2.12.3 MDS analysis showing the structural reorientation of HtrA4 model upon binding with β -casein peptide

RMSD plot generated from MDS analysis of HtrA4- β -casein complex, (PMDB ID: PM0081893) showed fluctuation in the N-terminal domain, linker region, and PDZ domain when compared to the unbound HtrA4. Among these three regions, N-terminal in the β -casein bound complex deviated the most, where it tended to relax as compared to the unbound HtrA4 by 0.2 nm (2 Å). Linker region started fluctuating after five ns and then tends to stabilize after 10ns. Highest deviation value for the linker region was 0.3 nm (3 Å) in bound HtrA4, which was 0.1 nm (1 Å) less than the highest RMSD obtained by the linker region in unbound HtrA4. Subtle movement in the overall RMSD value for PDZ domain was also observed upon binding with the β -casein peptide. (Figure 4.19 A and B).

Deviation of the H3 helix was observed upon H-bond interaction formed by S394 in H3 with the β -casein peptide (Figure 4.19 C). Apart from that L383 of $^{382}\text{YLGL}^{385}$ motif in PDZ domain interacts with the peptide resulting deviation of both the linker region and $^{382}\text{YLGL}^{385}$ motif from the starting unbound structure. The motif tends to move away to accommodate the heptameric β -casein peptide. Moreover, loop movement in the SPD domain contributed in the reorientation of the catalytic triad, where L2 and L4 loops come closer to each other bringing the H218 and S326 closer to each other and LB loop move away from L4 causing an increment in the distance between H218 and D248. (Figure 4.19 C). These arrangements, when compared with other serine proteases, are conducive for substrate binding and catalysis. For example, similar movements are observed in L1, L2 and LD loops of HtrA2 when an activator peptide binds to it, resulting in reorientation of the catalytic triad residues [141].

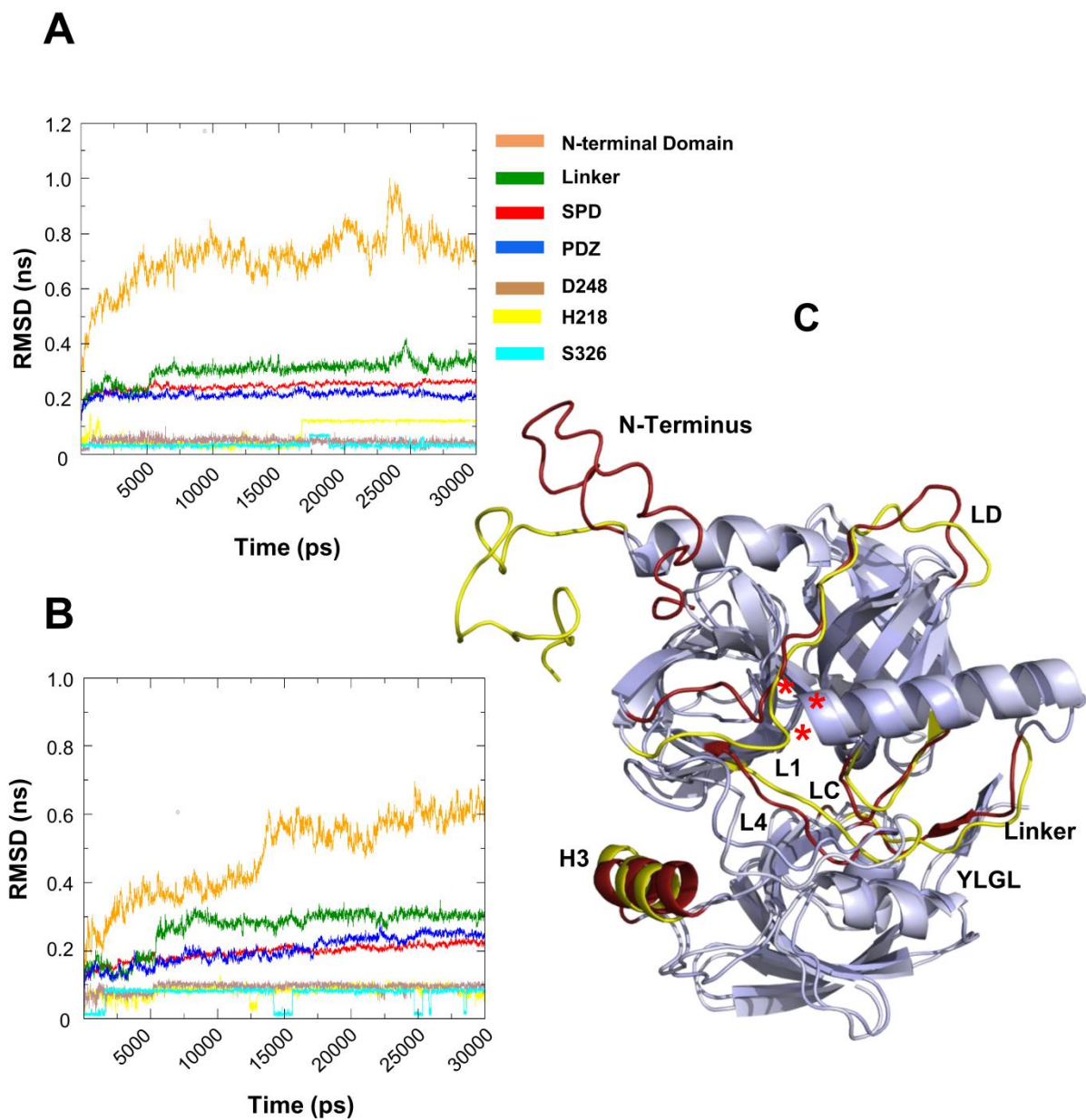


Figure 4.19: MDS analysis of HtrA4- β -Casein complex. RMSD plot for A) unbound HtrA4 B) bound HtrA4 showing the difference in fluctuations for important domains and catalytic triad residues. C) unbound HtrA4 (light-blue) and bound HtrA4 (blue-white) are aligned to show the movement of the loop and helix regions. Important fluctuating regions are marked as maroon for unbound and yellow for bound. An asterisk indicates location of each catalytic triad residue.

4.2.12.4 Comparative analysis of HtrA2 and HtrA4 catalytic triads to understand their role in enzymatic activity

Unbound HtrA4 model (PM0081859) and HtrA2 structures were aligned to compare the orientation of their catalytic triads. The distance between nitrogen (N ϵ 2) atom H65 and oxygen (O γ) atom of S173 for mature HtrA2 is 4.1 Å; whereas nitrogen (N δ 1) atom of H65 is 2.9 Å away from oxygen (O δ 1) atom of D95 [141]. Similar distance analysis for unbound HtrA4 model showed the distance between N ϵ 2 atom H218 and O γ atom of S326 as 8.5 Å and N δ 1 atom of H218 and O δ 1 atom of D248 as 5.6 Å (Figure 4.20 A). Upon binding with β casein peptide, the distance between H218 and S326 tends to decrease to 7.5 Å and increase to 6.2 Å for H218 and D248. The overall angular distance between N δ 1 atom of H218, O δ 1 atom of D248 and O γ atom S326 decrease to 56.4° from 59.3° upon binding of β -casein substrate. Compared to HtrA2, the catalytic triads in HtrA4 are far from each other, which might affect the catalytic activity of the HtrA4 (Figure 4.20 B and C).

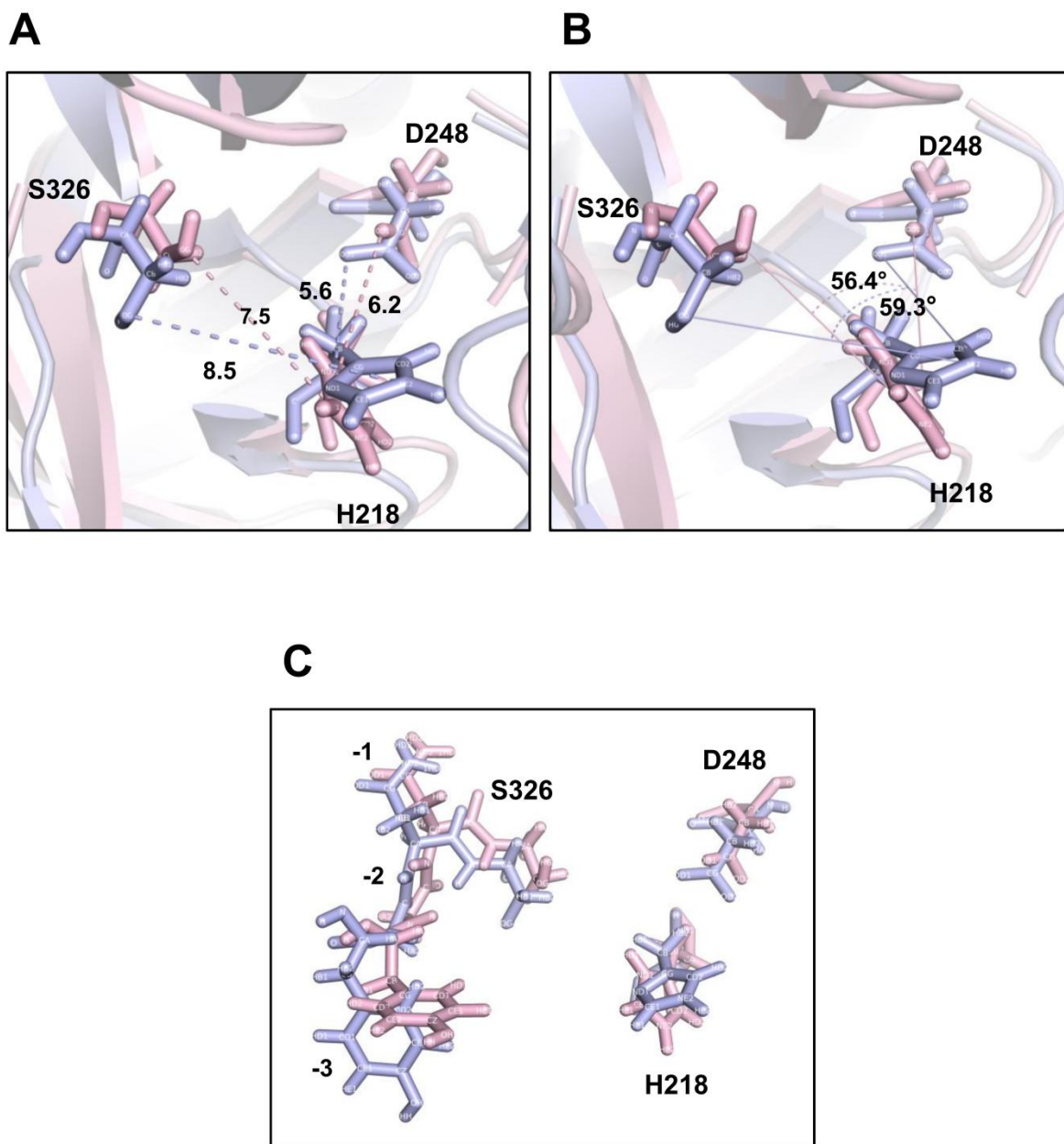


Figure 4.20: Structural comparison of catalytic triad and oxyanion hole residues. Comparison of the A) linear distances and B) angular distances between unbound (blue) and bound (pink) catalytic triad residues (Ser 326, Asp 248 and His 218) of HtrA4. C) Oxyanion hole orientation in peptide bound HtrA4 (pink) and unbound HtrA4 (blue) forms. Oxyanion hole residues namely, N325, G324, and Y323 are labeled as -1, -2, -3 respectively, where S326 is considered as 0.

4.3 Discussion and Conclusion

HtrA family members have similar domain architecture and perform various functions in the cell, and deregulation of their normal functions leads to various diseases [22, 33, 178–183]. Among human HtrA homologs, HtrA1 and HtrA2 are well characterized with available high-resolution crystal structures. HtrA1 and HtrA2 cleave a wide variety of targets mostly involved in cell death [36, 184–186]. The human HtrA homologs have an N-terminal region, serine protease domain and PDZ domain, the role of these domains in regulating protease activity is very well characterized in case of HtrA1 and 2 [36]. However, HtrA4 is the least described human HtrA protease concerning both structure as well as its functions. The role of HtrA4 in cellular physiology and pathology has recently started to emerge. HtrA4 levels are altered in many cancers, and elevated levels of HtrA4 was observed in pre-eclampsia (PE) and hence has been suggested to be used as a biomarker of PE [10, 22, 33]. However, none of the studies could define its mode of regulation and functions, which are a prerequisite for delineating its role in various biological pathways and diseases. Therefore, an intricate dissection of HtrA4 structure with an understanding of its functional reciprocity becomes imperative to harness its properties with desired characteristics.

Several studies revealed that HtrA2 is autocatalytically processed at the N-terminus, exposing an IAP Binding Motif (IBM) and resulting in a 36-kDa catalytically active mature protein [79, 145, 146]. Our extensive search for conservative motifs and consensus sequence resulted in identifying the N-terminal ¹⁴⁴AVPV residues, which are similar to the HtrA2 ¹³³AVPS motif. Endogenous levels of HtrA4 in various cell lines also showed a ~36 kDa band along with full-length protein. Based on these observations, we speculated that maturation site and processing of

HtrA4 might be identical to that of HtrA2. Hence we cloned HtrA4 starting from¹⁴⁴AVPV residues; the proteins produced in bacteria (starting from AVPV residues) are enzymatically active and cleaved β -casein indicating that the proteins are stable and well folded. These observations further substantiated with enzymatic assays and various spectroscopic methods.

Prokaryotic HtrA family members are capable of forming pyramidal 3-mers into higher-order complexes consisting of up to 24 molecules have been reported [34, 149, 150]. Human HtrA homologues forms 3-mers [53, 59, 60]. From our gel filtration analysis, we could observe a small fraction of monomeric population (~20%) along with dominant trimeric population (~80%), this might be due to the less stability of trimeric assembly as compared to HtrA2. N-SPD shows a trimeric ensemble only that implicates PDZ might be having a destabilizing effect on the trimeric assembly of the protease. It has been reported that the N-terminal region is prerequisite for the formation of oligomeric architecture as well as for proper protease functions in prokaryotic and human HtrAs [36]. Interestingly, our constructs devoid of N-terminal region such as SPD-PDZ and SPD eluted as monomers reiterating the importance of the N-terminal region in homo-trimerization. These results were further substantiated with the protease assays where only the trimeric forms of the proteins are active. From our results, it is evident that the constructs which have N-terminal region showed enzymatic activity and constructs which lack N-terminal region is found to be completely inactive and did not cleave the β -casein. These observations also highlight the importance of the N-terminal region for HtrA4 trimerization and activity.

Both gel-based and quantitative assays showed that the HtrA4 is less active when compared to HtrA2. From the quantitative studies, the activity of HtrA2 has been found to be 3.6×10^5 fold higher than HtrA4. From the gel-based assays, we could also see the striking difference in the cleavage pattern. HtrA2 cleaves β -casein into a single band whereas HtrA4 cleaves it into

multiple bands. HtrA4 also shows allosteric behavior like HtrA2 (Hill coefficients for HtrA4 and HtrA2 are 1.3 and 2.8, respectively), and the putative allosteric sites differ from each other in terms of size and nature of residues present [61]. Moreover, ligand docking studies in combination with Molecular Dynamics Simulation (MDS) showed that conformational movements underlying in this mechanism is different in HtrA4. The higher distance among the catalytic triad residues and fluctuations (RMSD) of the main loop regions (L1, L4, LC, and linker) in HtrA4 are some of the deviations observed. These subtle dissimilarities in conformational changes might be responsible for low activity in case of HtrA4. Above observations corroborate with temperature-based enzyme activity assays. HtrA2 is highly active at 55°C, T_m is around 74°C [61], while HtrA4 is highly active at 40°C with T_m of ~58°C, indicating the underlying conformational changes induced by temperature might be different in both of these proteases. Subtle structural variations in the dynamic loop regions and around the active-site might be responsible for the difference in protease activity, and hence functional diversity within the protease family.

For an active catalytic triad formation, the distances among the triad residues range from 2.7 Å to 5.7 Å for most serine proteases, both prokaryotes, and eukaryotes [4]. However, recently solved crystal structure of HtrA3 (PDB ID: 4RI0) shows that the active triad distance as far as 8.5 Å is able to form a stable oxyanion hole conducive for enzyme-substrate interactions [53]. Moreover, for our model HtrA4, one of the templates was HtrA3 (PDB ID 4RI0), and hence our model also showed catalytic triad distance as far as 8 Å [53]. Besides that, for an allosteric mode of regulation, the catalytic triad reorientation which is seen in HtrA2 has also been observed in bound HtrA4 structure [141]. So overall, HtrA4 also might be a unique case like HtrA3 where

distantly located triad residues interact among themselves to induce activity and cleavage of substrates.

Based on high sequence identity and similar substrate specificity, we hypothesized that HtrA family members are functionally redundant and have synergistic effects in the cellular milieu. To understand the above aspect, we aimed to explore the well known natural substrates and binding partners of HtrA1, HtrA2, and HtrA3 and test them as HtrA4 substrates or binding partners. In this study, we used one of the most well studied HtrA2 natural substrate, i.e., XIAP. Our preliminary *in vitro* data demonstrates cleavage of XIAP by HtrA4 thus implicating it to be a substrate of the protease. Further *ex vivo* studies are necessary to substantiate this result as well as to show its proapoptotic functions in the cell.

Post-translational modifications such as phosphorylation, acetylation, methylation, ubiquitination, and O-glycosylation play an important role in protein folding, protein-protein interactions, and other cellular function [187, 188]. Bacterially produced proteins are not subjected to any modifications as the bacteria lack the enzymes and cellular compartments responsible for modification. However, this is the first ever study to understand the biophysical and enzymatic properties as well as structure of HtrA4. We also aimed at identifying its substrates and binding partners in the apoptotic pathway if any. Therefore, obtaining highly pure and homogeneous HtrA4 protein in a large quantity became necessary and hence we used bacterial expression system. In our studies, we have found that the purified protein is stable and enzymatically active, suggesting that it has folded properly. However, further cell biology experiments are down the pipeline and will be done by other members of the lab to look into its functions in the cellular milieu.

To summarize, in the present study, we delineated the role of HtrA4 and its subdomains in enzyme catalysis as well as oligomerization status. We performed structural, biophysical as well as functional comparison of HtrA4 with its family members. Results in the present study highlight the importance of the N-terminal region in oligomerization. The kinetics of HtrA4 has been found to be lower than HtrA2 and substantially active at higher temperatures (>30 °C). Using β -casein, we investigated the substrate specificity and cleavage site residue selectivity, which has been found to be similar across the family. Sequence analysis identified the IAP binding motif in HtrA4; HtrA4 binds and cleaves XIAP in a time-dependent manner. Our data suggest that HtrA4 might have a role in cell death as it has been found to cleave antiapoptotic XIAP similar to HtrA2. Subtle structural variations in the dynamic loop regions and around the active-site might be responsible for the difference in protease activity and hence functional diversity within the protease family. Discerning the whole behavioral and functional aspects will assist us in devising strategies for modulating HtrA4, thereby developing an approach that increases HtrA4 proteolytic activity towards its antiapoptotic substrates like XIAP, which might be a promising tool in cancer treatment. In some of the cancers where XIAP is overexpressed, apoptosis can be triggered via caspase-dependent pathway by degrading XIAP along with a combination of other chemotherapeutic agents [169, 189]. Based on the above findings, we propose a working model of HtrA4 mode of action (Figure 4.21). We propose that HtrA4 exists in both trimeric and monomeric forms; trimeric one is the dominant and most favorable native oligomeric state. Addition of substrate also enhanced the conversion of the residual population of monomers to trimers. The model also suggests that initial binding of the β -casein peptide at SBP_HtrA4 leads to conformational rearrangement of the N-terminal region and loops at and around the catalytic triad. The significant role of the N-terminal region in fostering HtrA4's

activity and maintaining its trimeric form is evident from the fact that both SPD-PDZ and SPD monomers, which are devoid of the N-terminal region and are inactive. Hence, it further emphasizes the importance of trimerization to acquire a catalytically competent structure and indicates that the serine protease domain alone is not sufficient for catalytic activity. This work is the *first* structural, biophysical and enzymatic characterizations of serine protease HtrA4. Moreover, our study is also the pioneer to show that anti-apoptotic XIAP is a binding partner cum substrate of HtrA4.

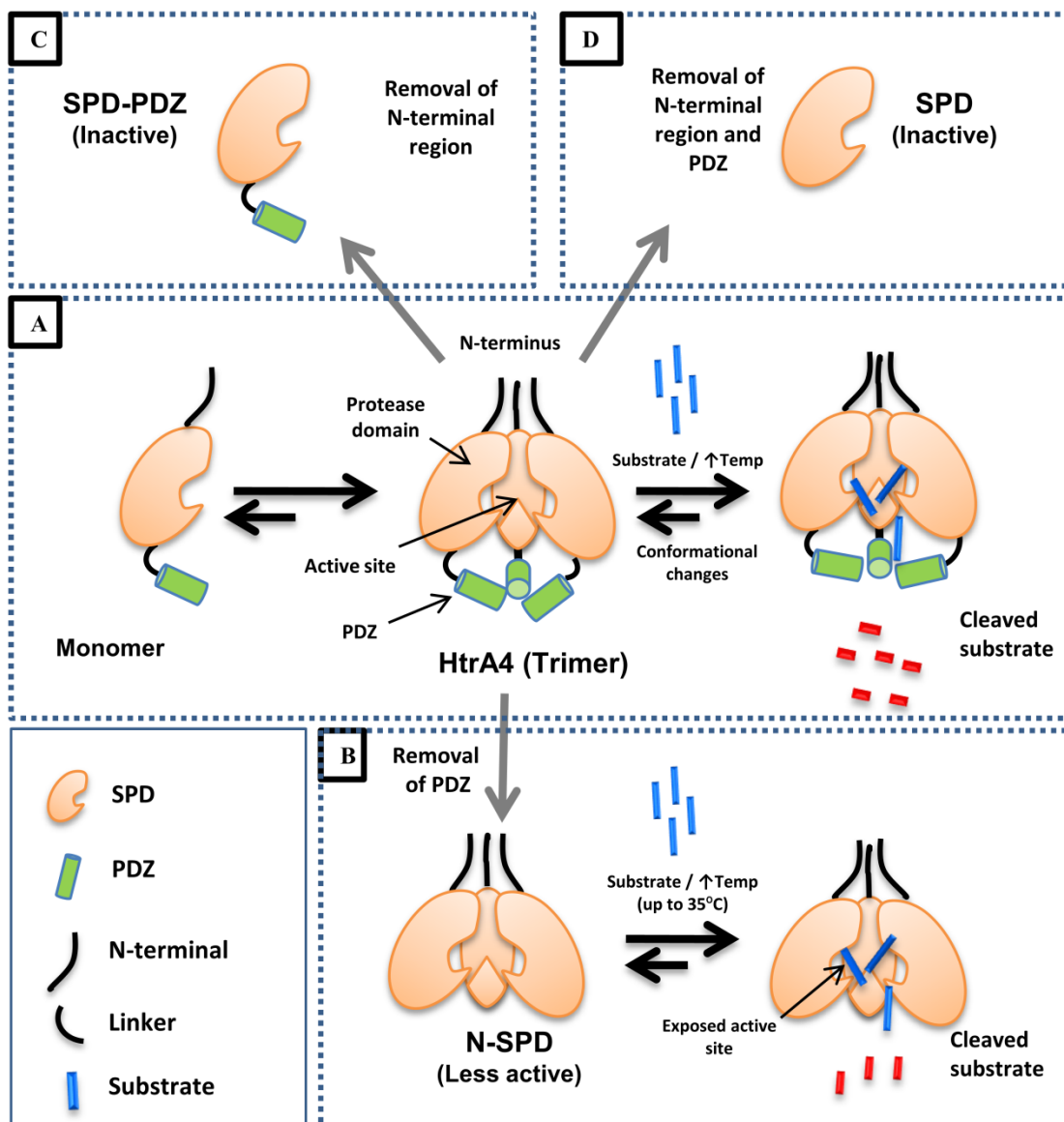


Figure 4.21: A proposed simplistic model for HtrA4 mechanism of action: The model illustrates the existence of HtrA4 primarily as a trimer with a small amount of monomeric population. The trimeric population is stabilized upon substrate binding. **A)** In trimeric HtrA4, initial substrate binding or increase in temperature leads to conformational changes in regulatory loops and makes protease active and cleaves substrates into shorter fragments. **B)** In trimeric N-SPD with the partially exposed active site and no regulatory PDZ domain, activity is less. **C)** Removal of N-terminal makes protease monomer, and hence, no catalytic activity is observed. **D)** Removal of both N-terminus and PDZ also generates monomeric protease, which lacks proteolytic activity.

CHAPTER – 5

**TO UNDERSTAND THE
INTERACTION BETWEEN
HTRA2 AND ITS BINDING
PARTNER– GRIM-19**

CHAPTER 5: TO UNDERSTAND THE INTERACTION BETWEEN HTRA2 AND ITS BINDING PARTNER–GRIM-19

5.1 Introduction

To maintain homeostasis, multi-cellular organisms tightly couple the rate of cell proliferation and cell death. Disruption of this fine balance due to altered regulation of apoptosis leads to diseases including cancer, atherosclerosis, aging and neurodegenerative disorders [190]. Tremendous progress in apoptotic research in the past decade has identified caspases to be the key players, although evidence of caspase-independent apoptosis also exists in literature [191]. Once activated, caspases can be inhibited by the inhibitor of apoptosis (IAP) family of proteins, which in turn can be antagonized by mitochondrial proapoptotic proteins Smac/DIABLO and HtrA2/Omi [192, 193]. Although HtrA2 and Smac bind IAPs in a similar fashion through their N-terminal tetrapeptide upon release from the mitochondria, HtrA2 also induces apoptosis in a caspase-independent manner. This unique property has made it an interesting target especially in cases where caspase activation is prevented either due to inhibition of caspase activity or genetic inactivation of a key caspase.

HtrA2 protein belongs to a unique family of serine proteases that are conserved from prokaryotes to humans [194]. The most elaborately studied protein in this family is *E. coli* periplasmic protein DegP/HtrA that has a dual temperature-dependent, chaperone-protease activity, the precise mechanism of which is still elusive. To date, four human homologs (HtrA1-HtrA4) of

DegP have been identified of which HtrA2 has pro-apoptotic activity [195] while detailed information on other human HtrAs is lacking. Although, HtrA2 has primarily been identified as an IAP-binding pro-apoptotic protein, its other functions such as caspase-independent induction of apoptosis and serine protease activity are poorly characterized. Recent studies have identified a few anti-apoptotic substrates of HtrA2 suggesting that its pro-apoptotic function is also regulated by its protease activities [191]. Based on the information from literature, the majority of its identified partners and substrates such as IAPs, Pag, Mxi-2, and Pea-15 are cytoplasmic suggesting HtrA2 interacts with them only after being released from the mitochondria [192, 196–198]. Based on the chaperoning ability of its bacterial counterpart DegP, and little evidence from the literature [199, 200], it was suggested that HtrA2 might also play a protective role in the mitochondria under normal conditions. Therefore, regulating HtrA2 activity might give rise to therapeutic possibilities in various diseases it is associated with.

To modulate HtrA2 functions with desired characteristics, understanding its mechanism of action, identifying its natural substrates and deciphering its biological functions become imperative. Till date, HtrA2 is reported to interact with IAPs, cytoskeletal proteins, anti-apoptotic proteins such as Hax1 and Pea-15 as well as with the cell death regulatory protein called GRIM-19 [201]. GRIM-19 or Gene associated with retinoic and interferon-induced mortality 19 protein, also known as NADH dehydrogenase [ubiquinone] 1 alpha subcomplex subunit 13, is a part of mitochondrial electron transport system [202]. GRIM-19 is either mutated or exhibits loss of expression in many cancers. Furthermore, viral proteins such as E6 protein of papillomavirus (high risk types), vIRF1 protein of Herpes virus 8, LT protein of SV40 and many other viral proteins also inhibit GRIM-19 which leads to cellular transformation [203]. GRIM-19 also interacts with STAT-3 and inhibits its gene stimulatory functions [204]. In addition, it

interacts with p16 and brings about cell cycle arrest. Thus, collectively these observations suggest that GRIM-19 could be a tumor suppressor gene [203]. *Kalvakolanu et al.*, have identified GRIM-19 as a potential activator of HtrA2. In the presence of GRIM-19, the pro-apoptotic activity of HtrA2 is amplified resulting in elevated rate of apoptosis [205]. Despite this important information, the region involved in this interaction, binding affinity as well as the mechanism of activation is still elusive. This offers an excellent opportunity towards designing activators for HtrA2 that could modulate its functions with desired characteristics against diseases associated with it. Delineating the mechanism of interaction between HtrA2 and GRIM-19 will therefore be a step towards this goal.

5.2 Results

5.2.1 Cloning, expression, and purification of GRIM-19

5.2.1.1 Cloning and expression standardization of human GRIM-19 protein

The *GRIM-19* gene of size 454bp was PCR amplified and cloned into a pET28a (+) bacterial expression vector. Positive clones were confirmed by restriction digestion and DNA sequencing. pET28a-GRIM-19 was transformed into BL21(DE3) *E.coli* strain and expressed using varying concentrations of IPTG starting from 0.2mM to 0.8mM IPTG for 12 hours at 18°C. His tagged GRIM-19 protein expression was found relatively equal in different IPTG concentrations (Figure 5.1). The overexpressed protein identity was confirmed using mass spectrometry.

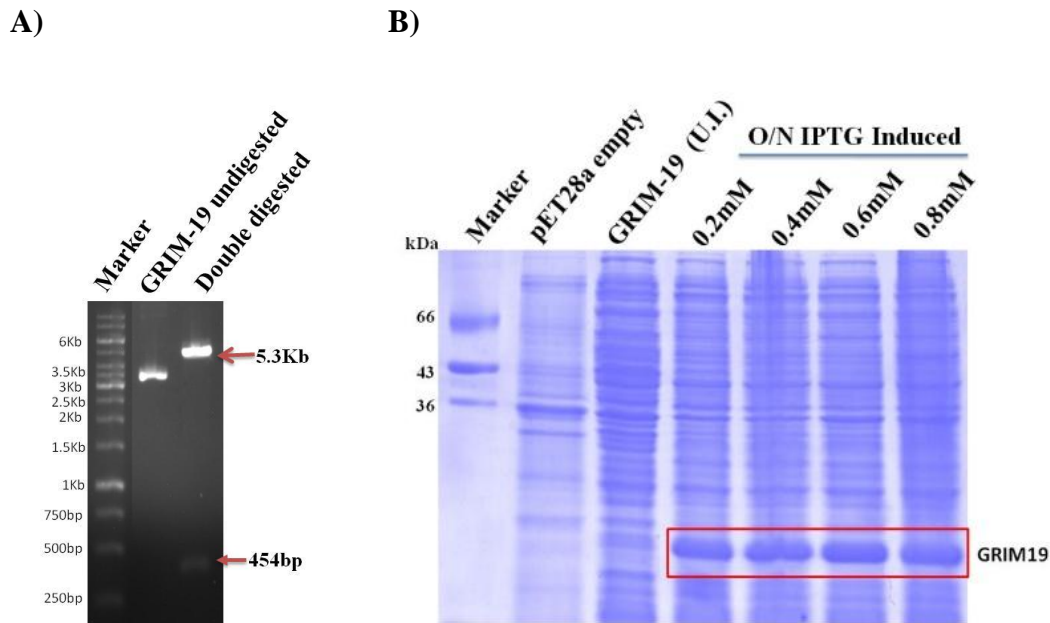


Figure 5.1: Cloning and expression standardization of human GRIM-19 protein A) GRIM-19 gene in pET28a (+) clone confirmed with restriction digestion B) SDS gel showing the GRIM-19 protein expression in different IPTG concentrations. (U.I- Uninduced; O/N- Overnight)

5.2.1.2 GRIM-19 protein solubility analysis

His tagged GRIM-19 protein was not soluble in different lysis buffers. The solubility of GRIM-19 was enhanced using different buffers comprising salts, additives, and detergents. Buffers with 0.6% sarkosyl retained 30-40% of the protein as soluble fraction, but detergent interfered with binding to NI-IDA column. So, we cloned GRIM-19 gene in soluble tag containing vectors like GST.

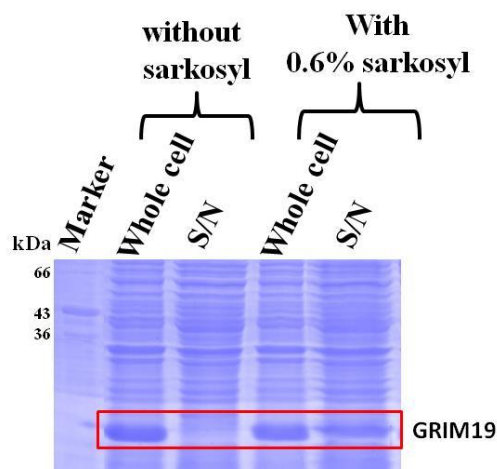
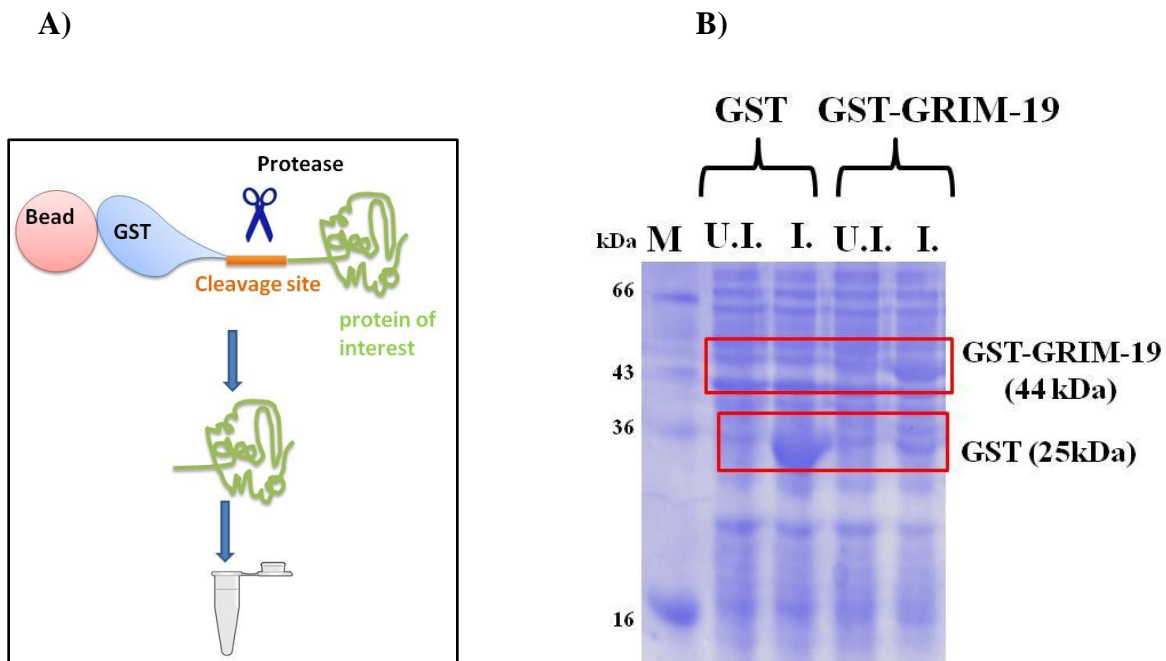


Figure 5.2: GRIM-19 protein solubility analysis. SDS gel showing solubility of GRIM-19 with and without detergent, with sarkosyl GRIM-19 protein found to be soluble, but it did not bind to Ni-IDA beads. (S/N- Supernatant)

5.2.1.3 GST tagged GRIM-19 purification

To increase the solubility of GRIM-19 protein, we further subcloned it into GST (pGEX6p-1, with precision protease site) tagged vector. The clone with gene of interest was further confirmed with restriction digestion and DNA sequencing. GST tagged GRIM-19 clone was expressed in *E. Coli* BL21 (DE3) pLysS strain. With the presence of GST tag, GRIM-19 protein was expressed in soluble fractions. Further GST tagged GRIM-19 was purified using standard GST tagged protein purification method. Schematic representation of purification strategy has been mentioned in figure 5.3. To separate GRIM-19 protein from the GST tag, on-column cleavage was performed using the precision protease. The eluted GRIM-19 protein analyzed for its purity,

and it was observed that along with GRIM-19 some other bacterial proteins were also co-eluting. Using mass spectrometry, we identified that impurities belong class of bacterial chaperones known as GroL1. To separate these chaperones from the GRIM-19, several buffer combinations containing MgCl_2 and ATP (1-10mM) were used [206]. However, these chaperones did not separate from GRIM-19. We assumed that bacterially expressed chaperones were not sufficient to fold the protein and we co-expressed GRIM-19 protein with a chaperone over expressing plasmid system.



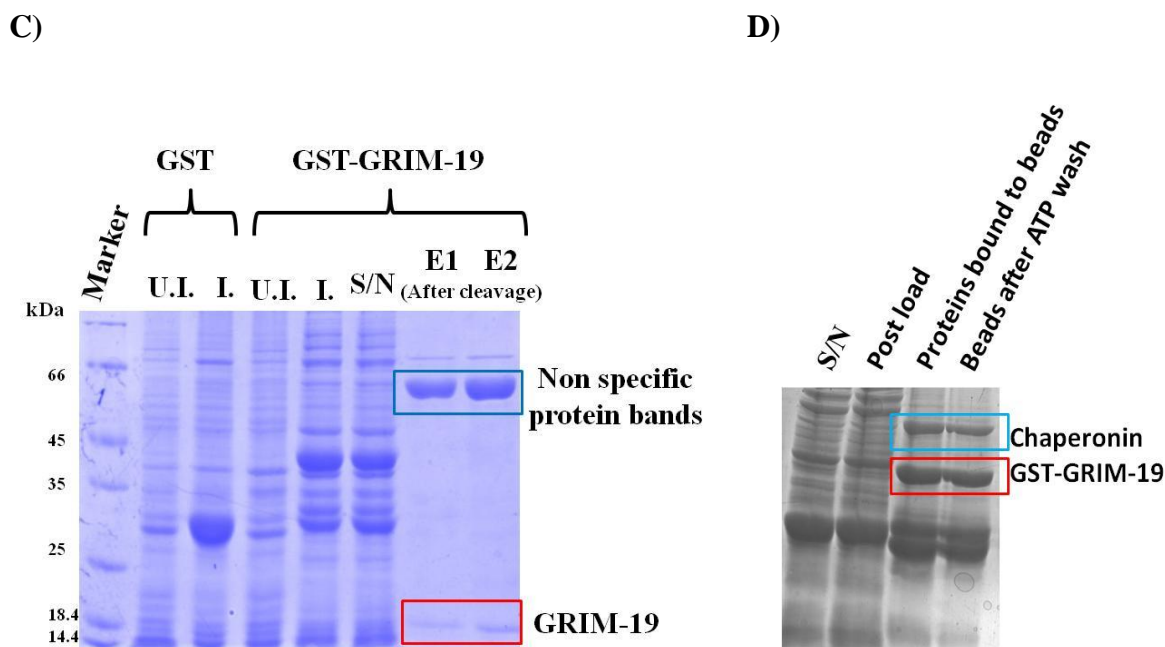


Figure 5.3: GST tagged GRIM-19 purification. A) Schematic representation of purification strategy of (GST tagged) GRIM-19 B) GST-GRIM-19 (44kDa) expressed in *E.coli* cells at 18°C for 12 hours C) After binding the GST-tagged GRIM-19 to beads, we used precession protease to separate GRIM-19 from GST (on-column cleavage). When GRIM-19 protein analyzed for its purity, it was observed that along with GRIM-19 some other bacterial proteins were also co-eluting. D) Beads washed with ATP and $MgCl_2$ were loaded on SDS gel for analysis. (U.I- Uninduced; I- Induced; S/N- Supernatant)

5.2.1.4 Co-expression and purification with chaperones

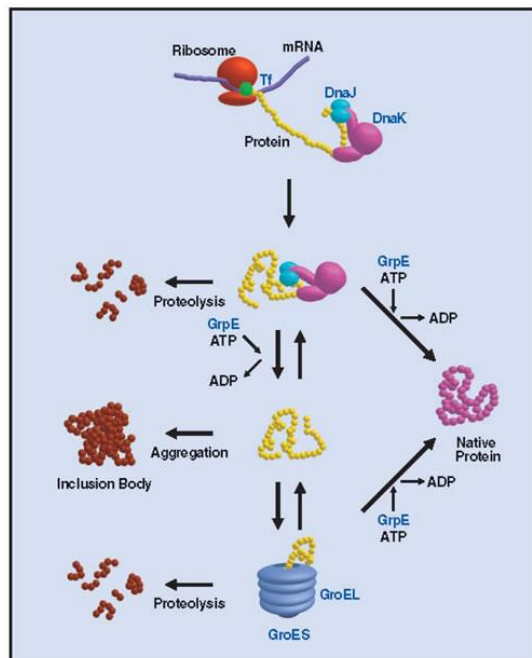
To enhance the GRIM-19 protein solubility, it was co-expressed with commercially available chaperone plasmids (pG-KJE8, pGro7, pKJE7, pG-Tf2, pTf16) (Table 5.1). We speculated that co-expression of GRIM-19 with these chaperones might enable optimal protein expression and folding. Co-expression with chaperones is known to reduce protein misfolding and increase the recovery of soluble protein [207]. The possible mechanism is explained in Figure 5.4 A.

GRIM-19 was successfully expressed as a soluble protein in presence of these chaperone plasmids. However, during protein purification GRIM-19 co-eluted with chaperones (Figure 5.4 C). Hence we proceeded to a Urea denaturation method to obtain purified GRIM-19 protein.

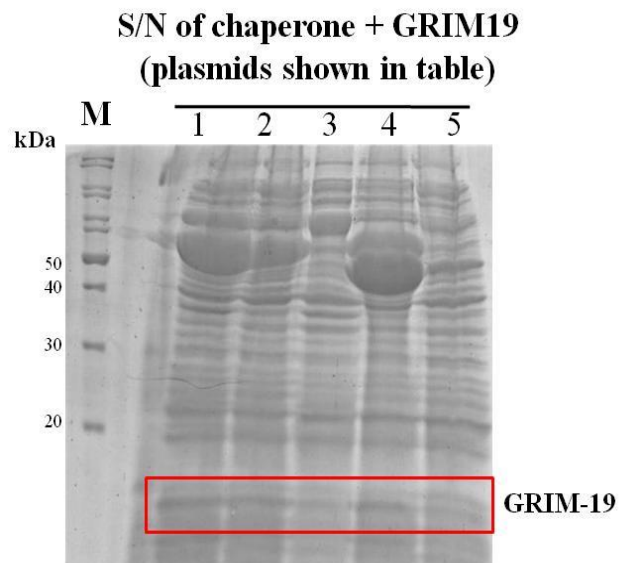
Table 5.1: Table showing list of chaperone plasmids used for the co-expression studies

No.	Plasmids	Chaperone	Inducer	Promoter
1	pG-KJE8	dnaK-dnaJ-grpE groES-groEL	L-Arabinose Tetracycline	araB Pzt-1
2	pGro7	groES-groEL	L-Arabinose	araB
3	pKJE7	dnaK-dnaJ-grpE	L-Arabinose	araB
4	pG-Tf2	groES-groEL-tig	Tetracycline	Pzt-1
5	pTf16	tig	L-Arabinose	araB

A)



B)



C)

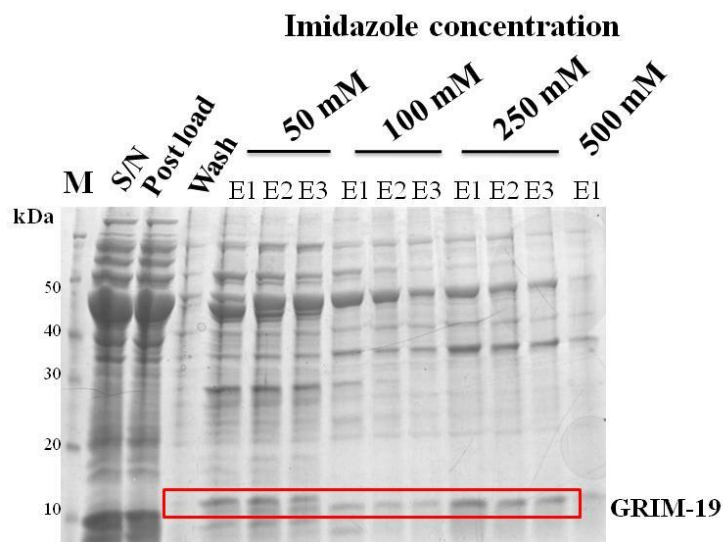


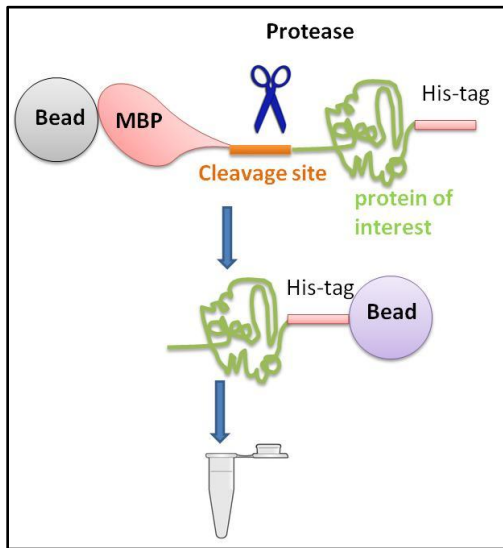
Figure 5.4: Co-expression and purification with chaperones A) Schematic representation of chaperone-assisted protein folding in *E. coli* [207] B) SDS gel showing the GRIM-19 protein in soluble fraction after co-expression with chaperone plasmids. The numbers represent the

plasmid set used in co-expression study are mentioned in Table 5.1 respectively C) GRIM-19 protein purified from (pG-KJE8) chaperone overexpressing bacterial cells. SDS gel showing the GRIM-19 protein eluted along with chaperone protein. The elutes which were giving color in Bradford protein assay test were loaded on the gel for analysis. GRIM-19 protein is highlighted with red box. (E-Elute; S/N- Supernatant)

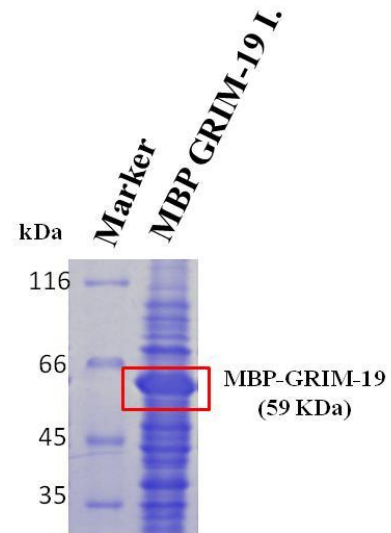
5.2.1.5 MBP tagged GRIM-19 purification

To solubilize GRIM-19 protein, we further subcloned it into MBP (modified pMAL-c5E with c-terminal His₆ tag and TEV cleavage site) tagged vectors. This clone was further confirmed with restriction digestion and DNA sequencing. This MBP-tagged GRIM-19 clone was expressed in *E. coli* BL21 (DE3) pLysS strain. In presence of the MBP-tag, GRIM-19 was expressed in soluble fraction (Figure 5.5 B). GRIM-19 construct with N-terminal MBP tag was purified by affinity chromatography using amylose resin (Figure 5.5 C). Schematic representation of purification strategy has been mentioned in Figure 5.5 A. After purifying the MBP-GRIM-19, we used TEV protease to separate GRIM-19 from MBP tag. Post cleavage, GRIM-19 with c-terminal His tag bound to Ni-IDA column and after appropriate washes, His tagged protein was eluted with a 250mM imidazole gradient. The eluted GRIM-19 protein analyzed for its purity, from SDS PAGE, it was observed that GRIM-19 co-eluting with MBP (Figure 5.5 D). We presume that GRIM-19 protein might be interacting with MBP with either by electrostatic or hydrophobic interaction; To disrupt this interaction we used buffer containing high salt concentration, mild detergents and low amount of urea during washes. After appropriate washes GRIM-19 was eluted with imidazole and analyzed for purity on SDS PAGE. From our results it has been observed that GRIM-19 strongly binds to MBP and the interaction could not be disrupted even under harsh buffer conditions.

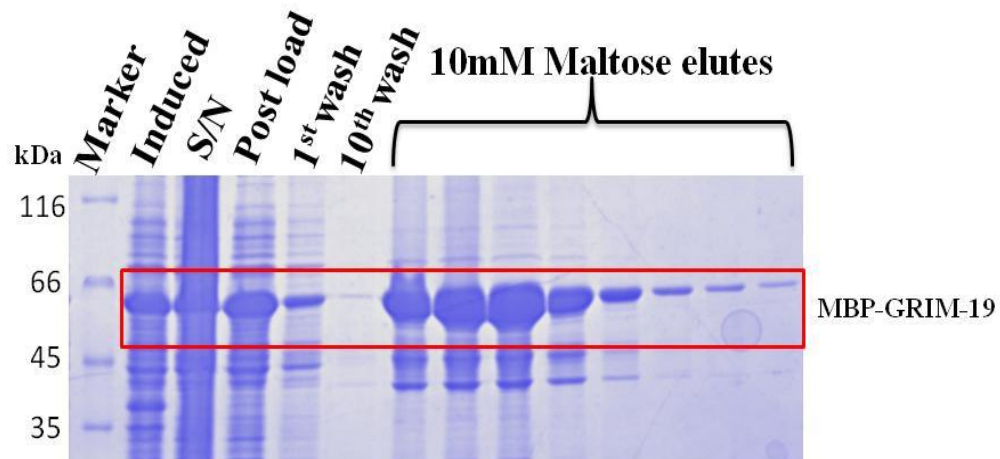
A)



B)



C)



D)

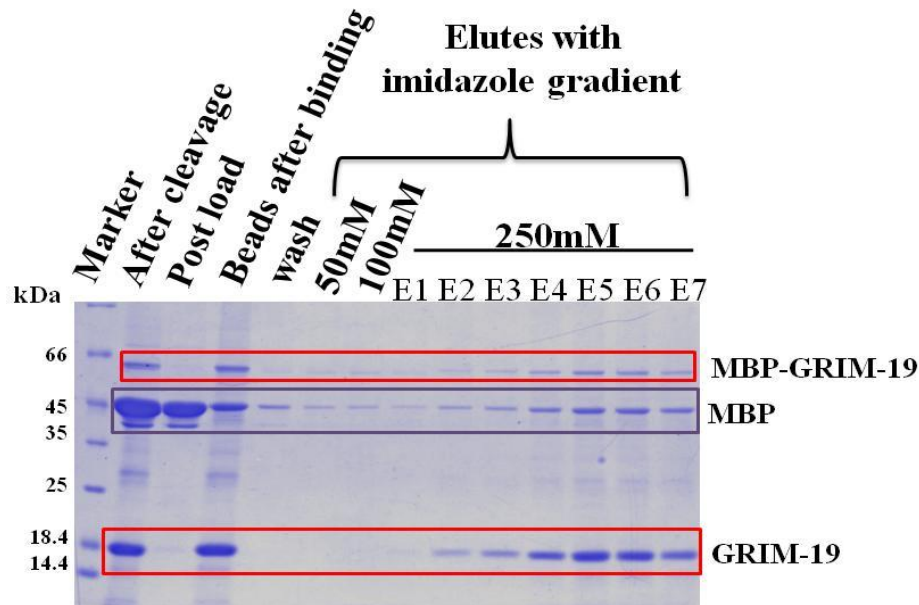


Figure 5.5: MBP tagged GRIM-19 purification. A) Purification strategy of MBP-Tagged GRIM-19 protein. B) SDS PAGE gel showing the overexpressed MBP-GRIM-19 of size 59kDa. C) SDS PAGE gel showing the purified MBP-GRIM-19 eluted with 10mM maltose. D) Post cleavage GRIM-19 with c-terminal his tag bound to NI-IDA column and after appropriate washes, His tagged protein was eluted with 250mM imidazole. From SDS PAGE analysis it was observed that GRIM-19 co-eluting with MBP. (I- Induced; S/N- Supernatant; E-Elute)

5.2.1.7 GRIM-19 protein Purification with urea denaturation method

E. coli expressed His tagged GRIM-19 was found to be in the insoluble fraction. Therefore, GRIM-19 protein from the insoluble fractions from small scale culture (250ml) was purified using 8M urea. Urea-denatured GRIM-19 protein was refolded and dialyzed to remove the additives (which helps in refolding). After refolding the GRIM-19 protein yield was very low hence, we have modified the purification protocol, with the following three steps: a) GRIM-19

was purified from the 2 liter bacterial culture, b) while refolding, concentration of urea in the buffer was sequentially decreased from 8M to 2M, c) further to decrease the protein precipitation, concentration of L-Arginine in the refolding dialysis buffer was increased from 0.5M to 0.75M. Using this modified procedure, approximately 70% of GRIM-19 was refolded with a significant decrease in precipitation.

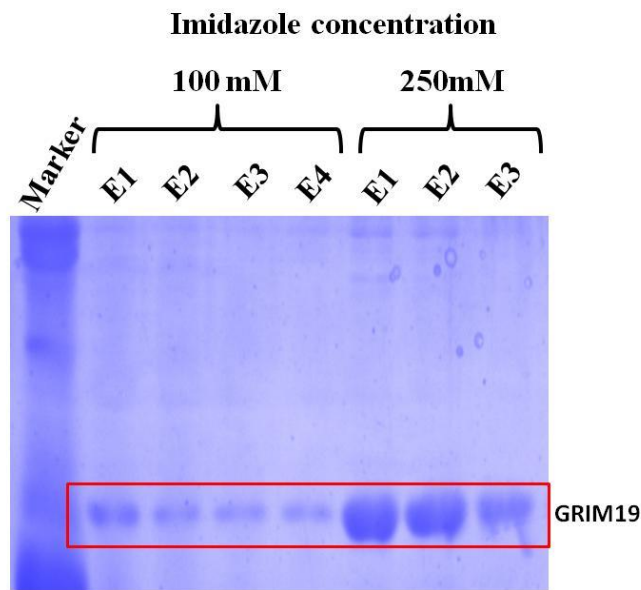
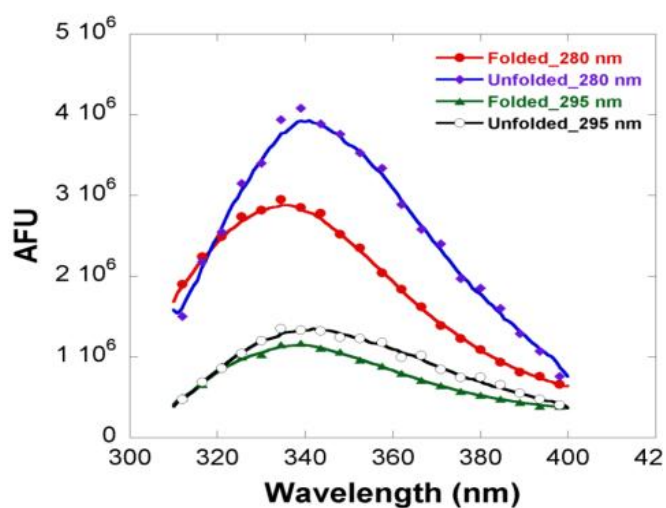


Figure 5.6: GRIM-19 protein purification with urea denaturation method. His tagged GRIM-19 protein purified by Ni-affinity chromatography with modified urea denaturation protocol. The protein was purified using Ni-IDA resin, approximately 3 fractions analyzed on 15% SDS-PAGE gel and stained with coomassie blue. E1-E3 are different elutes of the protein. E1 represents elute1 which was collected after adding either 100 or 250 mM concentration of imidazole as competitive binder to elute the His-Tagged protein.

5.2.2 Biophysical and structural characterization of GRIM-19 protein

5.2.2.1 Tertiary structure analysis of GRIM-19

Fluorescence emission maxima scans were collected to confirm whether the protein has refolded properly. Trp and Tyr have absorption maxima at 280 nm, 277 nm respectively (extinction coefficients $5563 \text{ cm}^{-1}/\text{M}$ and $1220 \text{ cm}^{-1}/\text{M}$, respectively). Trp absorbs 5 times more than the Tyr at 280 nm. At 280 nm both the Trp and Tyr will be excited. At 295 nm only tryptophan is excited. The extinction coefficient of Trp at 295 is $1614 \text{ cm}^{-1}/\text{M}$ and of Tyr is only $56 \text{ cm}^{-1}/\text{M}$, i.e., at 295 nm Trp absorbs ~30 times more than the Tyr at 295 nm. There are five Trp and six Tyr in GRIM-19 protein, Fluorescence emission of GRIM-19 ($2\mu\text{M}$) was measured by Fluorolog-3 spectrofluorometer. Fluorescence spectra were recorded with 280 and 295nm excitation followed by emission between 310-400 nm. Refolded protein showed blue shift ($\sim 7\text{nm}$) in emission maxima when compared to unfolded, suggesting that the protein has folded properly (Figure 5.7). Further protease assays were performed with this refolded GRIM-19.



Emission max 280 unfolded: 342nm

Emission max 280 folded: 335nm

Emission max 295 unfolded: 343nm

Emission max 295 folded: 336nm

Figure 5.7: Fluorescence Emission scans of unfolded and refolded GRIM-19. Fluorescence emission spectra of urea denatured and renatured GRIM-19 at 280, 295nm and excitation at 310 to 400 nm emission wavelengths. The refolded proteins have low emission maxima and show considerable blue shift indicating that GRIM-19 protein is well folded.

5.2.2.2 In-silico modelling of GRIM-19

Since we did not find any suitable template for homology modeling, we proceed with Ab Initio modeling using I-TASSER Server. Five models were given by I-TASSER whose C-score ranged from -3.08 to -2.00 (Figure 5.8). Ramachandran plot validation of the models showed that model 1 contains 66.2% of the residues in the core region and 15.5% of the residues in the outlier region (Figure 5.8 A). Model 2, 3 and 5 had 50.7%, 69.7% and 62.3% in the core region and 21.8%, 11.3% and 19.0% in the outlier region, respectively (Figure 5.8 B, C and E). However, model 4 showed the highest percentage of residues, i.e., 73.2% in the core region, as well as highest C-score -2.00 (Figure 5.8 D). Though model 4 had 12% of the residues in the outlier region, due to the higher number of core region residues and C-score value, it was chosen as the best model and subjected to ModLoop refinement.

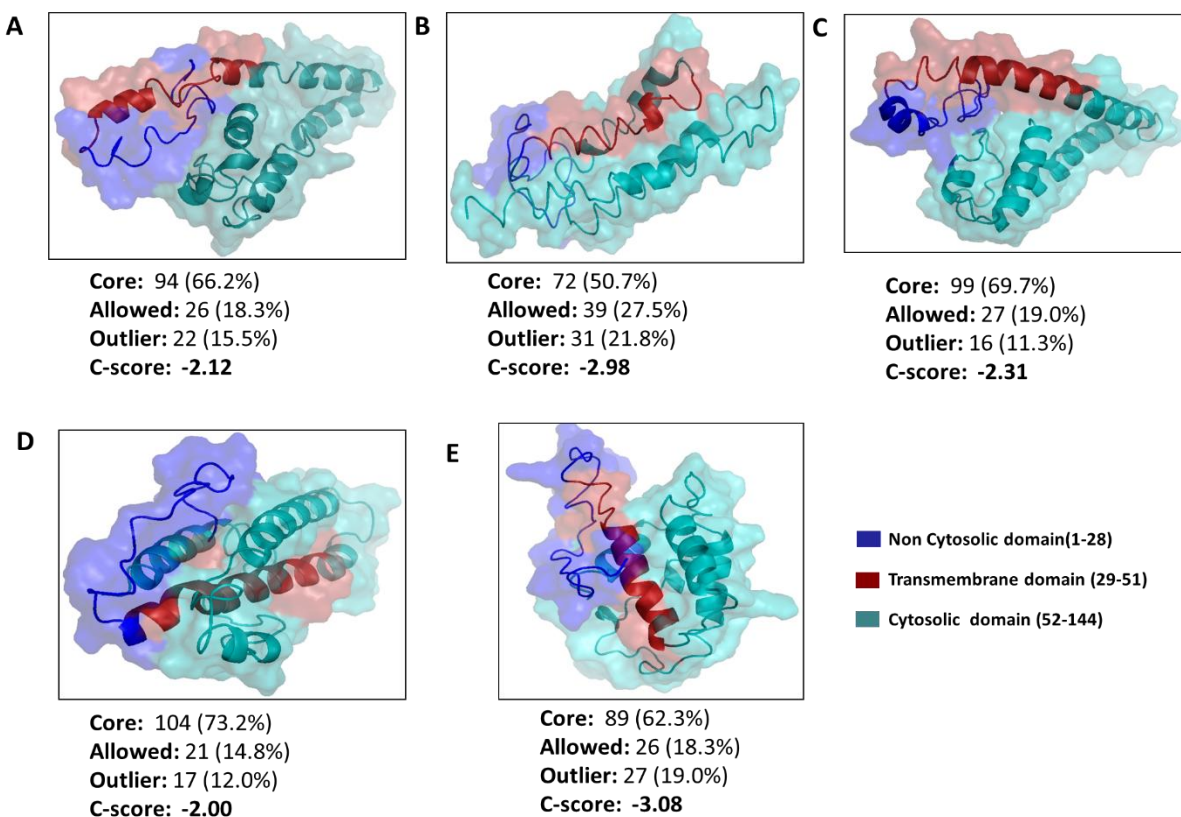


Figure 5.8: Quality analysis of the I-TASSER generated GRIM-19 models. The number of residues belonging to the energetically favored core, allowed and outlier regions along with their C-score values are shown for **A) Model 1**, **B) Model 2**, **C) Model 3**, **D) Model 4** and **E) Model 5**. For all the models, non-cytosolic domain of GRIM-19 is shown in blue, transmembrane domain in red and cytosolic domain in teal.

ModLoop refined model 4 was further validated using Ramachandran plot which revealed that refined structure contains no outlier residues and the number of residues in core region increased from 104 (73.2%) to 137 (96.5%).

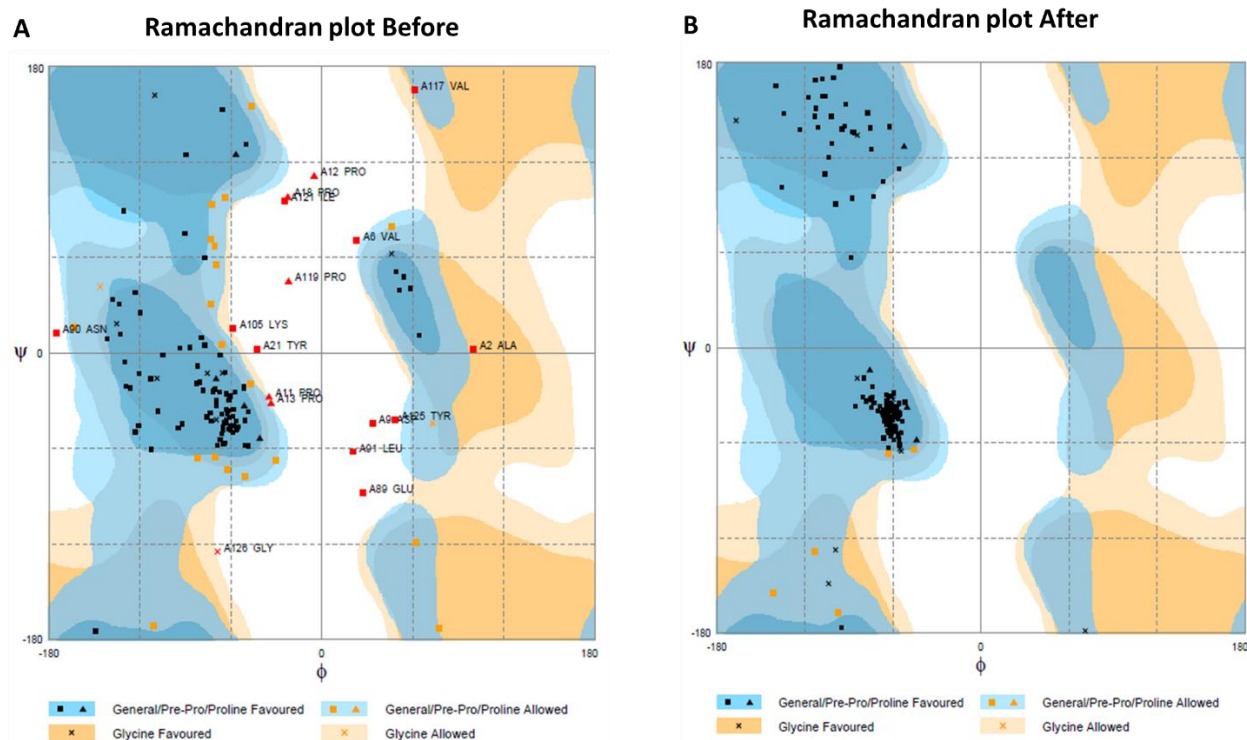


Figure 5.9: Ramachandran plot analysis of the GRIM-19 model. Ramachandran plot analysis of the GRIM-19 model **A)** before ModLoop refinement **B)** after ModLoop refinement showing an increase in the number of core region residues and elimination of the outlier residues.

5.2.3 Mapping the minimal binding region important for interaction

5.2.3.1 Docking of full-length GRIM-19 with HtrA2

The best GRIM-19 model was subjected to blind docking with HtrA2. Protein-protein docking between these proteins generated complexes which were ranked on the basis of docking score calculated using MM-GBSA scoring pattern, present in Bioluminate platform (Schrödinger, LLC, New York, NY, 2018). The energetically most favored docked complex was given for interaction analysis, which showed that the GRIM-19 residues exhibit surface interaction with HtrA2. A C-terminal long stretch of GRIM-19 residues, namely, Ala136, Ser137, Tyr138,

Gly139, Phe140, Met141, Trp142, Tyr143, and Thr144 interact with HtrA2 residues encompassing predominantly the SPD (Serine Protease Domain) region (Figure 5.10 A). This stretch of GRIM-19 residues belongs to its cell-death inducing domain, among which Tyr138 and Gly139 form H-bond interaction with Arg42, present in the SPD of HtrA2. Apart from the C-terminal stretch four other residues, namely, Trp104, Val106, Ser109 and Phe111 in the cell-death inducing domain of GRIM-19 form H-bond and van der Waal's interactions with HtrA2 (Figure 5.10 B).

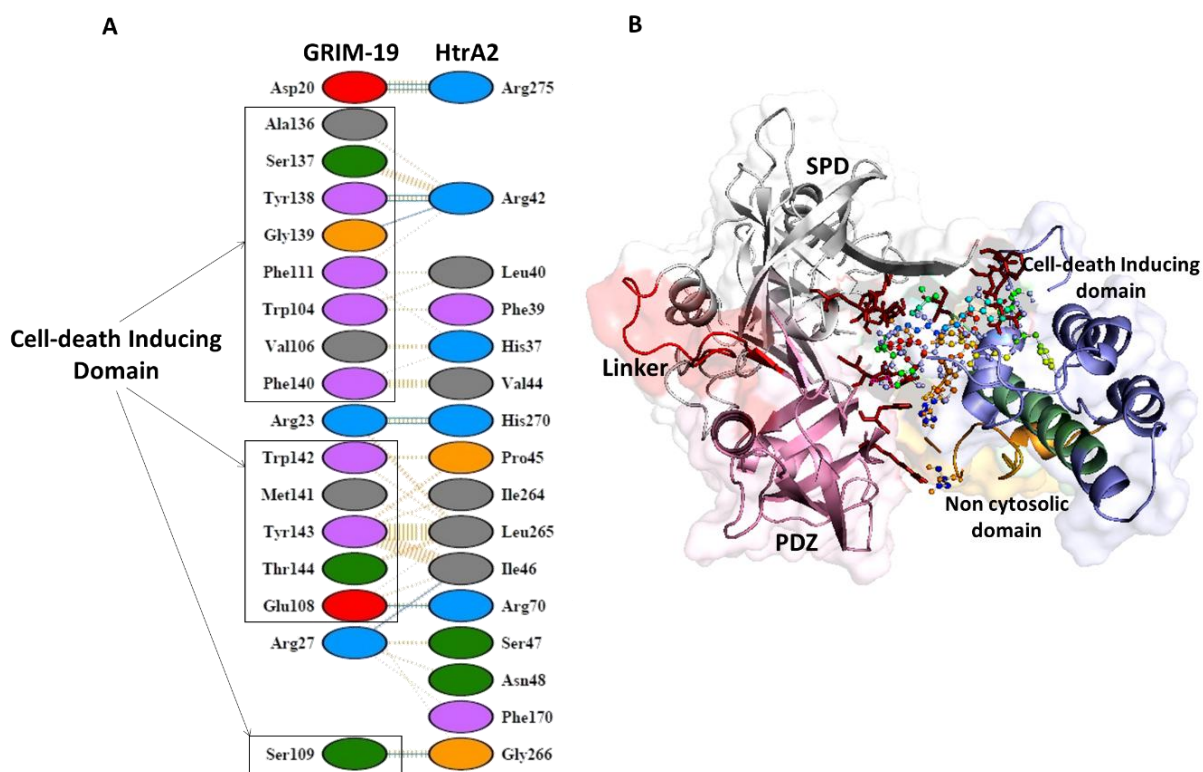
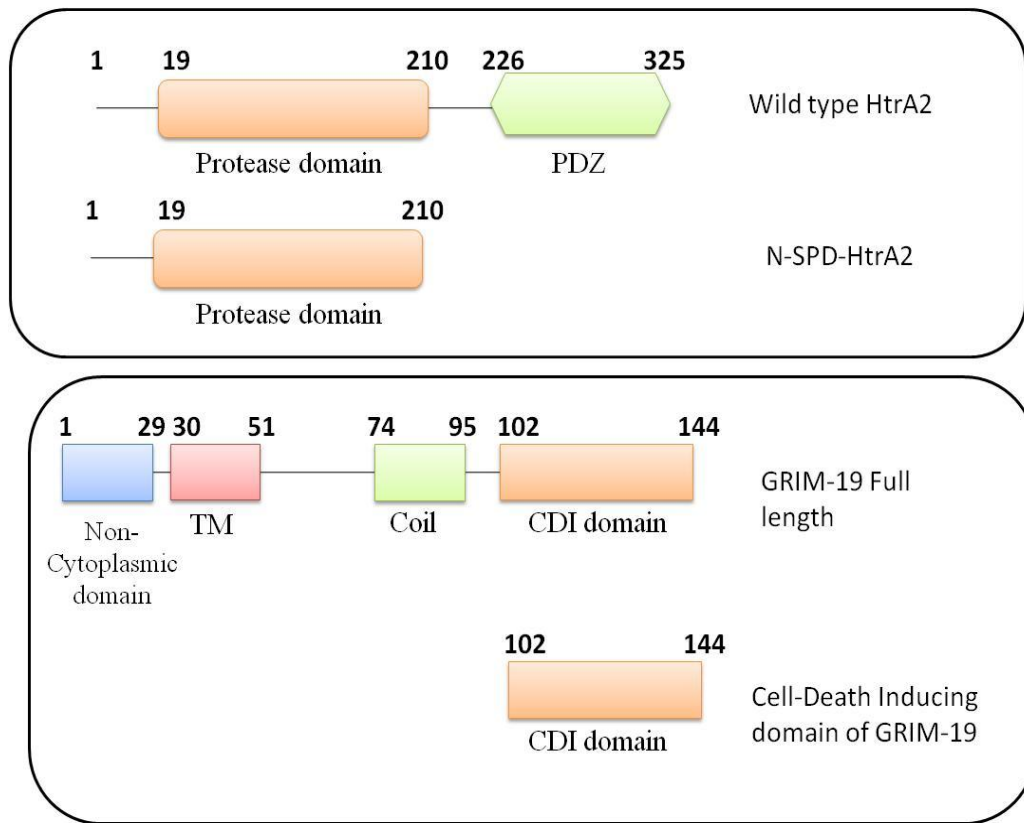


Figure 5.10: Interaction analysis of HtrA2 and GRIM-19 docked complex. A) PDBSum summary of HtrA2 and GRIM-19 interactions showing the residues, belonging to cell-death inducing domain form interaction with HtrA2. Green lines indicate H-bond and yellow dashed lines indicate van der Waal's interactions. B) Cartoon representation of the docked complex where the interacting residues are represented as rainbow sticks.

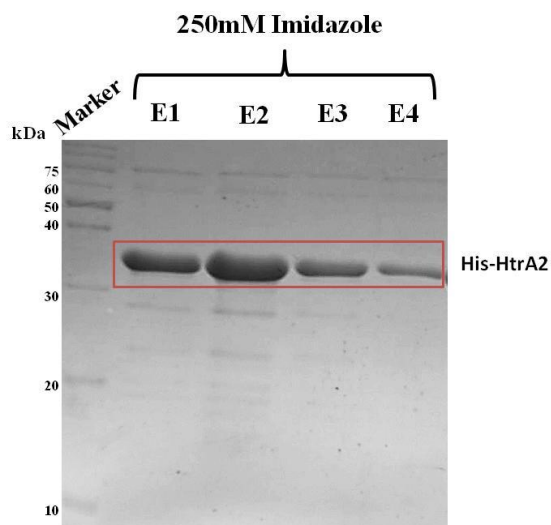
5.2.3.2 Binding assays of HtrA2 and GRIM-19

Although it has been previously demonstrated that HtrA2 binds to GRIM-19 and enhance the rate of apoptosis[205], the corresponding minimal binding region and critical residues involved in HtrA2 and GRIM-19 are not known. Therefore, pull-down studies were performed with MBP fused recombinant GRIM-19 as bait and HtrA2 variants as prey. HtrA2 variants used for these studies were HtrA2 full length and N-SPD domain (PDZ deleted variant), and their purifications were shown in figure 5.11. Pull-down experiments demonstrated that full-length GRIM-19 interacts with HtrA2 (Figure 5.12 A). From our *in silico* docking results it has been observed that most of the residues of GRIM-19 involved in the interaction belong to cell death-inducing domain. Hence we purified cell death-inducing domain of GRIM-19 (Figure 5.11 D) and performed pull down assays. From our results it is clear that both full-length GRIM-19 and cell death-inducing domain of GRIM-19 interacts with full-length and the serine protease domain of HtrA2 (Figure 5.12 B and C). No pull-down was detectable using MBP control alone.

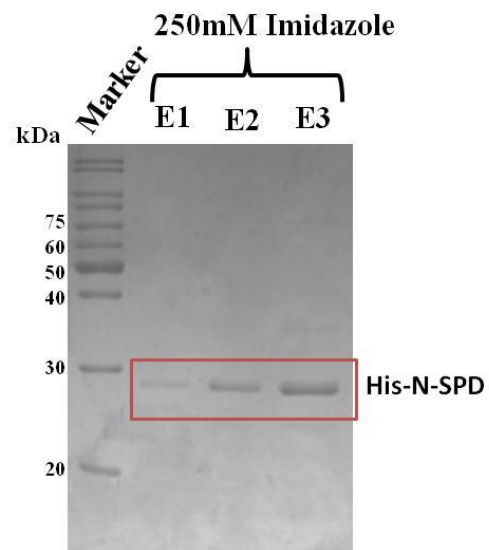
A)



B)



C)



D)

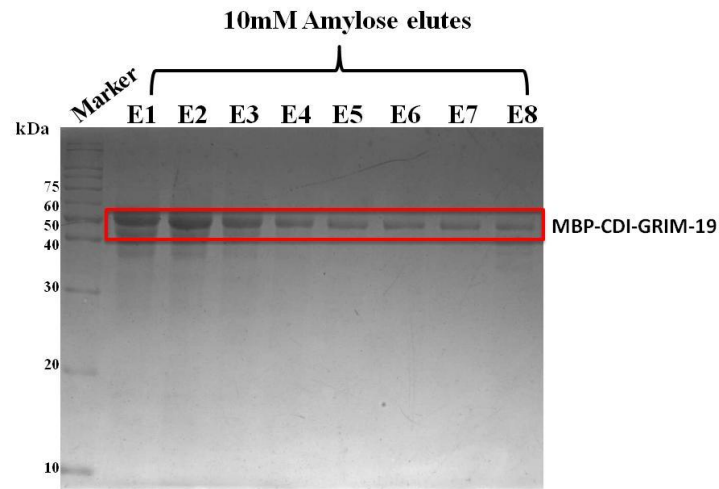


Figure 5.11: Purification of HtrA2 and GRIM-19 variants. SDS-PAGE gels representing purified proteins for HtrA2-GRIM-19 domain-wise pull-down assay. A) Schematic representation of different GRIM-19 and HtrA2 constructs used for HtrA2-GRIM-19 interaction studies. B) His tagged full-length HtrA2 (S174A), and C) His tagged N-SPD was purified by Ni-IDA affinity chromatography and D) MBP GRIM-19 cell death-inducing (CDI) domain purification using amylose resin. (E indicates elute)

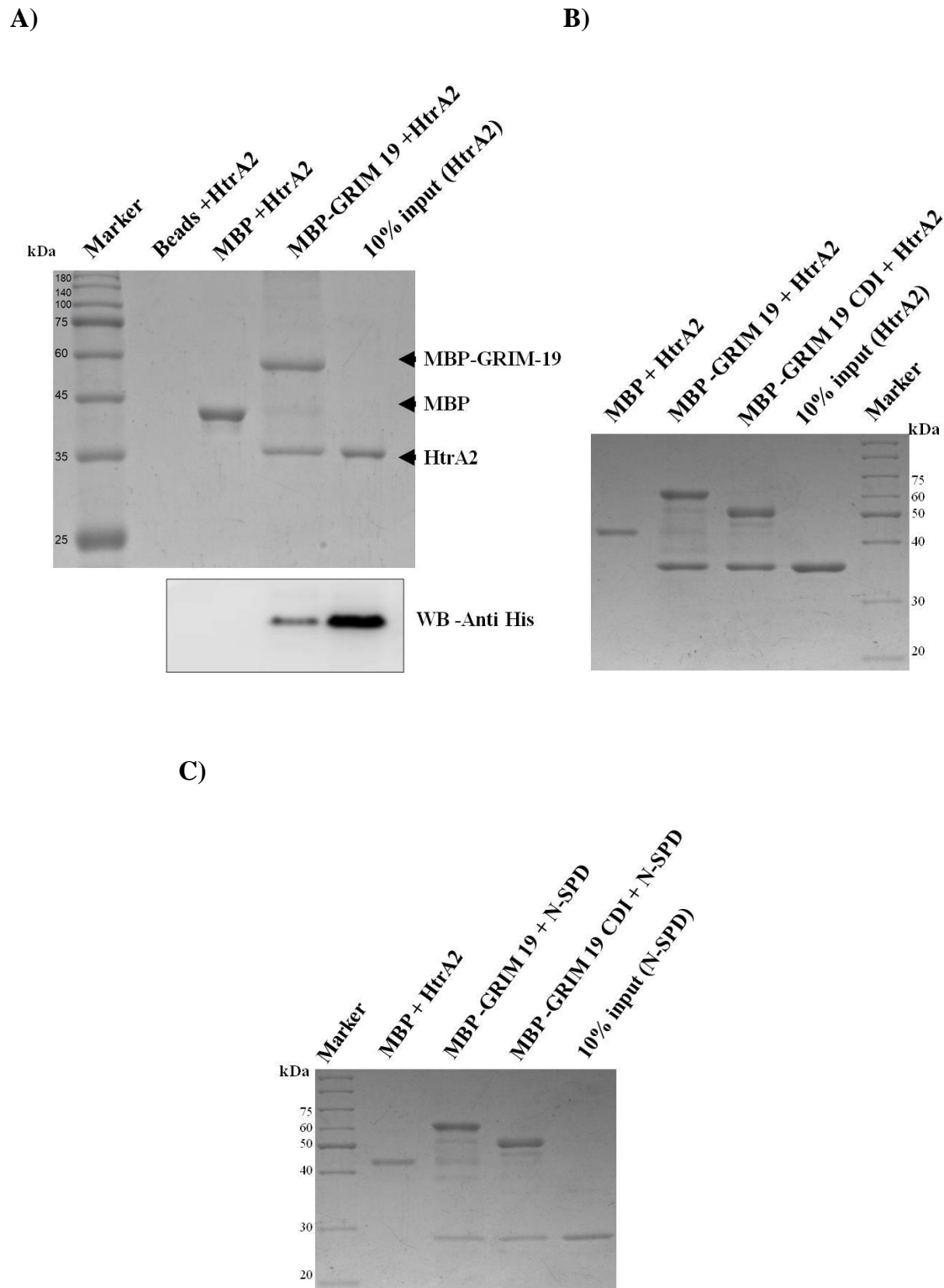


Figure 5.12: Pull-down assay with different *HtrA2* variants with various *GRIM-19* constructs.
A) MBP pull-down assay. Pull down was performed using MBP-GRIM-19 as bait and HtrA2 as prey. The interaction was further validated by western blotting using anti-His antibody. **B, C)**

MBP fused GRIM-19 and its cell death inducing (CDI) domain is used as bait and purified HtrA2 variants (B. HtrA2 wild type and C. N-SPD) are used as prey. 10 µg of recombinant MBP-GRIM-19 bound to amylose resin was incubated with the recombinant 100 µg of HtrA2 for 12 hrs at 4 °C. The reaction was stopped with Laemmli buffer at 100 °C, and proteins were separated by SDS-PAGE followed by coomassie blue staining.

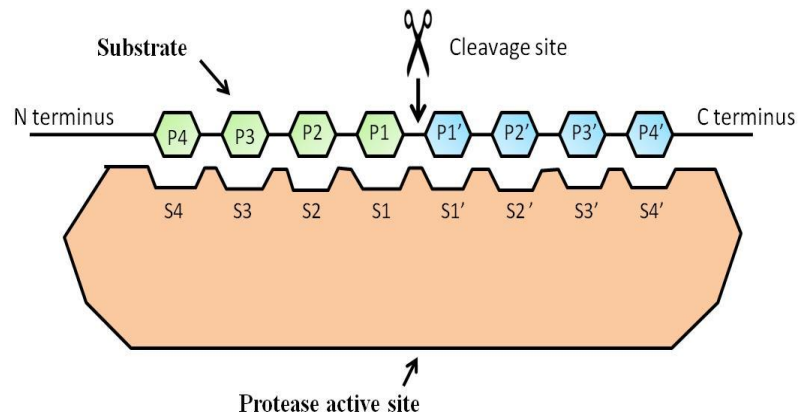
5.2.4 Substrate specificity of HtrA2 determined using natural substrate GRIM-19

The substrate specificity of classical serine proteases is mainly defined by the residue positions at carboxyl-terminal (P1', P2', P3') and amino-terminal (P1, P2, P3) to the cleavage site which are anchored by enzyme subsite residues (S3 to S3') in specificity pocket [208] (Figure 5.13 A). Substrate specificity of HtrA2 is limited to only two published reports, which showed the strong specificity profile at the residue positions P1, P2, P1' and P2' [209, 210]. The first studies reported by Martin and co-workers focused on the determination of the primary sequence specificity of HtrA2 protease activity using combinatorial peptide library. In the second report, Walle et al. used a proteomic approach to identify the optimal substrate cleavage site for HtrA2 protease. In this study, to understand substrate specificity of HtrA2 we used one of the natural substrate GRIM-19. Gel-based protease cleavage studies were performed with GRIM-19 as a putative substrate and either HtrA2 or HtrA2ΔPDZ (N-SPD) as the enzyme. Both HtrA2 and HtrA2ΔPDZ (N-SPD) variants cleaved GRIM-19 suggesting that GRIM-19 is a novel substrate of HtrA2 (Figure 5.13 B and C).

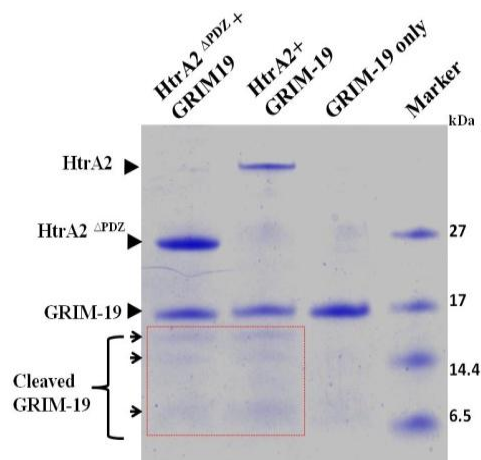
Further to gain insights into HtrA2 cleavage site specificity, proteolytically cleaved fragments (~15, 13, 12, 9.5, 6 and 5 kDa) of GRIM-19 were subjected to N-terminal sequencing by Edman degradation. The specificity profile of N-terminal sequence analysis of these fragments identified

six preferred cleavage sites on GRIM-19 (Figure 5.13 D and Table 5.2). The first cleavage site is between 19I–20D, second between 40I–41G, the third cleavage site is between 49S–50I, fourth cleavage site is between 68R–69I, fifth cleavage site is between K97–100D and the sixth cleavage site is between 108E–109S amino acids respectively. Cleavage at single or multiple sites resulted in a combination of different peptide fragments as shown in Figure 5.13 E. We performed a sequence analysis of the identified cleavage products to determine the specificity of the HtrA2. The specificity profile of HtrA2 mentioned in the literature and our N-terminal sequencing analysis of cleaved peptides residues are shown in Table 5.3. The observed frequencies of amino acids in the P1 position indicated a strong preference for aliphatic (I) and polar residues (S,R,K and E). At P2 position HtrA2 preferred aliphatic (A and M) and aromatic (W) residues. At P3 and P4 position HtrA2 accommodates aliphatic (G, I and V), polar (H and E) and aromatic (Y and F), aliphatic (A,G and I) residues respectively. At the P1' position, HtrA2 preferred polar (S and D) and aliphatic amino acids (G and I). At P2' position preference goes to aromatic (Y) and aliphatic (M, A, V) residues. At P3' position HtrA2 preferred polar (K and P) and aliphatic (L) residues. At P4' position it showed a preference for mostly aromatic (W), aliphatic (I and L) and polar (R, D and H) residues. This preference corroborates well with the previously published data and further to gain an insight into the structural determinants of HtrA2 substrate recognition and specificity, mutations in prime and non-prime cleavage residues and a high-resolution crystal structure of HtrA2 in complex with protein substrate is required.

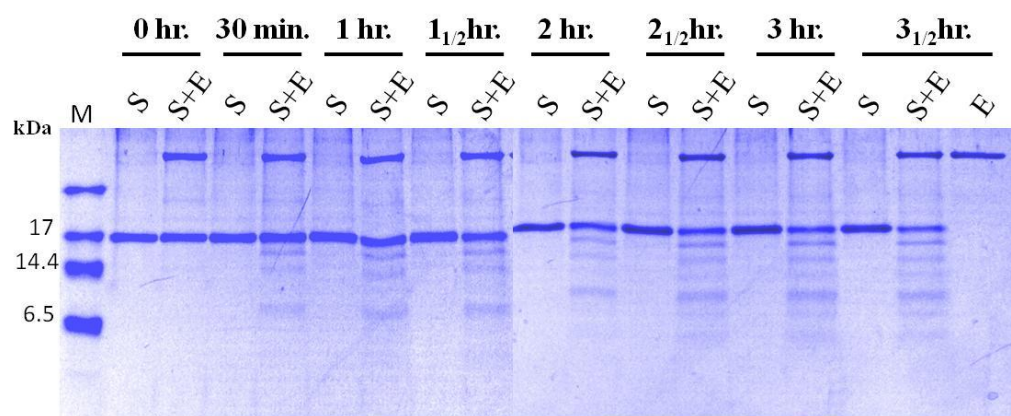
A)



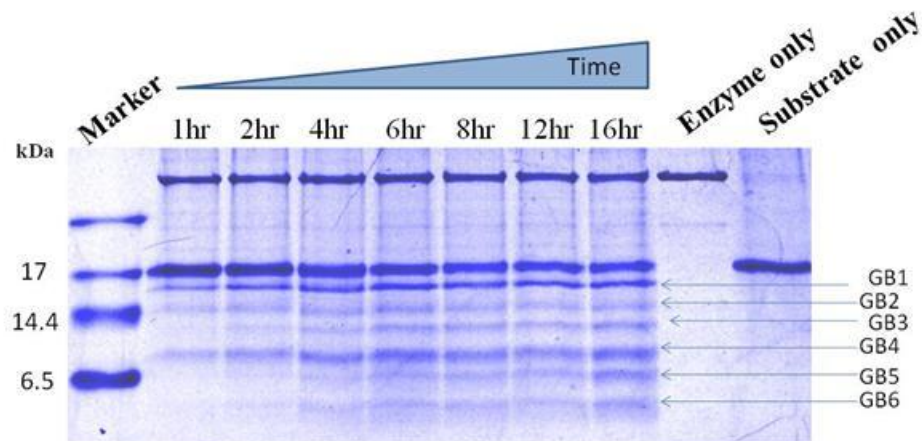
B)



C)



D)



E)

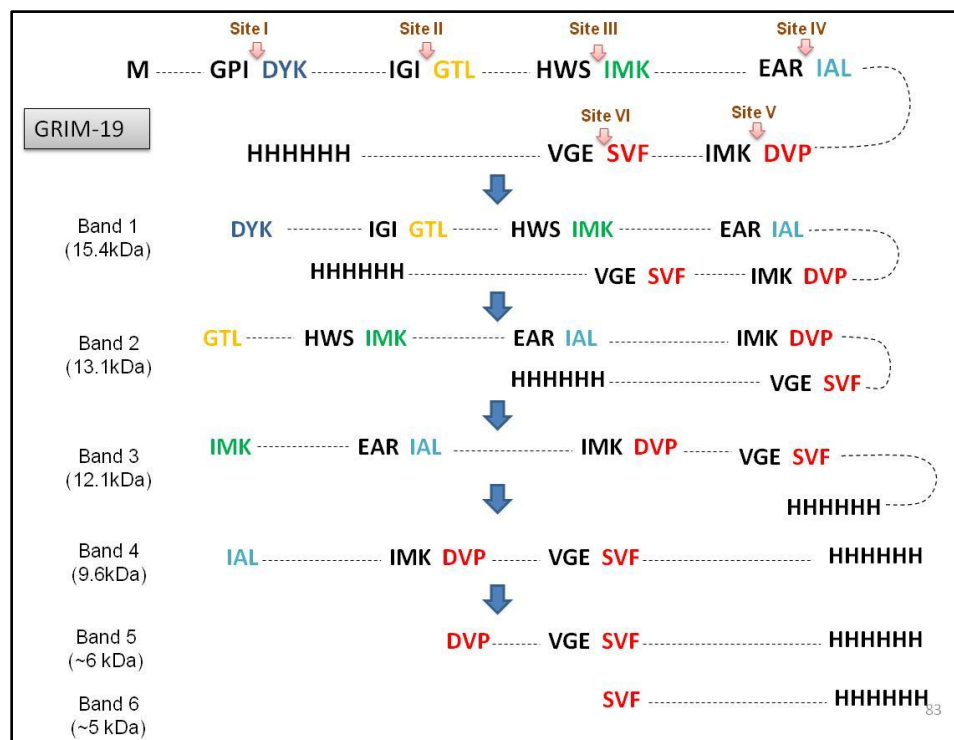


Figure 5.13: Proteolytic activity of HtrA2 and its variants with GRIM-19 as a substrate. A) Cartoon representation of substrate specificity of typical protease **B)** For each 20 μ l reaction mixture, 4 μ g of HtrA2 wild type and HtrA2 Δ PDZ was incubated with GRIM-19 (5 μ g) in assay

buffer for 12hr at 37°C. The reactions were stopped with SDS-PAGE sample buffer and were analyzed by 15% Tris-Tricine SDS-PAGE followed by Coomassie Blue staining. C) GRIM-19 incubated with only full-length HtrA2 starting from 0hr to 3_{1/2} hrs. E indicates enzyme (HtrA2) and S represents substrate (GRIM-19) D) Gel showing five different bands generated after cleavage were labelled as GB1, GB2, GB3, GB4, GB5, and GB6. These five bands were sent to N terminal sequencing to understand the cleavage specificity of HtrA2. E) Schematic representation of cleavage products observed on the gel after proteolysis. The GRIM-19 is cleaved into various fragments after incubating with HtrA2, initially, cleavage at site I and II generated fragments B1 (~15 kDa) and B2 (~13 kDa), upon further incubation, cleavage at site III generated B3 (~12 kDa). Further, cleavage at different sites generated B4 (~9.6 kDa) B5 (6 kDa) and B5 (<5 kDa) bands.

Table 5.2: Substrate specificity of HtrA2 using GRIM-19 as a substrate: Prime (P) and nonprime (P') residues at the cleavage sites were determined by N-terminal sequencing. GB1, GB2, GB3, GB4, GB5, and GB6 are the peptide fragments sent for the N-terminal sequencing as shown in Figure 5.13 D.

	P4	P3	P2	P1	-	P1'	P2'	P3'	P4'	P1' residue
GB1	Y	G	P	I	-	D	Y	K	R	Asp20
GB2	A	I	G	I	-	G	T	L	I	Gly41
GB3	G	H	W	S	-	I	M	K	W	Ile50
GB4	F	E	A	R	-	I	A	L	L	Ile69
GB5	I	I	M	K		D	V	P	D	Asp100
GB6	K	V	G	E		S	V	F	H	Ser109

Table 5.3: Substrate specificity of HtrA2

Positions	Literature [209, 210]	In case of GRIM-19
P1	A, I, S, R	I, S, R, K, E
P2	A, M, R, L	P, W, A, M, G
P3	K, F, M, A	H, E, G, I, V
P4	Y, L, P, I, V	Y, F, A, G, I, K
P1'	G, I, S, A	D, G, I, S
P2'	Y, F, S, M, A	Y, T, M, A, V
P3'	K, S, P, Y, F	K, L, P, F
P4'	I, F, Y, S, A	R, D, H, I, W, L

Aliphatic

Aromatic

Polar charged

Polar uncharged

5.2.5 Activation assays of HtrA2 with GRIM-19

It was reported in the literature that GRIM-19 enhances the pro-apoptotic activity of HtrA2 in *ex vivo*[205]. The minimal binding region of GRIM-19 which activates HtrA2 and the allosteric changes in HtrA2 associated with GRIM-19 binding is not known. The activation assay was performed in the presence of GRIM-19, from our docking and pull-down studies cell death-inducing domain of GRIM-19 is known to interact with HtrA2 and we employed this domain of

GRIM-19 for activation assays as well. The activity of HtrA2 was monitored after pre incubation with full length and cell death-inducing domain of GRIM-19. To determine the kinetic parameters, we measured the initial rates of substrate cleavage for different β -casein concentrations. It was observed that HtrA2 cleavage of β -casein follows a sigmoidal curve with a Hill constant of 2.8 (Figure 5.14). Therefore, the positive cooperativity upon substrate cleavage suggests that binding of one substrate (β -casein) molecule to one subunit of HtrA2 trimer favors the consequent binding of others. Interestingly, upon pre-incubation of HtrA2 with GRIM-19 the catalytic efficiency (k_{cat}/K_m) increased by approximately 2 fold and with cell death-inducing domain it increased to 2.8 fold (Table 5.4). The results might suggest greater stabilization of the relaxed (active) state of protease upon GRIM-19 binding. However, the substrate concentration at half-maximal velocity (K_m) remained unchanged, even in presence of GRIM-19 implying the existence of a similar binding pocket. The activity of HtrA2 was monitored after pre-incubation with GRIM-19 and the V_{max} was found to be altered without significantly altering the apparent K_m (with L2 specificity pocket mostly unaltered) and hence follow the 'V system' of allosteric modulation[211]. In his system, both the relaxed (R) and the tensed (T) states bind the substrate at the active site with similar affinity while the activator at the allosteric site binds the R and T states with different affinity. This differential affinity of the activator towards the binding site along with R state stabilization shifts the equilibrium towards R state thus positively influencing its turnover rate and hence catalytic efficiency which has been observed in case of HtrA2 in the presence of GRIM-19. Thus, GRIM-19 acts as an activator to allosterically modulate HtrA2 to form a catalytically active enzyme, which then cleaves β -casein. This observation suggests interaction of GRIM-19 with HtrA2 brings about rearrangement around the active site of the enzyme by positively influencing its activity thus behaving as an allosteric regulator.

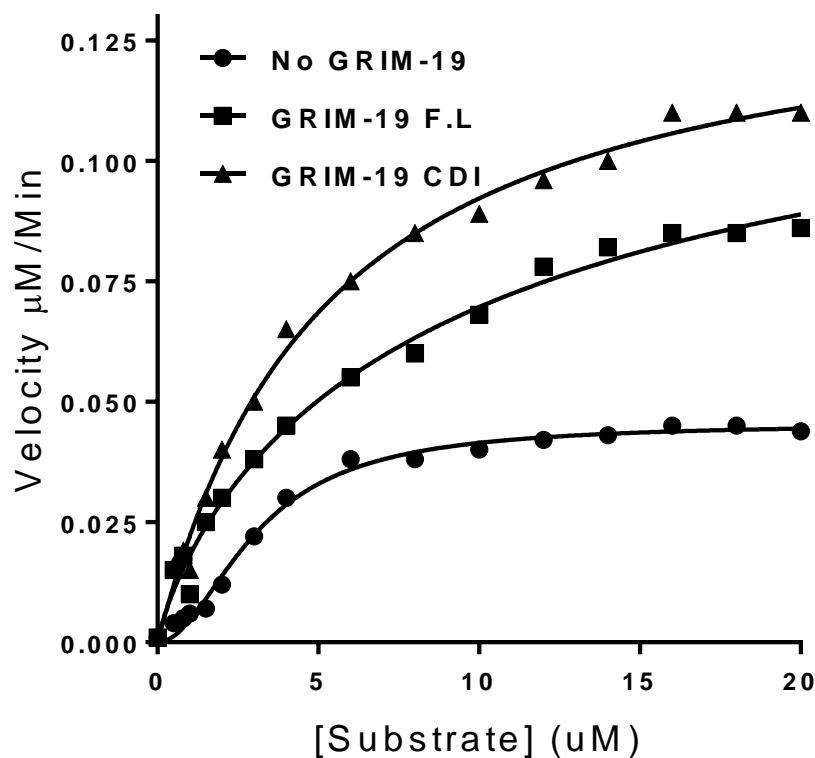


Figure 5.14: Activity of wild-type HtrA2 in presence or absence of activator. The steady-state kinetics of β -casein cleavage by wild-type HtrA2 (200 nM) has been done in the presence of saturating concentration of GRIM-19 full length (20 μ M) and cell death-inducing domain (25 μ M) of GRIM-19. The solid lines are nonlinear least-squares fit of the data to the Hill form of the Michaelis-Menten equation: $\text{velocity} = V_{\text{max}} / (1 + (K_m / [\text{substrate}])^n)$.

Table 5.4: Enzymatic parameters for HtrA2 in the presence of GRIM-19 full length and CID domain (cell death-inducing domain). The initial rates for substrate cleavage in the presence or absence of GRIM-19 protein were measured and fitted to Hill form of Michaelis-Menten equation to determine the steady-state kinetic parameters (Figure 5.14). The values are mean \pm S.E.M (n=3).

		K_m	Hill constant	Maximum velocity V_{max} (M/s)	k_{cat} (s^{-1})	Catalytic efficiency k_{cat}/K_m ($M^{-1} s^{-1}$)
WT-HtrA2 only		4.60 ± 0.5	2.8 ± 0.2	4.08×10^{-9}	0.02 ± 0.004	4.5×10^3
WT-HtrA2	GRIM-19 Full length	4.62 ± 0.5	1.8 ± 0.2	$8.16 \pm 0.2 \times 10^{-9}$	0.04 ± 0.006	8.7×10^3
WT-HtrA2	GRIM-19 Cytoplasmic domain	4.63 ± 0.5	1.6 ± 0.2	$11.4 \pm 0.2 \times 10^{-9}$	0.057 ± 0.006	12.4×10^3

5.2.6 Structural changes in HtrA2 associated with GRIM-19 peptide binding

5.2.6.1 Docking analysis of the GRIM-19 peptides with HtrA2 trimer

From our activation assay experiments, it is evident that full length and cell death-inducing domain of GRIM-19 activates HtrA2 significantly. To understand more about interacting surface, in-depth analysis of HtrA2 and GRIM-19 interacting residues were analyzed using docking studies with the peptides of GRIM-19. Since cell death-inducing domain has high potential to activate HtrA2, the peptide library prepared only from cell death-inducing domain of GRIM-19 (amino acid sequence 102 to 144). Heptameric GRIM-19 peptides from the designed

peptide library were docked with HtrA2 trimer at the best binding site (site 1) generated from the SiteMap output (Table 5.5). The top five docked complexes were shortlisted for interaction analysis whose docking score ranged from -9.191 kCal/mol to -7.928 kCal/mol. Interaction analysis showed that the peptides tend to bind into the trimeric interface of the HtrA2, predominantly forming H-bond interaction with Asp165 (belongs to SPD) residue present in the interface. Moreover, other SPD residues like Ala167, Lys191 and Ala194 were the most common residues which either formed H-bond or van der Waal's interaction with the GRIM-19 peptides (Figures 5.15 A and B).

Table 5.5: SiteMap analysis of the putative binding sites of HtrA2

Site number	Residues present	Site Score
Site 1	A132, L133, Q134, N135, T136, T138, S139, G140, D165, A166, A167, I168, D169, N188, T189, N190, K191, V192, T193, A194, G195, I196, S197, R247, E248	1.01
Site 2	V21, E22, G41, R42, E43, A55, A56, D57, G58, P276, G277, D278, V279	0.81
Site 3	R42, E43, A55, A56, T193, A194, G195, E248	0.79
Site 4	V21, E22, S139, G140, T193, A194, G195, I196, S197	0.72

Figure 5.16: Ligplot of the docked complexes ranked from 2 to 5. Ligplot showing the details of the interaction between **A) DWVGES** (denoted by Chain D) **B) LYGLRTT** (denoted by Chain D) **C) EEALHAS** (denoted by Chain D) **D) VHFTTRW** (denoted by Chain D) and HtrA2. H-bond interactions are represented as green dotted lines and semi-circular red dashed lines indicate van der Waal's interactions.

Table 5.6: Docking analysis showing the H-bond interactions and docking score

Docked Complex	H-bond Interactions		Docking Score (kCal/mol)
	HtrA2	GRIM-19(peptides)	
HtrA2-HGFMWYT	Asp165, Ala167	Tyr6	-9.191
HtrA2-DWKVGES	Asp165, Ala194	Trp2, Val4	-8.417
HtrA2-LYGLRTT	Lys191	Thr7	-8.343
HtrA2-EEALHAS	Arg247, Ala194	Leu4, His5	-7.961
HtrA2-VHFTTRW	Ser139, Asp165, Ala167, Asp169	Thr4, Trp7	-7.928

5.2.6.2 Structure-based comparative analysis of the GRIM-19 peptide bound and unbound HtrA2 using MD simulation

To understand more about conformational changes associated with peptide binding, we performed molecular dynamics simulations with GRIM-19 peptide bound and unbound HtrA2. Among all the peptides, HGFMWYT yielded the highest docking score of -9.191 kCal/ mole and was chosen for comparative MD simulation analysis with unbound HtrA2. Conformational changes in HtrA2-HGFMWYT complex during MD simulation indicated large fluctuation in the N-terminal region (1-32) (Figure 5.17 A and B) when compared to unbound HtrA2. The RMSD difference between bound and unbound HtrA2 in the N-terminus was found to be 1.2 Å. In comparison to the unbound HtrA2, overall SPD domain movements (33-209) in the bound HtrA2 seemed to get relaxed by 0.9Å (Figure 5.17 A and B). However, significant deviation in the

RMSD of the regulatory LD and L1 loops were observed in the bound complex, ranging from 1.1 Å to 1.6 Å (Figure 5.17 C). Movement of these loops could be significant for the opening of the catalytic pocket of HtrA2, which were further concluded from the active site and oxyanion hole reorientation in the bound complex (Figure 5.18). Nonetheless, there were not many movements were seen in the hinge region as the GRIM-19 peptide tend to bind in the SPD region. Due to SPD binding no such signal from the PDZ domain was required to be transferred via the hinge region which further corroborate with the very little movement seen in the hinge region (Figure 5.17 C).

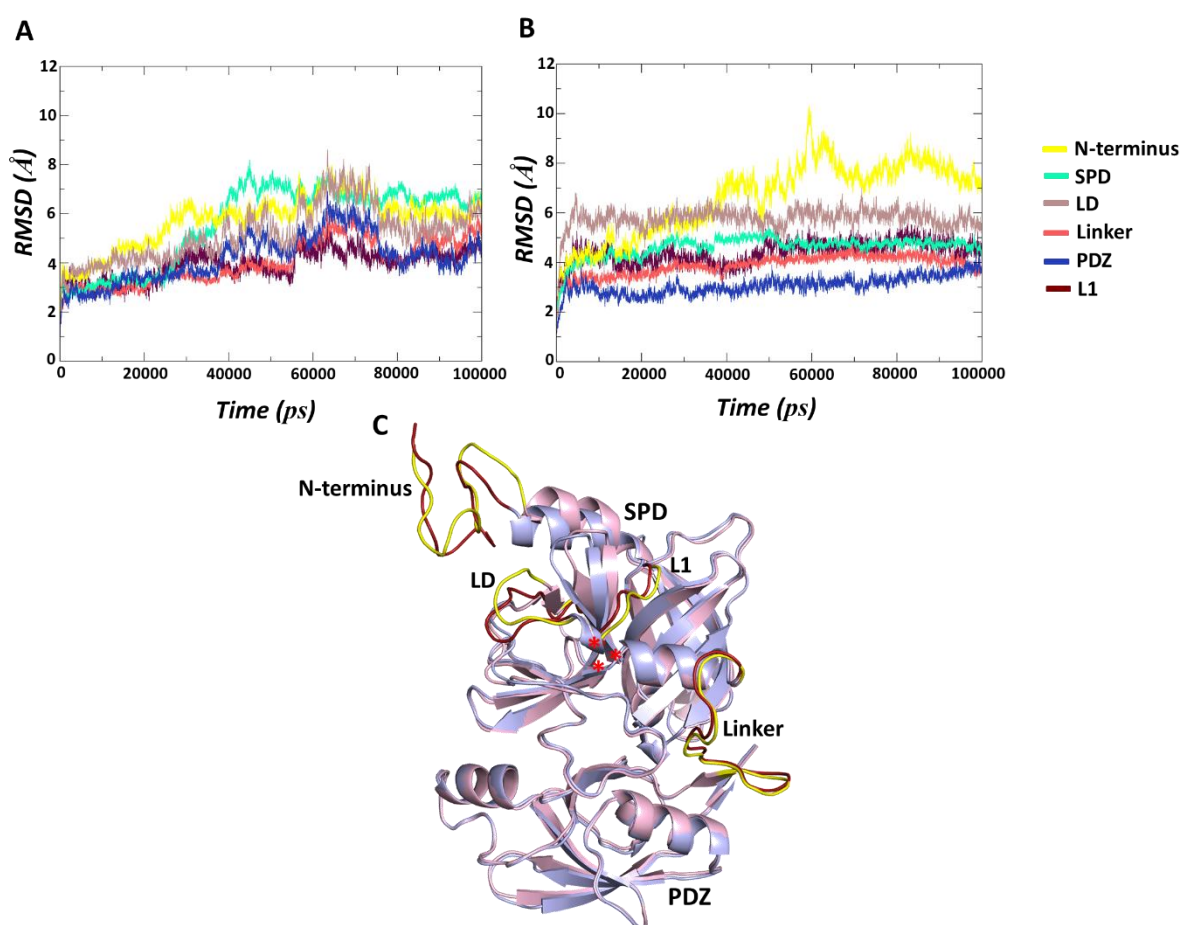


Figure 5.17: Domain specific conformational changes in HtrA2 resulted from the GRIM-19 (HGFMWYT) peptide binding. RMSD plot is showing domain-wise deviations in the **A) unbound HtrA2 and B) bound HtrA2** over 100 ns of MD simulation. **C) Superimposed cartoon representation of one of the chains (Chain A) for the unbound (light blue) and bound (pink) HtrA2**, showing the loop movements, where the loops are indicated in yellow for unbound and red for bound. The red asterisk indicates each residue in the catalytic triad.

Atomic distance analysis of the catalytic triad residues in the HtrA2-HGFMWYT complex showed that distances between nitrogen (N ϵ 2) atom of H65 and oxygen (O γ) atom of S173 increased by 0.5 Å when compared to unbound HtrA2 (Figure 5.18 A). However, the distance between nitrogen (N δ 1) atom of H65 and oxygen (O δ 2) atom of D95 decreased by 0.6 Å for HtrA2-HGFMWYT with reference to the unbound HtrA2 (Figure 5.18 A). Moreover, conformational changes were also observed in the relative orientation of oxyanion hole residues, namely F170, G171 and N172. The aromatic ring of F170 exhibited an anti-clockwise flip moving away from the imidazole ring of H65 in the bound complex creating a void space large enough to accommodate a substrate (Figure 5.18 B).

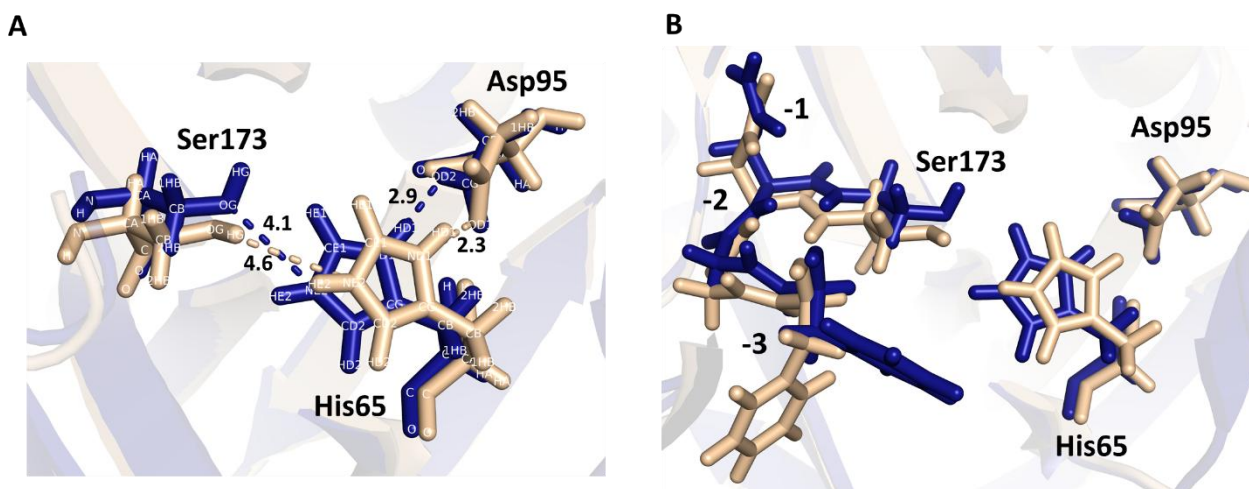


Figure 5.18: Interatomic distance analysis resulting structural reorientation of the catalytic triad and oxyanion hole residues. *A) Overlay of the bound (light yellow) and unbound HtrA2 (blue) showing catalytic triad movements, where H65 moves away from the S173, subsequently D95 moves closer to H65. All the distances are given in Å. B) Superimposed structure of bound (light yellow) and unbound HtrA2 (blue) showing flip of -3 oxyanion hole residue to create a pocket for accommodating a substrate. Here, positions of the oxyanion residues namely N172 G171 and F170 are denoted by -1, -2 and -3 respectively, keeping S173 at 0th position.*

5.3 Discussion and conclusion:

HtrA2 is a nuclear-encoded serine protease that performs several critical cellular functions in a coordinated fashion. Although, HtrA2 has primarily been identified as an IAP-binding proapoptotic protein, its other functions such as caspase-independent induction of apoptosis and serine protease activity are poorly characterized. Despite numerous reports on HtrA2 induced apoptosis, little is known about its mode of regulation, and the mechanism of interaction with its substrates involved in mediating this function. The available crystallographic data on mature substrate-unbound form of HtrA2 provided a broad overview of its structural organization. However, these studies could not define its mode of activation, which is a prerequisite for understanding its role in various biological pathways and diseases. Furthermore, delineating the basis and global mode of HtrA2 activation might give rise to therapeutic possibilities in various pathophysiological conditions such as cancer and neurodegenerative disorders. To delineate the structural correlates of HtrA2 activation, substrate recognition and specificity, comprehensive binding studies with its interacting partners is necessary. In the present work we dissected the molecular mechanism of HtrA2 with its interacting partner GRIM-19. Although previous studies

have reported that interferon-induced GRIM-19 interacts and activates HtrA2, which leads to cell death [212], the interacting region, critical residues involved in interaction, and allosteric activation mechanism associated are not known. It is well established in the literature that PDZ domain of HtrA2 is involved in interacting with different cellular proteins. Contrary to previous reports that suggest only PDZ domain of HtrA2 interacts with GRIM-19 our studies demonstrated the role of SPD and in the interaction. This complex mode of interaction involving both SPD and PDZ region might be required for enhancing the affinity of individually weaker interactions and allows for greater binding affinity with GRIM-19. Enzymology studies with wild-type HtrA2 delineated that GRIM-19 as novel substrate of HtrA2. Our primary sequence specificity based on the N-terminal sequencing displayed a broad specificity for HtrA2 toward the residues in vicinity of cleavage site. Although previous reports suggest that HtrA2 has preference towards aliphatic residues at P1 position, our studies indicated that polar (K and E) residues are also equally preferred at P1. In uniformity with the literature for selectivity of A and S at P1', our results demonstrated additional preference for acidic residue (D) at the P1'. Previous reports suggest that P2 prefers basic (R) and aliphatic (L) residues, while P2' position displays preference for aromatic (Y and F) residues[196]. Interestingly, our data demonstrate that polar (P and T) and aromatic (W and Y) residues are also preferred at P2 and P2' positions. This apparent discrepancy in cleavage site specificity between peptide and protein substrates of HtrA2 might be due to conformational constraint of a potentially susceptible sequence in proteins. Moreover, variations in the natural frequency of occurrence of amino acids in endogenous proteins may be an additional parameter that might help explain the differences between peptide and protein cleavage site specificities. It is likely that this specificity partly determines the choice of residues selected by HtrA2 within a target protein as well as post-translational modifications in the

protein. However, the selection of target proteins may also be dependent on which proteins are bound to the PDZ domain or other regions of HtrA2 and thus brought into proximity with the active site region.

PhosphoSitePlus® (PSP) is a resource for studying experimentally observed PTMs in the regulation of biological processes. It includes coverage of commonly studied PTMs such as phosphorylation, acetylation, methylation, ubiquitination, and O-glycosylation [213]. From the database, we could observe four different kinds of post-translational modifications that occur in GRIM-19. Acetylation at K22, methylation at R81, ubiquitination at K22, K99, K105, and phosphorylation at T79, Y125 residues were observed [213]. There are several post-translational modifications associated with HtrA2 functions [213]. Kalvakolanu et al., identified GRIM-19 as an interacting partner of HtrA2 using Yeast Two Hybrid system and validated using Immunofluorescence studies in MCF-7 cell lines [112]. In our study, we used bacterially overexpressed proteins for *in vitro* pull-down and enzymatic assays. Further experiments will be done in the lab in future to understand more about how post-translational modifications affect HtrA2-GRIM-19 interaction and other cellular functions.

From substrate specificity data, it is clear that there are six sites present in GRIM-19 which are accessible for HtrA2 cleavage. Out of the five I-TASSER-generated models of GRIM-19, the fourth one exhibits maximum residues in the allowed region of the Ramachandran plot. Moreover, the residues at the cleavage sites are found to be exposed and hence more accessible to the protease. Asp20 (GB1) is an exposed residue situated in the loop region of the model; Gly41(GB2) is a partially buried residue located in the Helix 3. Ile50 (GB3) and Ile 69(GB4) are exposed residues situated in Helices 3 and 4 respectively. Also, Asp100 (GB5) is an exposed residue located in the Helix 5 and Ser109 (GB6) is an exposed residue present in the loop region

of model 4. Although, many of these residues are exposed or partially exposed in the other models as well, the best match in terms of allowed regions and accessibility is observed in model 4. Activation assays with wild-type HtrA2 using substrate β -casein in the presence of varying effectors such as full-length GRIM-19, its cell death-inducing domain showed significant increment in the cleavage rate of the protease. From our *in silico* data binding of GRIM-19 peptides at N-terminus of HtrA2 allosterically modulates the protease and shifts the intrinsic equilibrium from tense to relaxed conformation thereby increasing the overall catalytic efficiency. Studies on HtrA2 optimal binding peptides showed that these peptides interact at the distal sites away from the catalytic pocket, preferably in the PDZ domain[214]. However, in our study we have designed peptides from the cell-death inducing domain of GRIM-19 which bind to the protease domain residues. Interestingly, the binding pocket is away from the catalytic or orthosteric pocket of HtrA2, which further hints towards allosteric mode of activation for HtrA2 [215]. Our *in silico* studies show that upon binding to the GRIM-19 peptides, LD and L1 loops show slight movements away from the active site which are conducive toward forming a catalytically active orthosteric pocket. Moreover, these loop movements lead to a cascade of events, which result in movements of His65 away from the Ser173 and towards Asp95. These structural reorientations corroborate with the earlier studies where similar movements are observed in presence of activator peptides, which are in turn instrumental for proper oxyanion hole and open catalytic pocket formation [141]. Hence, developing strategies to positively regulate HtrA2 functions using GRIM-19 peptide might open up possibilities toward modulating HtrA2 functions for therapeutic benefit.

CHAPTER – 6

CONCLUSIONS AND FUTURE PERSPECTIVES

CHAPTER 6: CONCLUSIONS AND FUTURE PERSPECTIVES

Part 1: Discerning the mechanism of action of HtrA4 and functional redundancy:

HtrA family members have similar domain architecture and perform various functions in the cell, deregulation of their normal functions leads to various diseases [18, 20, 22, 33, 137–139, 216]. Among human HtrA homologs, HtrA1 and HtrA2 are well characterized with available high-resolution crystal structures. HtrA1 and HtrA2 cleave a wide variety of targets mostly involved in cell death [36, 57, 58, 62]. The human HtrA homologs have an N-terminal region, serine protease domain and PDZ domain, the role of these domains in regulating protease activity is very well characterized in case of HtrA1 and 2 [36]. However, HtrA4 is the least described human HtrA protease concerning both structure as well as its functions. The role of HtrA4 in cellular physiology and pathology has recently started to emerge. HtrA4 levels are altered in many cancers, and are found to be up-regulated in pre-eclampsia (PE) and hence has been suggested to be used as a biomarker of PE [10, 22, 33]. However, none of the studies could define its mode of regulation and functions which are a prerequisite for delineating its role in various biological pathways and diseases. Therefore, an intricate dissection of HtrA4 structure with an understanding of its functional reciprocity becomes imperative to harness its properties with desired characteristics.

To summarize, in the present study, we delineated the role of HtrA4 and its sub domains in enzyme catalysis as well as oligomerization status. We performed structural, biophysical as well as functional comparison of HtrA4 with its family members. Results in the present study

highlight the importance of the N-terminal region in oligomerization. The kinetics of HtrA4 which was found to be lower than HtrA1, HtrA2 and HtrA4 is substantially active at higher temperatures ($>30\text{ }^{\circ}\text{C}$). Using β -casein, we investigated the substrate specificity and cleavage site residue selectivity which found to be similar across the family. Sequence analysis identified the IAP binding motif in HtrA4; HtrA4 binds and cleaves X-linked inhibitor of apoptosis protein (XIAP) in a time-dependent manner. Our data suggest that HtrA4 may have a role in cell death like proapoptotic HtrA2 and XIAP acts as its novel substrate. Subtle structural variations in the dynamic loop regions and around the active-site might be responsible for the difference in their protease activity, and hence functional diversity within the protease family. Based on above findings, we propose a working model of HtrA4 mode of action. We propose that HtrA4 exists in both trimeric and monomeric forms; trimeric one is the dominant and most favorable native oligomeric state. Addition of substrate also enhanced the conversion of the residual population of monomers to trimers. The model also suggests that initial binding of the β -casein peptide at SBP_HtrA4 leads to conformational rearrangement of the N-terminal region and loops at and around the catalytic triad. The significant role of N-terminal region in fostering HtrA4's activity and maintaining its trimeric form is evident from the fact that both SPD-PDZ and SPD monomers, which are devoid of N-terminal region and are inactive. Hence, it further emphasizes the importance of trimerization to acquire a catalytically competent structure and indicates that the serine protease domain alone is not sufficient for catalytic activities.

Part 2 : To understand the interaction of HtrA2 with its binding partner– GRIM-19

HtrA2 levels are known to be altered in many cancers such as chronic lymphocytic leukemia (CLL), renal carcinoma, ovarian cancer, breast cancer and prostate cancers [22]. Two major approaches in cancer therapies, such as chemotherapy or radiotherapy induce DNA damage and activate apoptosis [217]. Tumor samples from various cancers show elevated expression of IAPs, which are known to inhibit caspase activation, thereby preventing activation of apoptotic pathways in cancer cells. As evading apoptosis is one of the hallmarks of cancer [218], a complete understanding of HtrA2-mediated apoptotic pathway will help researchers devise strategies that will promote cancer cells to undergo cell death. HtrA2 has been found to have basal proteolytic activity which is enhanced several folds during apoptosis through a complex allosteric mechanism [4]. Thus developing a strategy that enhances the proteolytic activity of HtrA2 towards its substrates could be a promising tool in cancer treatment in combination with other chemotherapeutic agents such as cisplatin and paclitaxel [10]. Understanding the interaction between HtrA2 with its known activator GRIM-19 has the potential to be the cornerstone in designing peptide and small molecule activators of HtrA2. Apart from enhancing our knowledge about the proteases, our studies will help deduce their roles in several cellular processes. Studies have established that the tumor suppressor protein GRIM-19 to be a binding partner of HtrA2. Despite this information, the structural details, stoichiometry and mechanism of HtrA2-GRIM-19 interaction still needed to be elucidated. Thus, we aimed at structural and functional characterization of HtrA2-GRIM-19 interaction.

In this study, we provided the comprehensive binding analysis of HtrA2-GRIM-19 interaction. Our binding studies demonstrated that serine protease domain of HtrA2 interacts with both full length as well as cell death inducing domain region of GRIM-19. Enzymology studies with

GRIM-19 suggest that it is an allosteric activator of HtrA2 as it enhances the protease activity several fold. This might lead to activation of HtrA2 with the cleavage of several critical cellular proteins thus triggering apoptosis. Furthermore, our substrate specificity studies with GRIM-19 highlight that HtrA2 has broad substrate specificity toward the residues in the vicinity of its cleavage sites. We hypothesize that this broad specificity might be required for cleaving a variety of substrates by HtrA2 that commensurate very well with its diverse physiological functions. Proteolytic activity of HtrA2 has been reported to be critical in inducing apoptosis in prostate and ovarian cancer cells in presence of stress inducing agents [219]. These studies show the possibility of targeting HtrA2 in cancer therapy. Our advancement in understanding toward HtrA2 mechanism of action will help in developing tailored allosteric effectors that might enhance the proteolytic activity of HtrA2 towards its substrates.

Future perspective:

Apoptosis induction in cancer cells provides one of the greatest possibilities to fight this life-threatening disease. Classically, external apoptotic stimuli or signals generated from within the cell activate different signal transduction pathways involving a family of cysteine proteases (caspases), which are the key players in apoptosis. However, the complexity of cancer biology draws interest in search of new molecules that can potentially modulate the cell death pathway.

1) Among human HtrA homologs, HtrA1 and HtrA2 are well characterized with available information on their functions, cellular substrates along with high-resolution crystal structures . HtrA1 and HtrA2 cleave a wide variety of targets mostly involved in cell death [36, 57, 58, 62]. However, HtrA4 is the least described human HtrA protease concerning both structure as well as

its functions. HtrA4 shows differential expression in glioblastoma multiforme, breast carcinoma, and metastatic prostate cancer, which makes it an emerging therapeutic target [22]. Moreover, it is up-regulated in PE and hence has been suggested to be used as a biomarker of PE [33]. Discerning the whole behavioral and functional aspects will assist us in devising strategies for modulating HtrA4, thereby developing an approach that increases HtrA4 proteolytic activity towards its antiapoptotic substrates like XIAP which might be a promising tool in cancer treatment. In some cancers XIAP is over-expressed, in such a case we can trigger the apoptosis via caspase-dependent pathway by degrading XIAP along with a combination of other chemotherapeutic agents [220].

2) The broad objective of HtrA2-GRIM-19 study is to understand the complex allosteric behavior of HtrA2 so as to establish a unified model of its mechanism of action. This in turn will help develop ways in which proteolytic activity of HtrA2 can be regulated. There are several ways to regulate HtrA2: i) designing allosteric activators based on sequence and structure of allosteric peptides ii) searching and modulating alternative allosteric sites iii) designing inhibitors based on active site architecture and known substrate specificity. Information obtained on the allosteric modulators of HtrA2 can be utilized for high throughput screening of pharmaceutical grade peptide modulators. The information obtained on the mode of interaction of HtrA2-GRIM-19 as a result of our studies can be harnessed for generating peptidomimetics. Active HtrA2 cleaves IAPs; literature reports suggest that a wide variety of primary tumor samples and cancer cell lines show elevated levels of IAPs, which further results in inactivation of caspases thereby preventing cancer cells from dying via apoptosis. Developing ways to increase the proteolytic activity of HtrA2 could enhance apoptotic cell death in cancer cells along with other chemotherapeutic agents. One such study is with renal cells treated by cisplatin, where HtrA2 is

translocated into the cytosol and triggers apoptosis by degradation of XIAP. Therefore, if this proteolytic activity of HtrA2 can be stimulated, apoptosis might be intensified. Another study shows imatinib-induced caspase-independent cell death is associated with the release of HtrA2 from the mitochondria to the cytosol. Therefore, if imatinib treatment is coupled with increase in HtrA2 activity, cell death could be enhanced as well. Apart from this, increase in HtrA2 proteolytic activity might slow down formation of amyloid deposits in brains of patients with Alzheimer's disease. Increased HtrA2 activity might also serve to maintain mitochondrial homeostasis in Parkinson's disease [10]. Therefore, HtrA2 holds great potential in devising therapeutic strategies against several disorders.